TESIS DE LA UNIVERSIDAD DE ZARAGOZA

2024 219

César Alonso Arzola Silva

Controllability in timed continuous Petri nets: a structural approach

http://zaguan.unizar.es/collection/Tesis

Director/es
Ramirez Treviño, Antonio
Florentín Mahulea, Cristian

ISSN 2254-7606

Prensas de la Universidad
Universidad Zaragoza

Universidad de Zaragoza
Servicio de Publicaciones

ISSN 2254-7606

Universidad Zaragoza
1542

Tesis Doctoral

CONTROLLABILITY IN TIMED CONTINUOUS PETRI NETS: A STRUCTURAL APPROACH

Autor

César Alonso Arzola Silva

Director/es

Ramirez Treviño, Antonio
Florentín Mahulea, Cristian

UNIVERSIDAD DE ZARAGOZA
Escuela de Doctorado

Programa de Doctorado en Ingeniería de Sistemas e Informática

2024

Repositorio de la Universidad de Zaragoza – Zaguan http://zaguan.unizar.es

Universidad Zaragoza
1542

Tesis Doctoral

Controllability in timed continuous Petri nets: a structural approach

Autor

Cesar Alonso Arzola Silva

Director/es

Dr. Cristian Mahulea
Dr. Antonio Ramírez Treviño

Universidad de Zaragoza
Departamento de Informática e Ingeniería de Sistemas

2023

Repositorio de la Universidad de Zaragoza – Zaguan http://zaguan.unizar.es

Universidad Zaragoza

Controllability in timed continuous Petri nets: A structural approach

Cesar Alonso Arzola Silva

PhD Thesis

Dirección:
Dr. Cristian Mahulea
Dr. Antonio Ramírez Treviño

Universidad de Zaragoza

Departamento de Informática e Ingeniería de Sistemas

2023

Agradecimientos

Aprovecho este espacio para agradecer a las personas que han contribuido en la realización de esta tesis:

Primero que nada, quisiera agradecer a mis directores de tesis: Cristian Mahulea, muchas gracias por compartir tu experiencia y brindarme una orientación valiosa durante este trabajo doctoral. Tú visión y dirección han contribuido de manera significativa para que este proyecto pudiese alcanzar su realización; Antonio Ramírez Treviño, "el Doc Treviño", aprecio enormemente el tiempo y la dedicación que has invertido en la realización de esta tesis (incluidos domingos y días festivos). Tu amistad y confianza son invaluables, y ha sido un honor contar contigo como guía durante todos estos años. Además, quisiera expresar mi más profundo agradecimiento a mi estimado director, Manuel Silva. Su fallecimiento repentino dejó un impacto significativo en todos los que tuvimos el privilegio de conocerlo. Manuel fue un mentor excepcional cuya sabiduría y dedicación fueron fundamentales para el desarrollo de este proyecto. A pesar de su ausencia, su legado perdura en cada página de este trabajo.

A mi hijo Cédric, gracias por todo ese apoyo y cariño infinito. Pero sobre todo gracias por siempre ayudarme a recordar, con sólo una sonrisa, que hay un mundo más allá de las redes de Petri. Gracias por la paciencia que has tenido con mis interminables días/noches de café y estrés.

A mis padres, Alfredo y María, por el apoyo incondicional que siempre he recibido de su parte. Soy lo que soy gracias a ustedes.

A mis compañeros de la universidad, gracias por su amistad y por hacerme sentir en casa, incluso a 8860 km de distancia. Gracias por todas las pausas de café, los asados, los conciertos, las cervezas, las noches de karaoke, las excursiones, las recomendaciones musicales, las sesiones de ganchillo, las kalimotxo sessions, etcetera. Pero sobre todo, por ayudarme a no morir en el intento (aún ante la presencia del Puma Escarlata, el cual ha atacado de nuevo...). Agradezco de manera infinita su compañia durante esta etapa de mi vida.

Al personal del departamento de informática e ingeniería de sistemas. No solo he tenido el privilegio de trabajar rodeado de profesionales altamente calificados, sino también de personas de buen corazón que han hecho de mi experiencia académica un verdadero placer.

Finalmente, quiero agradecer al CONACYT por el apoyo económico brindado por medio de la beca con No. 710039.

Gracias Totales.

Summary

In the literature, numerous results exist for the analysis of discrete event dynamic systems (DEDS) using the formalism of Petri nets (PN). These nets find applications in various fields such as manufacturing systems, supply chains, traffic systems, and healthcare systems, to mention a few. However, the computational complexity in analyzing these systems can easily grow due to different factors, such as a large size of the net (structure), a large marking (population), or a high interconnection between network nodes. Such situations lead to the well-known state explosion problem, where the set of reachable markings grows exponentially. This has led to the proposal of an alternative approach: the analysis of discrete event systems using continuous models, known as fluidification.

This thesis focuses on the study of timed continuous Petri nets (TCPNs) under infinite server semantics (ISS), considered a potential approximation of stochastic Petri nets with a Markovian interpretation. The main advantage of this approach, in contrast with traditional methods that involve enumerating states, is that it provides more efficient means to analyze the system behavior while maintaining a good level of accuracy with respect to the behavior of the discrete model. This formalism allows representing DEDS as a family of hybrid systems, specifically belonging to piecewise affine systems (PWA) with polyhedral regions and constrained inputs. A TCPN can be seen as a PWA system where the number of linear modes composing it depends on the number of join transitions of the net.

Particularly, we are interested in the study of controllability and the controller synthesis for TCPN systems under ISS. Controllability is one of the most important properties of any dynamic system since it indicates whether the state of the system can be driven in a desired way. The latter refers to the design and implementation of controllers to impose a specific behavior on a given system.

The analysis of controllability of TCPNs, however, is not trivial. It is well-known that checking certain controllability properties, even for very simple PWA systems are undecidable problems. To deal with that, the study of the controllability for the particular case of TCPNs under ISS has been largely addressed in the literature. These results, however, usually require analyzing each one of the polyhedral regions of the system (whose number grows exponentially in the size of the PN), are only centered in the analysis for subclasses of nets, and/or consider restrictive conditions, such as that all the transitions (events in the system) can be controlled. Similar issues arise in the existing literature on control synthesis for TCPNs, which has been largely addressed without tackling the controllability analysis and considering mainly particular cases in which this property trivially holds (for instance the case when all the transitions are controllable).

In this thesis, we deal with TCPN systems with the presence of uncontrollable transitions. In the literature, the commonly adopted goal for this case is to study controllability over the set of equilibrium markings of the system, which represent the stationary operating points of the modeled plant. This is a particularly challenging problem that has been addressed in the literature by using a local approach: by characterizing controllability over the set of equilibrium

markings in each polyhedral region, where the system behaves linearly, by using controllability matrices. Unfortunately, since the number of regions grows exponentially, the complexity of the controllability analysis, from this perspective, also grows exponentially.

Therefore, the main objective of this thesis is to provide tools for the analysis of controllability and control design while avoiding the exponential complexity associated with such analyses through the utilization of the current techniques. Particularly, we establish a structural approach (in terms of the Petri net structure) to deal with these problems. The main contributions of this thesis can be encompassed in the following 3 main categories:

Structural analysis of controllability: We deal with the analysis of controllability by proposing a novel structural approach (depending only on the information of the net structure). We propose a new property named the net rank-controllability (NRC), a structural property of the TCPN. Then, the relation between NRC and controllability is studied. It is shown that under the assumption of liveness, NRC is a sufficient condition for controllability over the equilibrium markings of multiple regions of the system.

More importantly, it is shown that this property can be characterized in terms of global structural objects of the net, thus, avoiding the analysis by regions. In this sense, some new structural conditions for NRC are derived for general TCPNs.

Finally, polynomial-time algorithms for the verification of NRC are provided.

Analysis of equilibria in TCPNs: In this part of the thesis, a study of the connectivity of the sets of equilibrium markings, within the different polyhedral regions of a given system, is presented and its importance for the analysis of controllability is addressed. By defining the connectivity graph of a given system, which represents the connections between the different equilibrium markings in its different polyhedral regions, we provide tools for its computation achieving a better performance than the brute force methods used in the literature. As it will be shown, this tool provides useful information for the analysis of controllability and synthesis of controllers in general TCPN systems.

To further particularize these results and by adopting a structural approach, a qualitative analysis of the equilibrium sets in Choice-Free (CF) TCPN systems is presented. It is based on the analysis of the slowest conservative subsystems of the system. This allows us to define a structural component named the Maximal Limiting Subnet (MLS). Then, some properties of the equilibrium sets in CF-TCPN systems are stated in terms of its MLS. Next, the connectivity of the equilibrium sets is studied for this subclass. It is shown that CF-TCPN systems always exhibit this property. Finally, the previous results are extended to Topologically Equal Conflict TCPN systems.

Control synthesis and applications to real-life systems: The implementation of the main results for the analysis of controllability and equilibria from the previous sections is presented. We implement several algorithms for this purpose in SimHPN, an available MATLAB toolbox for the analysis of hybrid Petri nets. This serves to facilitate their application in real-life systems.

Additionally, we propose a control scheme to optimize the behavior of TCPN systems with the presence of uncontrollable transitions. The scheme is based on an On-Off type control over the firing speed at the controllable transitions that reduce the marking error, i.e., the difference between the desired and actual state of the system. The proposed control law can be computed easily online, despite the complexity of a given system. The effectiveness of the

proposed control scheme is studied using simulation results and its use in different case studies.

Finally, we present some case studies by modeling two systems to showcase the capabilities of the studied formalisms: an industrial transport platform manufacturing process and the modeling of healthcare systems based on clinical pathways. For the former, we present a Generalized Stochastic Petri net to model and analyze the manufacturing process for transport platforms at the Alimak Group facility in La Muela, Spain. For the latter, we propose a TCPN model that allows for an efficient continuous-time analysis of the patient flow and resource utilization dynamics of a hip fracture clinical pathway at the Lozano Blesa University Clinical Hospital, in Zaragoza, Spain. For this second model, we also deal with the controllability analysis and control synthesis by using the previously presented results. We demonstrate the feasibility and effectiveness of the methodology presented in this thesis through this case study and some other examples.

Resumen

En la literatura, existen numerosos resultados para el análisis de sistemas dinámicos de eventos discretos (DEDS) utilizando el formalismo de las redes de Petri (PN). Estas redes encuentran aplicaciones en diversos campos como sistemas de manufactura, cadenas de suministro, sistemas de tráfico y sistemas de atención médica, por mencionar algunos. Sin embargo, la complejidad computacional en el análisis de estos sistemas puede aumentar fácilmente debido a diferentes factores, como el tamaño grande de la red (estructura), un marcado grande (población) o una alta interconexión entre nodos de la red. Tales situaciones conducen al conocido problema de explosión de estados, donde el conjunto de marcados alcanzables crece de manera exponencial. Esto ha llevado a la propuesta de un enfoque alternativo: el análisis de sistemas de eventos discretos utilizando modelos continuos, conocido como fluidificación.

Esta tesis se centra en el estudio de las redes de Petri continuas temporizadas (TCPNs) bajo la semántica de infinitos servidores (ISS), considerada como una aproximación potencial de las redes de Petri estocásticas con una interpretación de Markov. La principal ventaja de este enfoque, en contraste con los métodos tradicionales que implican la enumeración de estados, es que proporciona medios más eficientes para analizar el comportamiento del sistema, manteniendo un buen nivel de precisión con respecto al comportamiento del modelo discreto. Este formalismo permite representar DEDS como una familia de sistemas híbridos, específicamente pertenecientes a los sistemas afines a trozos (PWA) con regiones poliédricas y entradas acotadas. Un TCPN puede considerarse como un sistema PWA donde el número de modos lineales que lo componen depende del número de transiciones de sincronización de la red.

Particularmente, nos interesa el estudio de la controlabilidad y la síntesis de controladores para sistemas TCPN bajo ISS. La controlabilidad es una de las propiedades más importantes de cualquier sistema dinámico, ya que indica si el estado del sistema puede controlarse de la manera deseada. La síntesis de controladores se refiere al diseño e implementación de controladores para imponer un comportamiento específico en un sistema dado.

Sin embargo, el análisis de la controlabilidad de TCPNs no es trivial. Se sabe que verificar ciertas propiedades de controlabilidad, incluso para sistemas PWA muy simples, son problemas indecidibles. Para abordar esto, el estudio de la controlabilidad para el caso particular de TCPNs bajo ISS ha sido ampliamente abordado en la literatura. Sin embargo, estos resultados generalmente requieren analizar cada una de las regiones poliédricas del sistema (cuyo número crece exponencialmente con el tamaño de la PN), se centran solo en el análisis de subclases de redes, y/o consideran condiciones restrictivas, como que todas las transiciones (eventos en el sistema) puedan ser controladas. Problemas similares surgen en la literatura existente sobre síntesis de control para TCPNs, que se ha abordado en gran medida sin abordar el análisis de la controlabilidad y considerando principalmente casos particulares en los que esta propiedad se cumple trivialmente (por ejemplo, el caso en que todas las transiciones son controlables).

En esta tesis, estudiamos sistemas TCPN con la presencia de transiciones no controlables. En la literatura, el objetivo comúnmente adoptado para este caso es estudiar la controlabilidad sobre el conjunto de marcados de equilibrio del sistema, que representan los puntos de operación estacionarios de la planta modelada. Este es un problema particularmente desafiante que se ha abordado en la literatura mediante un enfoque local: caracterizando la controlabilidad sobre el conjunto de marcados de equilibrio en cada región poliédrica, donde el sistema se comporta linealmente, utilizando matrices de controlabilidad. Desafortunadamente, dado que el número de regiones crece exponencialmente, la complejidad del análisis de controlabilidad, desde esta

perspectiva, también crece exponencialmente.

Por lo tanto, el objetivo principal de esta tesis es proporcionar herramientas para el análisis de controlabilidad y el diseño de control evitando la complejidad exponencial asociada con tales análisis a través de la utilización de técnicas actuales. En particular, establecemos un enfoque estructural (en términos de la estructura de la red de Petri) para abordar estos problemas. Las principales contribuciones de esta tesis pueden englobarse en las siguientes 3 categorías principales:

Análisis estructural de la controlabilidad: Abordamos el análisis de la controlabilidad proponiendo un enfoque estructural novedoso (dependiendo solo de la información de la estructura de la red). Proponemos una nueva propiedad llamada net rank-controllability (NRC), una propiedad estructural de la TCPN. Luego, se estudia la relación entre NRC y la controlabilidad. Se muestra que bajo la suposición de vivacidad, NRC es una condición suficiente para la controlabilidad sobre marcados de equilibrio de múltiples regiones del sistema.

Más importante aún, se muestra que esta propiedad puede caracterizarse en términos de objetos estructurales globales de la red, evitando así el análisis por regiones. En este sentido, se derivan nuevas condiciones estructurales para NRC para TCPNs generales.

Finalmente, se proporcionan algoritmos de tiempo polinómico para la verificación de NRC.

Análisis de marcados de equilibrio en TCPNs: En esta parte de la tesis, se presenta un estudio de la conectividad de los conjuntos de marcados de equilibrio dentro de las diferentes regiones poliédricas de un sistema dado, y se aborda su importancia para el análisis de la controlabilidad. Al definir el grafo de conectividad de un sistema dado, que representa las conexiones entre los diferentes marcados de equilibrio en sus diferentes regiones poliédricas, proporcionamos herramientas para su cálculo logrando un mejor rendimiento que los métodos de fuerza bruta utilizados en la literatura. Como se mostrará, esta herramienta proporciona información útil para el análisis de la controlabilidad y la síntesis de controladores en sistemas TCPN generales.

Para particularizar aún más estos resultados y adoptar un enfoque estructural, se presenta un análisis cualitativo de los conjuntos de equilibrio en sistemas TCPN Choice-Free (CF). Se basa en el análisis de los subsistemas conservativos más lentos del sistema. Esto nos permite definir un componente estructural llamado la Maximal Limiting Subnet (MLS). Luego, se establecen algunas propiedades de los conjuntos de equilibrio en sistemas CF-TCPN en términos de su MLS. A continuación, se estudia la conectividad de los conjuntos de equilibrio para esta subclase. Se muestra que los sistemas CF-TCPN siempre exhiben esta propiedad. Finalmente, los resultados anteriores se extienden a sistemas TCPN con Conflictos Topológicamente Iguales.

Síntesis de controladores y aplicaciones a sistemas del mundo real: Se presenta la implementación de los principales resultados para el análisis de la controlabilidad y los equilibrios de las secciones anteriores. Implementamos varios algoritmos con este propósito en SimHPN, una toolbox de MATLAB disponible para el análisis de redes de Petri híbridas. Esto sirve para facilitar su aplicación en sistemas del mundo real.

Además, proponemos un esquema de control para optimizar el comportamiento de sistemas TCPN con la presencia de transiciones no controlables. El esquema se basa en un control tipo On-Off sobre la velocidad de disparo en las transiciones controlables que reduce el error en el marcado, es decir, la diferencia entre el estado deseado y real del sistema. La ley de control propuesta puede calcularse fácilmente en línea, a pesar de la complejidad de un sistema dado.

La efectividad del esquema de control propuesto se estudia mediante resultados de simulación y su aplicación en diferentes casos de estudios.

Finalmente, presentamos algunos casos de estudios modelando dos sistemas para mostrar las capacidades de los formalismos estudiados: un proceso de fabricación de plataformas de transporte industrial y la modelización de sistemas de atención médica basados en vías clínicas. Para el primero, presentamos una Red de Petri Estocástica Generalizada para modelar y analizar el proceso de fabricación de plataformas de transporte en las instalaciones de Alimak Group en La Muela, España. Para el segundo, proponemos un modelo TCPN que permite un análisis eficiente en tiempo continuo del flujo de pacientes y la dinámica de utilización de recursos de una vía clínica de fractura de cadera en el Hospital Clínico Universitario Lozano Blesa, en Zaragoza, España. Para este segundo modelo, también abordamos el análisis de la controlabilidad y la síntesis de control utilizando los resultados presentados anteriormente. Demostramos la viabilidad y eficacia de la metodología presentada en esta tesis a través de este caso de estudio y algunos otros ejemplos.

Contents

1 Introduction **1**

1.1 Motivation 1

1.2 Contributions 5

2 Concepts and notations **7**

2.1 Petri net systems 7

2.1.1 Structural concepts in Petri nets 10

2.2 Continuous Petri nets 11

2.3 Unforced timed continuous Petri nets 13

2.4 Controlled Timed Continuous Petri nets 15

2.4.1 Equilibrium markings in TCPNs 17

2.5 Controllability in linear-time invariant systems 20

2.6 State of the art: Controllability in TCPN systems 21

2.6.1 Controllability when all the transitions are controllable 22

2.6.2 Controllability with the presence of uncontrollable transitions 23

2.7 Main objectives 27

3 Net Rank-Controllability: A structural approach **29**

3.1 Introduction 29

3.2 Net rank-controllability and its relation to controllability 29

3.3 Influence of the controllable transitions 32

3.3.1 Influence definition 33

3.3.2 Influence verification 34

3.3.3 Influence as a necessary condition for NRC 35

3.4 Concluding remarks 37

4 Structural characterization of NRC **39**

4.1 Introduction 39

4.2 Uncontrollable invariant subpsaces 41

4.3 Structural characterization of UFIs 42

4.3.1 Uncontrollable structural flow invariants 42

4.3.2 Uncontrollable timed flow invariants 44

4.4 Structural conditions for net rank-controllability 48

4.5 Net rank-controllability verification . . . 50
4.6 Illustrative example: A Flexible Manufacturing System . . . 51
4.7 Concluding remarks . . . 52

5 Characterization of the controllability sets 55
5.1 Characterization of the controllability set . . . 56
5.1.1 Reducing the number of regions to analyze . . . 56
5.1.2 Connectivity verification of the controllability sets . . . 59
5.1.3 Results and Discussion . . . 60
5.2 Structural characterization of connectivity in subclasses . . . 61
5.2.1 Equilibrium markings and structural components in CF-TCPN systems . 61
5.2.2 Equilibria within a single region in CF-TCPNs . . . 68
5.2.3 Equilibrium sets in Choice Free TCPN systems . . . 70
5.2.4 Equilibrium sets in TEC-TCPN systems . . . 73
5.3 Concluding remarks . . . 73

6 Towards applications of structural controllability 75
6.1 Implementation in SimHPN . . . 75
6.1.1 Influence of controllable transitions . . . 77
6.1.2 Net rank-controllability test . . . 77
6.1.3 Equilibrium connectivity graph . . . 77
6.2 A Kanban-like flexible manufacturing system . . . 79
6.3 Analysis and optimization of clinical pathway . . . 82
6.3.1 Motivation . . . 82
6.3.2 TCPN model of the clinical pathway . . . 83
6.3.3 TCPN model validation . . . 85
6.3.4 Control and optimization of the fluid model . . . 87
6.3.5 Structural controllability analysis using SimHPN . . . 89
6.3.6 Control law implementation . . . 90
6.4 Concluding remarks . . . 93

7 Conclusions and Future Work 95
7.1 Concluding remarks . . . 95
7.2 Future work . . . 97
7.3 Observaciones finales . . . 99
7.4 Trabajo futuro . . . 101

References 103

A Analysis of an industrial manufacturing process **111**

A.1 Introduction 111

A.2 Production process of transport platforms 112

A.2.1 Assembly of the transport platforms 113

A.3 Petri net model of the manufacturing process 114

A.3.1 Model parameters 115

A.4 Performance analysis of the system 116

A.4.1 Discussion 118

A.5 Concluding remarks 118

Chapter 1

Introduction

1.1 — Motivation

Discrete Event Dynamical Systems (DEDS) refer to systems whose evolution is governed by occurrences of events, producing discrete changes in the state of the system, often with non-deterministic behavior [Cassandras and Lafortune, 2008]. This formalism encompasses a wide variety of systems such as manufacturing systems, traffic systems, healthcare systems, and communication systems, among many others.

The application of DEDS theory has proven to be successful in practical scenarios where it has played an important role in the analysis and design of diverse systems, demonstrating its usefulness in identifying and mitigating potential challenges. For instance, in manufacturing systems, DEDS theory has successfully aided in preemptively discovering bottlenecks, optimizing production workflows, and enhancing overall efficiency [Campos et al., 2018]. Additionally, its application in traffic systems has facilitated the modeling of complex traffic patterns, leading to improved traffic flow management strategies [Coogan et al., 2017]. Furthermore, modeling the dynamic interactions of healthcare systems has proven instrumental in the assessment of resources for optimal performance by the identification of bottlenecks, streamlining patient flow, and optimizing resource allocation [Jacobson et al., 2013].

DEDS theory is a branch of mathematics and engineering that emerges as a fundamental response to the need to comprehend and explain the intricate behaviors of numerous man-made systems. Different formalisms have been introduced over the years to describe and analyze those behaviors. Notable among these are *Process Algebras* [Baeten and Weijland, 1991], *Automata* [Ramadge and Wonham, 1989], and *Petri nets* [Murata, 1989], each offering a unique perspective to capture the essential attributes of a system.

In particular, Petri nets (PNs) are a widely accepted paradigm within the scientific community due to their efficacy in modeling, analyzing, and controlling DEDSs. They provide a powerful mathematical background, as well as a visually intuitive graphical representation, offering an appropriate framework for collaboration between researchers and practitioners. An

important feature of Petri nets is that they capture the main characteristics of DEDSs such as concurrency, parallelism, synchronization, and mutual exclusion, among others [Silva, 1985].

However, as systems become more complex, managing a large number of parts, components, and information, the analysis using these formalisms becomes challenging. Particularly in *heavily populated* and complex systems, DEDS formalisms suffer from the so-called *state explosion problem*. In the context of Petri nets, this problem has been tackled in the literature by following a classical relaxation: the fluidification of the system [David and Alla, 2010, Silva et al., 2011], leading to the concept of Continuous PNs (CPNs). Fluidization proposes to relax the integrality constraints of the discrete model system, and deals with a continuous approximation; this allows to make some computational problems decidable or more tractable in practice.

This thesis focuses on the study of the formalism of *timed continuous Petri nets* (TCPNs). TCPNs are continuous-state systems, originally introduced as a fluid relaxation of discrete PNs [David and Alla, 2010, Silva et al., 2011] to cope with the *state explosion problem*, present in the analysis of highly populated discrete event systems. This is achieved by fluidizing the state space, which allows the application of analysis techniques rooted in linear algebra, linear dynamic systems analysis, and control theory, among others. This approach contrasts with traditional methods that involve enumerating states, providing more efficient means to analyze the system's behavior while maintaining a good level of accuracy with respect to the behavior of the discrete model. Furthermore, it offers the benefit of leveraging the analysis and design techniques that have been developed specifically for TCPNs, that have been extensively addressed in the literature (steady-state throughput analysis [Mahulea et al., 2008b, Navarro-Gutiérrez et al., 2022a], fault diagnosis [Casas Carrillo et al., 2021, Mahulea et al., 2012], controllability [Vázquez et al., 2014], observability [Mahulea et al., 2010], among many others).

In this thesis, the main focus is to study TCPNs under *infinite server semantics* (ISS), whose evolution is described by *piecewise affine systems* (PWA) [Kloetzer et al., 2010, Xu and Xie, 2014] *with polyhedral regions and constrained inputs*. TCPNs under ISS provide a good approximation of the performance of timed interpretations of PNs, such as *Markovian Petri nets* [1] [Mahulea et al., 2009, Molloy, 1982], and they have been successfully used to model systems, such as epidemiological [Beccuti et al., 2013], health management [Dotoli et al., 2009a], or traffic [Júlvez and Boel, 2010], among others.

In particular, we are interested in the study of *controllability* and the controller synthesis for TCPN systems under ISS. The former is a valuable property that indicates whether a system can be driven to a required state by *reducing the firing speed* at the *controllable* transitions. The latter refers to the design and implementation of controllers to impose a specific behavior on the system. By following a control theory approach, the frequently established control objective consists of driving the TCPN system toward a desired target state, rather than the control

[1] Introduced as stochastic Petri nets in Molloy [1982], using exponentially distributed transition rates.

problems commonly addressed in DEDS (like disabling the occurrence of certain controllable events to avoid forbidden states). Moreover, these kinds of controllers can be designed for the fluid system and then applied to its discrete counterpart (see for instance, Vázquez and Silva [2009] for the stock-level control of a stochastically timed automotive assembly line model).

In the literature, the controller synthesis for TCPNs has been largely addressed without tackling the controllability analysis (*e.g.*, Mahulea et al. [2008a], Kara et al. [2009], Ross-León et al. [2010], Taleb et al. [2014]), considering particular cases in which this property trivially holds (for instance the case where *all* the transitions are controllable [Vázquez et al., 2014]). Nevertheless, to establish methods for the controller synthesis of more general systems, a first step is to improve the analysis techniques for controllability.

Since TCPNs correspond to PWA systems, a first natural step will be to use the available results for controllability for this type of systems. However it is well known that the controllability analysis for general PWA systems is not trivial [Xu and Xie, 2014]. A wide variety of works dealing with this subject can be found in the literature, *e.g.*, Bemporad et al. [2000], Xu and Xie [2005] and Habets et al. [2006]. In particular, the approach from Bemporad et al. [2000] requires the solution of a Mixed-Integer Linear Programming problem (MILP) to determine the controllability of a PWA system; in Xu and Xie [2005], the controllability of planar bimodal piecewise linear systems is studied; Habets et al. [2006] provided sufficient conditions for *reachability* in PWA systems based on the reachability inside the different polyhedral regions of a system, which can be extended to controllability. These results, however, can only be applied to TCPNs with a small number of state variables since the solution of MILPs is a computationally complex problem and the number of polyhedral regions composing a TCPN grows exponentially in the size of the PN [Silva et al., 2011]. Hence, these results do not provide useful information in general TCPNs.

The study of controllability for TCPNs under ISS has also been addressed in the literature [Jiménez et al., 2005, Mahulea et al., 2008b, Vázquez and Ramírez-Treviño, 2012, Vázquez et al., 2014]. These works take advantage of the continuous control theory and the structural analysis of PNs to derive more adequate results for the problem under consideration. In Jiménez et al. [2005], the controllability property in Join-Free TCPNs, fully described by a single linear system, was studied. In Mahulea et al. [2008b] it was stated that TCPN systems are frequently not controllable in the sense of continuous-state systems (where a continuous system is named controllable if all states in the state space can be reached from any other state in the state space), due to the existence of state invariants, related to marking conservation laws imposed by P-flows. In Vázquez et al. [2014], the analysis of controllability was divided into two cases: when all the transitions are controllable and when there exist uncontrollable transitions. In the first case, the *consistency* of the net is sufficient and necessary to guarantee controllability. In the second case, it was demonstrated that controllability over all of the reachable markings could not be achieved. Nevertheless, this property was defined as the possibility of transferring the

system between its potential steady states (equilibrium markings). This approach is of great interest since these states usually represent the potential stationary operating points of the modeled plants. That work derives necessary and sufficient conditions for *controllability over the set of equilibrium markings* in a given polyhedral region, where the system behaves linearly, by using controllability matrices. Unfortunately, as stated before, the number of regions *grows exponentially* in the size of the TCPN, hence the complexity of the controllability analysis, from this perspective, also grows exponentially.

Moreover, since the controllability is defined over the sets of equilibrium markings of the system, the analysis of these sets requires some attention too. In Vázquez et al. [2014] it is stated that if the system is controllable over the *equilibrium sets* in each region, a sufficient condition for controllability over the set of all equilibrium markings of the system is that such set is *connected*. In other words, issues appear if it is not connected since, even if the system is *locally* controllable in each region, it is not necessarily *globally* controllable.

Then, a deeper analysis of the equilibrium sets on TCPN systems is necessary to establish stronger controllability results. However, the study of equilibria in general piecewise-smooth dynamical systems is far from trivial [Bernardo et al., 2008]. Nevertheless, since TCPNs are continuous on the state and its derivative, we can exclude cases like pseudoequilibria or sliding manifolds and restrict our study to phenomena that have been observed in the context of TCPNs such as isolated equilibrium markings, sets of infinitely many equilibria, equilibria at the border of regions [Meyer, 2012, Vázquez et al., 2014] and oscillatory behaviors in steady-state [Mahulea et al., 2008b], for instance. The literature on the study of equilibria in TCPNs, however, is very limited. Usually, it is carried out by analyzing the dynamic matrix of each *linear mode* of the system (corresponding to its different regions). Nonetheless, the existence of a potentially exponential number of regions in general nets makes this a challenging problem.

Unlike the case of controllability and the study of equilibrium sets, the analysis of other properties such as diagnosability (Casas Carrillo et al. [2021]), steady state throughput analysis (Navarro-Gutiérrez et al. [2020] and Navarro-Gutiérrez et al. [2022b]), and observability (Mahulea et al. [2010], Aguayo-Lara et al. [2011] and Aguayo-Lara et al. [2014]) has greatly benefited from adopting a *structural approach*, which has emerged as a powerful methodology. In other words, this structural approach harnesses the information embedded within the Petri net structure itself to characterize specific properties without the exhaustive analysis of all linear modes within a given system. This technique, not new for TCPNs, parallels its classical application in the structural theory of discrete Petri nets, where it has been employed to study properties such as boundedness, liveness, deadlock-freeness, and many others [Silva et al., 1998].

As will be explained in the following, the main objective of this thesis is to establish a structural approach to deal with the controllability analysis in TCPN systems.

1.2 — Contributions

The main contributions of this thesis can be encompassed in the following 3 main categories:

• **Structural analysis of controllability**: This thesis deals with the analysis of controllability by using a structural approach. We propose a new property named the *net rank-controllability* (NRC), a *structural property* of the TCPN that indicates that the controllability matrices of all the linear modes of the system have the largest possible rank. Then, the relation between NRC and controllability is studied. *Under the assumption of liveness, it is shown that NRC is a sufficient condition for controllability; nevertheless, if liveness is not fulfilled, then controllability is not guaranteed by NRC.*

More importantly, we show that this new property can be characterized in terms of *global structural objects* of the net, thus avoiding the analysis by configurations. In this sense, some new structural conditions, one necessary and one sufficient for NRC are introduced for general TCPNs. Finally, polynomial-time algorithms for the verification of NRC are provided.

• **Analysis of equilibria in TCPNs:** In this part of the thesis, a study of the connectivity of the sets of equilibrium markings, within the different polyhedral regions of a given system, is presented and its importance for the analysis of controllability is addressed. By defining the connectivity graph of a given system, which represents the connections between the different equilibrium markings in its different polyhedral regions, we provide tools for its computation achieving a better performance than the brute force methods used in the literature. As it will be shown, this tool provides useful information for the analysis of controllability and synthesis of controllers in general TCPN systems.

In order to further particularize these results and by adopting a structural approach, a qualitative analysis of the equilibrium sets in Choice-Free (CF) TCPN systems is presented. It is based on the analysis of the *slowest conservative subsystems* of the system. This allows us to define a structural component named the *Maximal Limiting Subnet* (MLS). Then, some properties of the equilibrium sets in CF-TCPN systems are stated in terms of its MLS. Next, *connectivity* of the equilibrium sets is studied for this subclass. It is shown that CF-TCPN systems always exhibit this property. Finally, the previous results are extended to Topologically Equal Conflict TCPN systems. However, it is also shown that connectivity is not necessarily fulfilled in general systems.

• **Control synthesis and applications to real-life systems:** The implementation of the main results for the analysis of controllability and equilibria from the previous sections is presented. We implement several algorithms for this purpose in SimHPN [Júlvez et al., 2012], an available MATLAB toolbox for the analysis of hybrid Petri nets. This serves to facilitate their application in real-life systems.

Additionally, we propose a control scheme to optimize the behavior of TCPN systems with the presence of uncontrollable transitions. The scheme is based on an On-Off type control over the firing speed at the controllable transitions that reduce the marking error, i.e., the difference between the desired and actual state of the system. The proposed control law can be computed easily online, despite the complexity of a given system. The effectiveness of the proposed control scheme is studied using simulation results and its use in different case studies.

Finally, we present some case studies by modeling two systems to showcase the capabilities of the studied formalisms: an industrial transport platform manufacturing process and the modeling of healthcare systems based on clinical pathways. For the former, we present a Generalized Stochastic Petri net to model and analyze the manufacturing process for transport platforms at the Alimak Group facility in La Muela, Spain. For the latter, we propose a TCPN model that allows for an efficient continuous-time analysis of the patient flow and resource utilization dynamics of a hip fracture clinical pathway at the Lozano Blesa University Clinical Hospital, in Zaragoza, Spain. For this second model, we also deal with the controllability analysis and control synthesis by using the previously presented results. We demonstrate the feasibility and effectiveness of the methodology presented in this thesis through this case study and some other examples.

The structure of this thesis is the following: Chapter 2 gives an introduction to the basic concepts of Petri nets, continuous Petri nets, and timed continuous Petri nets used in this thesis. Moreover, it introduces the state of the art in the study of controllability in TCPNs, establishing the main goals of this thesis. Chapter 3 introduces the property of net rank-controllability and shows its relation to the study of controllability. Chapter 4 deals with the characterization of NRC from a structural point of view. It introduces structural conditions and algorithms to study this property in polynomial time. Chapter 5 deals with developing tools for the analysis of equilibria in TCPNs. Chapter 6 introduces some case studies to showcase the applicability of the results presented in previous chapters. Moreover, it includes the proposal of a control law for the optimization of the presented systems. Finally, Chapter 7 establishes the conclusions and proposes possible future works.

Chapter 2

Concepts and notations

This chapter is devoted to providing a comprehensive introduction to the fundamental concepts and definitions of discrete, continuous, and timed continuous Petri nets, as well as some concepts of linear time-invariant (LTI) systems and controllability. These topics form the basis of the proposed results and are crucial for understanding the subsequent chapters. For a more detailed introduction to these topics, we recommend consulting the following key references: Silva [1985], Murata [1989], David and Alla [2010], Silva et al. [2011], Vázquez et al. [2014] and Chen [1998].

In the sequel, the following notation is adopted: vectors and matrices are notated with bold lowercase and uppercase letters, respectively. Given a matrix $\mathbf{A}$ of dimension $n \times m$ and sets of ordered indexes $J = \{j_1, ..., j_s\}$ and $K = \{k_1, ..., k_r\}$ with $s \leq n$ and $r \leq m$ the restriction of matrix $\mathbf{A}$ to the elements in the rows indicated by J and the columns indicated by K is denoted as $\mathbf{A}[J, K]$. Similarly, given a vector $\mathbf{a}$, $\mathbf{a}[J]$ represents the vector built with the entries of $\mathbf{a}$ indicated in J. To denote a particular entry of a vector or a matrix: the j-th entry of vector $\mathbf{a}$ is denoted as $[\mathbf{a}]_j$, or simply as a_j if it does not cause confusion; $[\mathbf{A}]_{j,k}$, or $A_{j,k}$, denotes the j, k-th entry of matrix $\mathbf{A}$. $[\mathbf{A}]_{j,\bullet}$ and $[\mathbf{A}]_{\bullet,k}$ stand for the j-th row and the k-th column of matrix $\mathbf{A}$, respectively. Vector and matrix comparisons are bit-wise, *i.e.*, $\mathbf{a} > \mathbf{b}$ means that $\forall j$, $[\mathbf{a}]_j > [\mathbf{b}]_j$. The image of a matrix $\mathbf{A}$ (i.e., the set of all possible linear combinations of its columns) is denoted as $Img(\mathbf{A})$.

2.1 — Petri net systems

This section presents some basic concepts on discrete Petri nets.

Definition 2.1. *A* Petri net (PN) *structure is a directed bipartite graph defined as* $\mathcal{N} = \langle P, T, \mathbf{Pre}, \mathbf{Post} \rangle$ *where:* $P = \{p_1, \cdots, p_n\}$ *and* $T = \{t_1, \cdots, t_m\}$ *are finite non-empty disjoint sets of nodes named places and transitions, respectively;* **Pre** *and* **Post** *are* $n \times m$ *matrices, where* $[\mathbf{Pre}]_{j,k}, [\mathbf{Post}]_{j,k} \in \mathbb{N}_{\geq 0}$ *represent the weight of the* arc, (p_j, t_k), *connecting* p_j *to transition* t_k, *and the* arc, (t_k, p_j), *connecting* t_k *to* p_j, *respectively.*

Each node, place, transition and arc, have a graphical representation. Places are repre-

sented as circles, transitions are represented as boxes and arcs are represented by arrows from the source node to the ending node.

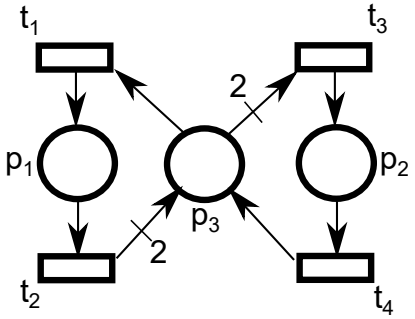

Figure 2.1. Petri net structure example.

Example 2.1. *In Figure 2.1 a PN structure is presented. The set of places is* $P = \{p_1, p_2, p_3\}$ *and the set of transitions is* $T = \{t_1, t_2, t_3, t_4\}$. *Matrices* **Pre** *and* **Post** *are:*

$$\mathbf{Pre} = \begin{bmatrix} 0 & 1 & 0 & 0 \\ 0 & 0 & 0 & 1 \\ 1 & 0 & 2 & 0 \end{bmatrix} \quad \mathbf{Post} = \begin{bmatrix} 1 & 0 & 0 & 0 \\ 0 & 0 & 1 & 0 \\ 0 & 2 & 0 & 1 \end{bmatrix}$$

A *subnet* of $\mathcal{N}$ is a Petri net structure $\mathcal{N}' = \langle P', T', \mathbf{Pre}', \mathbf{Post}' \rangle$ where $P' \subseteq P$ and $T' \subseteq T$ are subsets of places and transitions of $\mathcal{N}$, respectively; $\mathbf{Pre}' = \mathbf{Pre}[P', T']$ and $\mathbf{Post}' = \mathbf{Post}[P', T']$ are the **Pre** and **Post** matrices restricted to the entries related to the nodes in P' and T'. For pre- and postsets of places and transitions we use the conventional dot notation:

$$^\bullet p_j = \{t_k \in T | [\mathbf{Post}]_{j,k} \neq 0\}, \qquad p_j{}^\bullet = \{t_k \in T | [\mathbf{Pre}]_{j,k} \neq 0\}$$

$$^\bullet t_j = \{p_k \in P | [\mathbf{Pre}]_{j,k} \neq 0\}, \qquad t_j{}^\bullet = \{p_k \in T | [\mathbf{Post}]_{j,k} \neq 0\}$$

For example, in the PN of Fig 2.1, $t_3{}^\bullet = \{p_2\}$ and $^\bullet p_3 = \{t_2, t_4\}$. The pre- and postsets of subsets of nodes are defined analogously. The nodes of $\mathcal{N}$ can be classified based on their input and output nodes:

- $t_j \in T$ is a *join* if $|^\bullet t_j| > 1$.
- $t_f \in T$ is a *fork* if $|t_f{}^\bullet| > 1$.
- $p_a \in P$ is an *attribution* if $|^\bullet p_c| > 1$.
- $p_c \in P$ is a *choice* if $|p_c{}^\bullet| > 1$.
- Two transitions t_j and t_k are said to be in *conflict* if $^\bullet t_j \cap {}^\bullet t_k \neq \emptyset$.

- Two transitions t_j and t_k are in *topologically equal conflict* if $\exists \gamma > 0$ s.t.

$$\mathbf{Pre}[P, t_j] = \gamma \mathbf{Pre}[P, t_k]$$

In discrete Petri net systems, the *marking*, or *state*, is a vector $\mathbf{M} \in \mathcal{N}_{\geq 0}^{|P|}$ that assigns to each place of $\mathcal{N}$ a non-negative natural number.

Definition 2.2. *A* discrete Petri net *system is a PN structure together with an initial marking* $\mathbf{M}_0$*, denoted as* $\langle \mathcal{N}, \mathbf{M}_0 \rangle$.

The marking (state) of the system evolves according to the following rules: a transition $t_k \in T$ is *enabled* at a marking $\mathbf{M}$ if $\forall p_j \in {}^\bullet t_k$, $[\mathbf{M}]_j \geq [\mathbf{Pre}]_{j,k}$. The *enabling degree* of a transition, t_k, indicates the maximum amount it can be *fired* at a specific marking $\mathbf{M}$ and is given by:

$$enab(t_k, \mathbf{M}) = \min_{p_j \in {}^\bullet t_k} \left\lfloor \frac{[\mathbf{M}]_j}{[\mathbf{Pre}]_{j,k}} \right\rfloor$$

If a transition t_k is enabled, it can be fired in any amount $a \in \mathbb{N}$ such that $0 < a \leq enab(t_k, \mathbf{M})$, leading to a new marking $\mathbf{M}'$, computed as $\mathbf{M}' = \mathbf{M} + a \cdot \mathbf{C}[P, t_k]$, where $\mathbf{C} = \mathbf{Post} - \mathbf{Pre}$ is the *token-flow* matrix of the PN. Then, it is said that $\mathbf{M}'$ is *reachable* from $\mathbf{M}$, denoted by $\mathbf{M} \xrightarrow{at_k} \mathbf{M}'$.

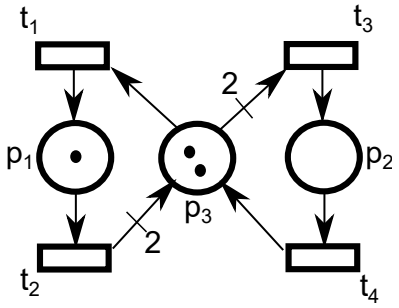

Figure 2.2. A Petri net system with marking $\mathbf{M}_0 = [1\ \ 0\ \ 2]^T$.

Example 2.2. *Regarding the PN in Figure 2.2,* t_4 *is the only transition that is not enabled at marking* $\mathbf{M}_0$*. Since* t_3 *is enabled, the marking* $\mathbf{M}_1$*, such that,* $\mathbf{M}_0 \xrightarrow{t_3} \mathbf{M}_1$ *can be computed as:*

$$\mathbf{M}_1 = \begin{bmatrix} 1 \\ 0 \\ 2 \end{bmatrix} + \begin{bmatrix} 1 & -1 & 0 & 0 \\ 0 & 0 & 1 & -1 \\ -1 & 2 & -2 & 1 \end{bmatrix} \begin{bmatrix} 0 \\ 0 \\ 1 \\ 0 \end{bmatrix} = \begin{bmatrix} 1 \\ 1 \\ 0 \end{bmatrix}$$

2.1.1. Structural concepts in Petri nets

Particular sets of nodes (components) in the structure of the Petri net can show interesting results about the behavior of the system. This approach is known as structural analysis [Silva et al., 1998], in which such components can be equivalently analyzed from the incidence matrix. Let us first introduce P- and T- flows, structures that will be useful in this document.

If $\mathbf{x} \neq \mathbf{0}$ (resp. $\mathbf{y} \neq \mathbf{0}$) is a solution of $\mathbf{Cx} = \mathbf{0}$ (resp. $\mathbf{y}^T\mathbf{C} = \mathbf{0}$) then it is named *T-flow* (resp. *P-flow*). Matrices $\mathbf{B}_x$ and $\mathbf{B}_y$ denote bases for the T-flows and the P-flows of $\mathcal{N}$, respectively. Thus, $rank(\mathbf{C}) = |T| - rank(\mathbf{B}_x) = |P| - rank(\mathbf{B}_y)$. Non-negative T-flows, $\mathbf{x} \geq \mathbf{0}$ (resp. P-flows, $\mathbf{y} \geq \mathbf{0}$), are called *T-semiflows* (resp. *P-semiflows*). $\mathcal{N}$ is *consistent*, denoted as Ct (resp. *conservative*, denoted as Cv) if there exists a T-semiflow $\mathbf{x} > \mathbf{0}$ (resp. P-semiflow $\mathbf{y} > \mathbf{0}$). The *support* of a $|T|$-sized vector $\mathbf{x}$ (resp. $|P|$-sized vector $\mathbf{y}$), denoted by $||\mathbf{x}||$ (resp. $||\mathbf{y}||$), is defined as the set $||\mathbf{x}|| = \{t_k \in T \mid [\mathbf{x}]_k \neq 0\}$ (resp. $||\mathbf{y}|| = \{p_j \in P \mid [\mathbf{y}]_j \neq 0\}$). A semiflow is said to be *minimal* when its support is not a proper superset of the support of any other, and the greatest common divisor of its elements is one.

Example 2.3. *Consider the PN in Figure 2.3 where the token-flow matrix is:*

$$\mathbf{C} = \begin{bmatrix} -2 & -1 & 1 & 2 \\ 1 & 0 & -1 & 0 \\ 0 & 1 & 0 & -1 \\ 0 & 0 & 1 & -1 \end{bmatrix}$$

$\mathbf{y} = \begin{bmatrix} 1 & 2 & 1 & 1 \end{bmatrix}^T$ *is a P-semiflow of the net. Then,* $\mathbf{y}^T\mathbf{M} = \mathbf{y}^T\mathbf{M_0} + \mathbf{y}^T\mathbf{C}\boldsymbol{\sigma} = \mathbf{y}^T\mathbf{M_0}$, *where* $\boldsymbol{\sigma} = \begin{bmatrix} a_1 & \dots & a_{|T|} \end{bmatrix}^T$ *is a vector containing the amount of firing of each transition. Then, the existence of the P-semiflow implies that the sum* $\mathbf{y}^T\mathbf{M} = [\mathbf{M}]_1 + 2[\mathbf{M}]_2 + [\mathbf{M}]_3 + [\mathbf{M}]_4$ *remains constant during the evolution of the system. Also,* $\mathbf{x} = \begin{bmatrix} 1 & 1 & 1 & 1 \end{bmatrix}^T$ *is a T-semiflow. Then,* $\mathbf{M} = \mathbf{M}_0 + \mathbf{Cx} = \mathbf{M}_0$ *meaning that by firing all the transitions one time, the marking reached is equal to the initial one,* $\mathbf{M}_0 \xrightarrow{t_2} \mathbf{M}_1 \xrightarrow{t_4} \mathbf{M}_2 \xrightarrow{t_1} \mathbf{M}_3 \xrightarrow{t_2} \mathbf{M}_0$. *Furthermore, since* $\mathbf{x} > \mathbf{0}$ *and* $\mathbf{y} > \mathbf{0}$, *the system is Ct and Cv.*

Definition 2.3. *Let* $\mathbf{y}_k$ *be a P-semiflow of* $\mathcal{N}$. *The* Conservative component *(Cv-component)* induced by $\mathbf{y}_k$ *is defined as* $\mathcal{N}_k = \langle P_k, T_k, \mathbf{Pre}_k, \mathbf{Post}_k \rangle$ *where* $P_k = ||\mathbf{y}_k||$, $T_k = P_k{}^\bullet$, $\mathbf{Pre}_k = \mathbf{Pre}[P_k, T_k]$ *and* $\mathbf{Post}_k = \mathbf{Post}[P_k, T_k]$.

Subclasses of nets defined according to their structure are:

1. $\mathcal{N}$ is Choice-Free (CF) if $\forall p \in P : |p^\bullet| \leq 1$.
2. $\mathcal{N}$ is Join-Free (JF) if $\forall t \in T : |{}^\bullet t| \leq 1$.

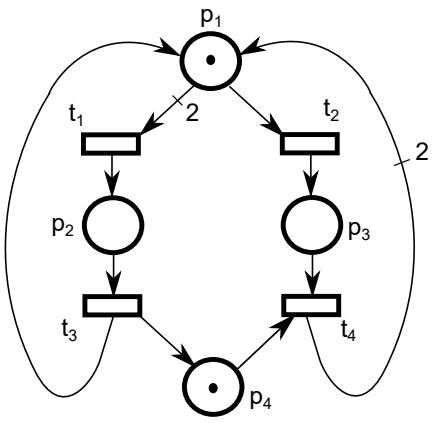

Figure 2.3. A conservative and consistent Petri net system.

3. $\mathcal{N}$ is Fork-Attribution (FA) if it is CF and JF.

4. $\mathcal{N}$ is Topologically Equal Conflict (TEC) if all the conflicts are topologically equal.

5. $\mathcal{N}$ is Mono-T-Semiflow (MTS) if it is Cv and has a unique minimal T-semiflow $\mathbf{x}$, s.t. $||\mathbf{x}|| = T$.

One of the advantages of the study of subclasses of nets is that, usually, the results obtained to analyze behavioral properties in general systems can be improved for the subclasses under consideration. For instance, while for general nets only structural necessary or sufficient conditions for liveness (an important property in PN systems) exist, for TEC systems, structural necessary and sufficient conditions can be stated [Silva et al., 2011](which can be verified in polynomial time).

JF systems are a generalization of the well-known subclass of State Machines. CF nets represent systems without structural conflicts; in particular, they comprise the subclass of Marked Graphs. JF and CF nets belong to the class of continuous TEC nets. These nets are able to capture the *cooperative* and *decision* processes occurring in a manufacturing system. Cooperative processes represent resource allocation to jobs and assembly operations; decision processes represent alternative processing routes followed by parts. It leads that TECs are able to represent a broad subclass of *flexible manufacturing systems* (FMS) that includes the Flow Shop and Job Shops, among other FMS subclasses, where the decision on which route a part may take, is not subordinated to the availability of idle resources.

2.2 — Continuous Petri nets

In this section, continuous Petri nets are presented. A continuous Petri net is a relaxation of the discrete PN model, implemented with the purpose of avoiding the state explosion problem

appearing in heavily populated discrete Petri nets [David and Alla, 2010]. In continuous Petri nets, a transition can be fired in any real amount between zero and its enabling degree. As a consequence, the number of tokens in each place can be a positive real number. This model is formally defined below.

Definition 2.4. *A* continuous Petri net (CPN) *system, $\langle \mathcal{N}, \mathbf{m}_0 \rangle$, is a PN structure provided with an* initial marking, *$\mathbf{m}_0 \in \mathbb{R}^n_{\geq \mathbf{0}}$. The evolution of the marking is governed by the following rules: The* enabling degree *of the system at marking $\mathbf{m}_r$, denoted by the $|T|$-sized vector $\mathbf{enab}(\mathbf{m}_r)$, is defined s.t. its k-th component is:*

$$[\mathbf{enab}(\mathbf{m}_r)]_k = \min_{p_j \in {}^\bullet t_k} \left\{ \frac{[\mathbf{m}_r]_j}{[\mathbf{Pre}]_{j,k}} \right\}$$

representing how much t_k can be fired *at $\mathbf{m}_r$; t_k is* enabled *at $\mathbf{m}_r$ if $[\mathbf{enab}(\mathbf{m}_r)]_k > 0$. An enabled transition t_k can be fired in any real amount α_k:*

$$0 < \alpha_k \leq [\mathbf{enab}(\mathbf{m}_r)]_k \tag{2.1}$$

leading to a new marking $\mathbf{m}_{r+1} = \mathbf{m}_r + [\mathbf{C}]_{\bullet,k}\alpha_k$. The firing count vector *$\boldsymbol{\sigma}_r = [\alpha_1 \ ... \ \alpha_m]^T$ indicates the amount of firing of each transition at $\mathbf{m}_r$ and it is* fireable *if each α_k fulfills (2.1). A* firing sequence, *$\boldsymbol{\sigma} = \boldsymbol{\sigma}_0 + \boldsymbol{\sigma}_1 + ... + \boldsymbol{\sigma}_r$ is defined s.t. $\boldsymbol{\sigma}_j$ is the j-th firing count vector of the sequence. A marking $\mathbf{m}$ is* reachable[1] *from $\mathbf{m}_0$ if there is a (finite or infinite) firing sequence, $\boldsymbol{\sigma}$, satisfying the fundamental CPN equation:*

$$\mathbf{m} = \mathbf{m}_0 + \mathbf{C}\boldsymbol{\sigma} \tag{2.2}$$

Given $\langle \mathcal{N}, \mathbf{m}_0 \rangle$, the set of all reachable markings from $\mathbf{m}_0$ is convex and it is denoted as $RS(\mathcal{N}, \mathbf{m}_0)$ [Silva et al., 2011].

Example 2.4. *Regarding the CPN in Figure 2.4, transitions t_1, t_3 and t_2 are enabled and its enabling degrees are $[\mathbf{enab}(\mathbf{m}_0)]_1 = 2$, $[\mathbf{enab}(\mathbf{m}_0)]_2 = 1$ and $[\mathbf{enab}(\mathbf{m}_0)]_1 = 1$, respectively. If transition t_2 is fired 0.5 times and t_3 0.3 times, simultaneously, the reached marking $\mathbf{m}'$ can be computed using Eq. (2.2):*

$$\mathbf{m}' = \begin{bmatrix} 1 \\ 0 \\ 2 \end{bmatrix} + \begin{bmatrix} 1 & -1 & 0 & 0 \\ 0 & 0 & 1 & -1 \\ -1 & 2 & -2 & 1 \end{bmatrix} \begin{bmatrix} 0 \\ 0.5 \\ 0.3 \\ 0 \end{bmatrix} = \begin{bmatrix} 0.5 \\ 0.3 \\ 2.4 \end{bmatrix}$$

A CPN system is *bounded* if $\forall \mathbf{m} \in RS(\mathcal{N}, \mathbf{m}_0)$ there exists a constant b s.t., $\forall p_i \in P$, $m_i \leq b$. It is *live* if $\forall t_j \in T$ and $\forall \mathbf{m} \in RS(\mathcal{N}, \mathbf{m}_0)$ there exists a successor $\mathbf{m}' \in RS(\mathcal{N}, \mathbf{m})$ s.t.

[1] This corresponds to the concept of *lim-reachability*, studied in Júlvez et al. [2003], in which markings reached by infinite firing sequences are considered reachable.

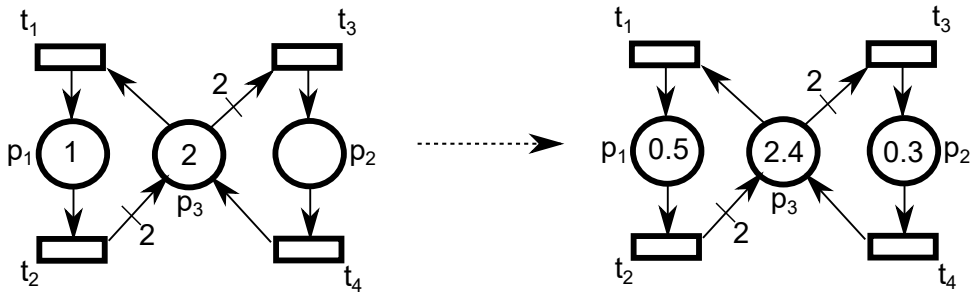

Figure 2.4. Evolution of a continuous Petri net.

$[\mathbf{enab}(\mathbf{m}')]_j > 0$. A reachable marking $\mathbf{m}_D$ is a *deadlock* if $\mathbf{enab}(\mathbf{m}_D) = \mathbf{0}$. In this thesis, we focus on live and bounded systems, which are frequently desired properties in practical systems. In order for a system to be live and bounded, it is necessary that $\mathcal{N}$ be Ct and Cv [Silva et al., 2011]. Hence, in this work, it will be assumed that the nets fulfill these properties.

Notice that, for every P-flow $\mathbf{y}$ of $\mathcal{N}$, every reachable marking $\mathbf{m}$ satisfies: $\mathbf{y}^T\mathbf{m} = \mathbf{y}^T\mathbf{m}_0$. In other words, linear dependencies appear between the markings, called *token conservation laws*.

Definition 2.5. *Given a Cv net, $\mathcal{N}$, every reachable marking of the system $\langle \mathcal{N}, \mathbf{m}_0 \rangle$ must belong to the* invariant *defined by:*

$$Class(\mathbf{m}_0) = \{\mathbf{m} \in \mathbb{R}_{\geq 0}^{|P|} \mid \mathbf{B}_y^T\mathbf{m} = \mathbf{B}_y^T\mathbf{m}_0\}$$

In particular, if $\mathcal{N}$ is Ct and Cv, the set $RS(\mathcal{N}, \mathbf{m}_0)$ is equal to $Class(\mathbf{m}_0)$ [Silva et al., 2011].

2.3 — Unforced timed continuous Petri nets

The notion of time may be included in CPN systems by timing the firing of their transitions. In that case, the marking and the firing sequence in (2.2) will be explicitly dependent on time τ:

$$\mathbf{m}(\tau) = \mathbf{m}_0 + \mathbf{C}\boldsymbol{\sigma}(\tau) \tag{2.3}$$

where $\boldsymbol{\sigma}(\tau)$ is assumed to be a smooth function.

Definition 2.6. *A* timed continuous Petri net (TCPN) *system is a time-driven continuous-state system described by the tuple $\langle \mathcal{N}, \boldsymbol{\lambda}, \mathbf{m}_0 \rangle$, where $\langle \mathcal{N}, \mathbf{m}_0 \rangle$ is a CPN system and the vector $\boldsymbol{\lambda} \in \mathbb{R}_{>0}^{|T|}$ is the* firing rate vector *or* timing *of the net, which assigns to each transition a positive real number representing its* firing rate. *The state equation of the timed system is obtained by*

taking the time derivative of (2.3):

$$\dot{\mathbf{m}}(\tau) = \mathbf{C}\mathbf{f}(\tau) \tag{2.4}$$

where $\mathbf{f}(\tau) = \dot{\boldsymbol{\sigma}}(\tau)$ *is the* firing flow *vector of the TCPN.*

There are different ways of defining the flow through the transitions, the two most important being *infinite server* or *variable speed* [Mahulea et al., 2009], and *finite server* or *constant speed* [David and Alla, 2010]. In this work, the flow vector is defined using *infinite server semantics* (ISS), which, for a broad class of net systems provides a better approximation of the performance of the system's discrete counterpart [Mahulea et al., 2009].

Definition 2.7. *Under ISS the flow of the k-th transition is defined as the product of its firing rate,* $\lambda_k = [\boldsymbol{\lambda}]_k$*, and its instantaneous enabling degree,* $[\mathbf{enab}(\mathbf{m}(\tau))]_k$*:*

$$[\mathbf{f}(\tau)]_k = \lambda_k[\mathbf{enab}(\mathbf{m}(\tau))]_k = \lambda_k \min_{p_j \in {}^\bullet t_k} \left\{ \frac{[\mathbf{m}(\tau)]_j}{[\mathbf{Pre}]_{j,k}} \right\} \tag{2.5}$$

The *min* operator in Eq. (2.5) allows describing the state evolution of a TCPN system as a *piecewise affine system* [Kloetzer et al., 2010]. The next concepts illustrate this:

Definition 2.8.

(1) *A* configuration *of the TCPN,* $\mathcal{C} = \{(p_{\alpha_1}, t_1), \cdots, (p_{\alpha_m}, t_m)\}$*, is a set of arcs, one per transition s.t.* $p_{\alpha_k} \in {}^\bullet t_k$*. The number of configurations is* $\prod_{t_k \in T} |{}^\bullet t_k|$ *(it grows exponentially in the presence of join transitions [Silva et al., 2011]).*

(2) *The* $|T| \times |P|$ configuration matrix $\mathbf{\Pi}_i$*, associated to the i-th configuration,* $\mathcal{C}_i$*, is defined as:*

$$[\mathbf{\Pi}_i]_{k,j} = \begin{cases} \frac{1}{[\mathbf{Pre}]_{j,k}} & \text{if } (p_j, t_k) \in \mathcal{C}_i \\ 0 & \text{otherwise} \end{cases} \tag{2.6}$$

(3) *A configuration* $\mathcal{C}_i$ *is said to be* active at $\mathbf{m}(\tau)$ *if* $\mathbf{\Pi}_i\mathbf{m}(\tau) = \mathbf{enab}(\mathbf{m}(\tau))$*. If* $\mathcal{C}_i$ *is active and* $(p_j, t_k) \in \mathcal{C}_i$*, it is said that* p_j constrains *the flow of* t_k *at* $\mathcal{C}_i$*.*

(4) *A* region $\mathcal{R}_i$ *is the convex subset of the reachable markings for which* $\mathcal{C}_i$ *is active:* $\mathcal{R}_i = \{\mathbf{m} \in Class(\mathbf{m}_0) | \mathbf{\Pi}_i\mathbf{m} = \mathbf{enab}(\mathbf{m})\}$ *[Silva et al., 2011]. According to (2.5), within region* $\mathcal{R}_i$*, the flow vector is given by:*

$$\mathbf{f}(\tau) = \mathbf{\Lambda} \cdot \mathbf{enab}(\mathbf{m}(\tau)) = \mathbf{\Lambda}\mathbf{\Pi}_i\mathbf{m}(\tau) \tag{2.7}$$

where $\mathbf{\Lambda}$ *is the diagonal matrix containing the entries of* $\boldsymbol{\lambda}$ *in its main diagonal*[2]*.*

(5) *A* linear mode *of a TCPN system,* Σ_i*, is the LTI system,* $\dot{\mathbf{m}}(\tau) = \mathbf{C}\mathbf{f}(\tau) = \mathbf{C}\mathbf{\Lambda}\mathbf{\Pi}_i\mathbf{m}(\tau)$*, that describes the evolution of the marking inside* $\mathcal{R}_i$*.*

[2]By definition, $\forall \mathbf{m} \in \mathcal{R}_i \cap \mathcal{R}_j$, it holds that $\mathbf{\Pi}_i\mathbf{m} = \mathbf{\Pi}_j\mathbf{m} = \mathbf{enab}(\mathbf{m})$. Thus, it implies that $\mathbf{f}(\tau)$ (and therefore, (2.4)) is continuous over $Class(\mathbf{m}_0)$, including the border between regions. This eliminates the possibility of Zeno behavior.

Definition 2.9. *The* T-coverture *of a configuration $\mathcal{C}_i$ is the set of places $\mathcal{TC}_i = \{p \in P | (p, t_j) \in \mathcal{C}_i,\, t_j \in T\}$.*

Regions constitute a partition, except on its borders, of the set of $RS(\mathcal{N}, \mathbf{m}_0)$ [Silva et al., 2011]. The previous concepts are exemplified in the system of Fig. 2.5. It has only two configurations and, at $\mathbf{m}_0$, $\mathcal{C}_2$ is active (the arcs in $\mathcal{C}_2$ are depicted in gray). The evolution of the *unforced* system (*i.e.*, fully uncontrolled) is shown as a dashed line in Fig. 2.6, together with its phase plane and $Class(\mathbf{m}_0)$.

Definition 2.10. *Let $\langle \mathcal{N}, \boldsymbol{\lambda}, \mathbf{m}_0 \rangle$ be a TCPN system. A marking $\mathbf{m}_{ss} \in Class(\mathbf{m}_0)$ that fulfills that $\mathbf{m}_{ss} = \lim_{\tau \to \infty} \mathbf{m}(\tau)$, $\mathbf{m}_{ss} \in \mathcal{R}_s$ and $\dot{\mathbf{m}} = \mathbf{C}\boldsymbol{\Lambda}\boldsymbol{\Pi}_s\mathbf{m}_{ss} = \mathbf{0}$ is named the* steady state *of the system.*

Notice that TCPNs are deterministic systems, thus, given a particular $\mathbf{m}_0$, its steady state marking is unique.

Definition 2.11. *[Silva et al., 2011] Let $\langle \mathcal{N}, \boldsymbol{\lambda}, \mathbf{m}_0 \rangle$ be a TCPN system whose marking evolution converges to the steady state $\mathbf{m}_{ss}$. Let $\mathbf{f}_{ss} = \boldsymbol{\Lambda}\boldsymbol{\Pi}_s\mathbf{m}_{ss}$ be the steady state flow (with $\mathbf{m}_{ss} \in \mathcal{R}_s$). Then:*

- $\langle \mathcal{N}, \boldsymbol{\lambda}, \mathbf{m}_0 \rangle$ *is* timed-live *if* $\mathbf{f}_{ss} > \mathbf{0}$.
- $\langle \mathcal{N}, \boldsymbol{\lambda}, \mathbf{m}_0 \rangle$ deadlocks *if* $\mathbf{f}_{ss} = \mathbf{0}$.

See, for instance, the system in Fig. 2.5 and its evolution from $\mathbf{m}_0$, depicted in Fig. 2.6 (dashed line). The steady state of the system is $\lim_{\tau \to \infty} \mathbf{m}(\tau) = \mathbf{m}_{d1} = [0\ 0\ 3]^T$, which is a deadlock ($\mathbf{f}_{ss} = \boldsymbol{\Lambda}\boldsymbol{\Pi}_1\mathbf{m}_{d_1} = \mathbf{0}$), hence, it is not timed-live. It is worth noticing that *if a CPN is live, then it is live for any timing* [Silva et al., 2011]. Thus, since we work under the assumption that the systems are live and bounded as untimed, as timed they will also be.

2.4 — Controlled Timed Continuous Petri nets

Control actions can be applied to TCPN systems to enforce a desired behavior. They consist of *local reductions of the unforced flow through the transitions* (a transition cannot work faster than its nominal speed).

Definition 2.12. *Transitions in which control actions can be applied are named* controllable. *The set of all controllable transitions is denoted by T_c and the set of* uncontrollable *transitions is $T_{nc} = T \setminus T_c$.*
The selector of controllable transitions *is a $|T| \times |T_c|$ matrix, $\mathbf{S}_c$, s.t., if $t_k \in T_c$, the elementary vector $\mathbf{e}_k$ is a column of $\mathbf{S}_c$ ($\mathbf{e}_k$ is a $|T|$-sized vector of zeros with $[\mathbf{e}_k]_k = 1$). The indices of its columns, $\mathbf{e}_k$, are in ascending order, guaranteeing its uniqueness.*

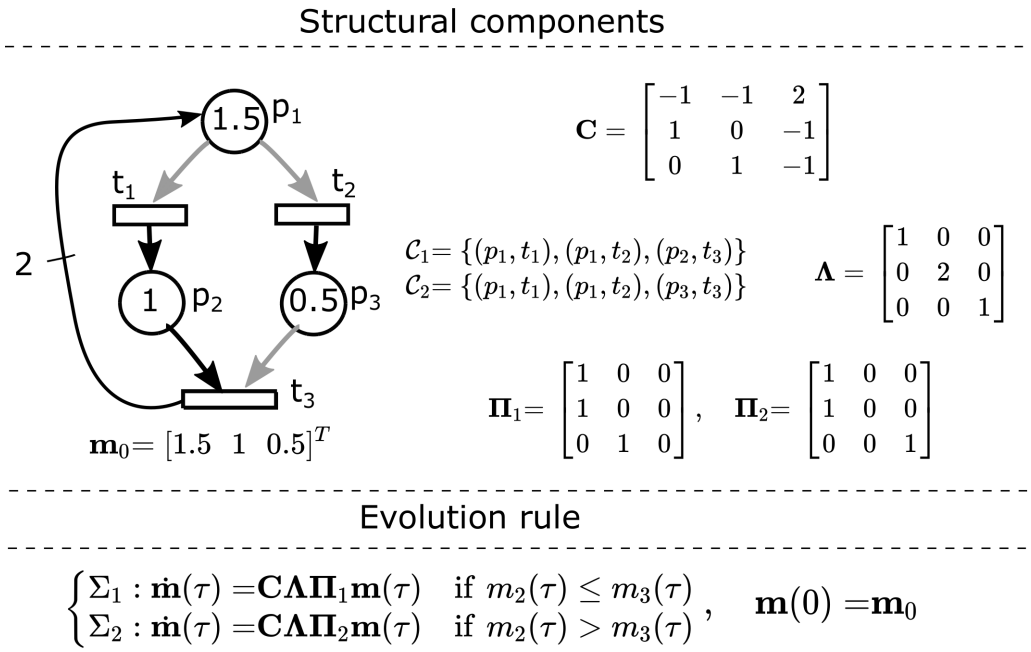

Figure 2.5. A non-live TCPN system. As untimed, it has two reachable dealocks, $\mathbf{m}_{d1} = [0\ 0\ 3]^T$ and $\mathbf{m}_{d2} = [0\ 3\ 0]^T$.

Definition 2.13. *The* control vector $\mathbf{u}(\tau) \in \mathbb{R}^{|T_c|}_{\geq \mathbf{0}}$ *is defined s.t.* $[\mathbf{u}(\tau)]_j$ *represents the control action on the* j*-th element of* T_c *(assuming that its elements are sorted so that their indices are in ascending order). A control vector is called* suitably bounded (SB) *if it fulfills that:* $\mathbf{0} \leq \mathbf{S}_c\mathbf{u}(\tau) \leq \mathbf{f}(\tau)$*. Only, SB control inputs can be applied.*
The effective flow of the controlled system *is given by*

$$\boldsymbol{w}(\tau) = \mathbf{f}(\tau) - \mathbf{S}_c\mathbf{u}(\tau) \tag{2.8}$$

Then, the behavior of a *forced* (or *controlled*) TCPN system, when $\mathbf{m}(\tau) \in \mathcal{R}_i$, is described by:

$$\begin{gathered} \dot{\mathbf{m}}(\tau) = \mathbf{C}\boldsymbol{w}(\tau) = \mathbf{C\Lambda\Pi}_i\mathbf{m}(\tau) - \mathbf{CS}_c\mathbf{u}(\tau), \\ \text{subject to} \quad \mathbf{0} \leq \mathbf{S}_c\mathbf{u}(\tau) \leq \mathbf{\Lambda\Pi}_i\mathbf{m}(\tau) \end{gathered} \tag{2.9}$$

In this work, it will be useful to consider *the evolution of the effective flow*, $\boldsymbol{w}(\tau)$, as a state equation. By taking the time derivative of (2.8), we obtain $\dot{\boldsymbol{w}}(\tau) = \dot{\mathbf{f}}(\tau) - \mathbf{S}_c\dot{\mathbf{u}}(\tau)$, where $\dot{\mathbf{f}}(\tau)$ can be computed by taking the derivative of (2.7) and substituting $\dot{\mathbf{m}}(\tau)$ by (2.9). Thus, the *effective flow system* (EFS) in $\mathcal{R}_i$ is described as:

$$\begin{gathered} \dot{\boldsymbol{w}}(\tau) = \dot{\mathbf{f}}(\tau) - \mathbf{S}_c\dot{\mathbf{u}}(\tau) = \mathbf{\Lambda\Pi}_i\mathbf{C}\boldsymbol{w}(\tau) - \mathbf{S}_c\dot{\mathbf{u}}(\tau), \\ \boldsymbol{w}(0) = \mathbf{\Lambda\Pi}_i\mathbf{m}_0 - \mathbf{S}_c\mathbf{u}(0) \end{gathered} \tag{2.10}$$

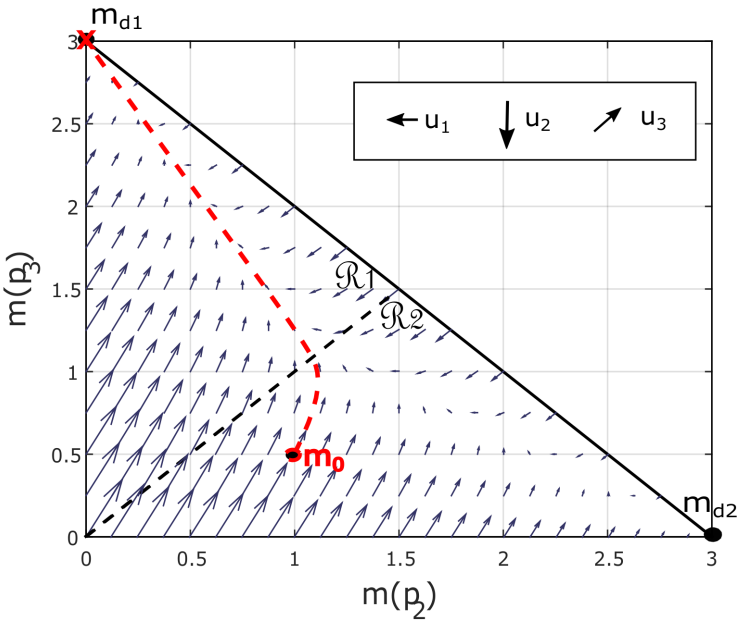

Figure 2.6. Phase portrait of the unforced system in Fig. 2.5, with timing $\boldsymbol{\lambda} = [1\ 2\ 1]^T$. For any initial condition in $Class(\mathbf{m}_0) \setminus \{\mathbf{m}_{d2}\}$, it always reaches the deadlock $\mathbf{m}_{d1}$. As forced, each arrow u_i represent the direction in which the phase portrait may be reoriented by controlling t_i.

2.4.1. Equilibrium markings in TCPNs

From an algebraic point of view, the equilibrium markings of a given TCPN system are the solutions of $\dot{\mathbf{m}} = \mathbf{C}\boldsymbol{\Lambda}\boldsymbol{\Pi}_i\mathbf{m} - \mathbf{C}\mathbf{S}_c\mathbf{u} = \mathbf{0}$ with $\mathbf{m} \in \mathcal{R}_i$ and a SB $\mathbf{u}$.

Definition 2.14. *A marking $\mathbf{m}_q$ for which $\exists \mathbf{u}_q$, SB, such that $\mathbf{C}(\boldsymbol{\Lambda}\boldsymbol{\Pi}(\mathbf{m}_q)\mathbf{m}_q - \mathbf{S}_c\mathbf{u}_q) = \mathbf{0}$ is called an* equilibrium marking. *The set of all equilibrium markings is denoted as $\mathbb{E}$. The set of equilibrium markings in $\mathcal{R}_i$ is $E_i = \{\mathbf{m} \mid \mathbf{m} \in \mathbb{E} \cap \mathcal{R}_i\}$.*

An interesting subset of E_i is the set of equilibrium markings where all the controllable transitions have a positive effective flow:

Definition 2.15. *[Vázquez et al., 2014] The set $E_i^* = \{\mathbf{m}_q \in E_i \mid \forall t_k \text{ in } T_c, 0 < [\mathbf{S}_c\mathbf{u}_q]_k < [\boldsymbol{\Lambda}\boldsymbol{\Pi}_i\mathbf{m}_q]_k\}$ is defined as the set of equilibrium markings at which the direction of all the inputs can be arbitrarily controlled (i.e., all the entries in $\mathbf{u}(\tau)$ can be increased o decreased w.r.t. their value at $\mathbf{u}_q$). The union of the sets E_i^*, in all the regions, is denoted as $\mathbb{E}^*$.*

It is worth noting that, in general, every $\mathbf{m} \in E_i \setminus E_i^*$ contains blocked activities or lies in the border of E_i (i.e., either $u_i^q = \lambda_i enab(t_i, \mathbf{m}^q)$ or $u_i^q = 0$ for some $t_i \in T_c$). Therefore, E_i^* *contains most of the interesting equilibrium markings in $\mathcal{R}_i$.*

The following example illustrates different types of equilibrium markings that can be found in TCPN systems.

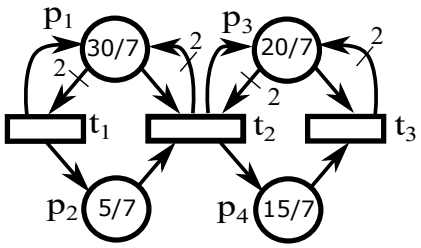

Figure 2.7. A Mono-T-Semiflow System.

Example 2.5. *Consider the TCPN system of Figure 2.7. Let us compute some of its equilibrium markings. For simplicity, let us consider the unforced case, i.e., s.t.* $\mathbf{u} = \mathbf{0}$. *The existence of P-semiflows* $\mathbf{y}_1 = [1\ 1\ 0\ 0]^T$ *and* $\mathbf{y}_2 = [0\ 0\ 1\ 1]^T$ *lead to the marking invariants* $[\mathbf{m}]_1 + [\mathbf{m}]_2 = 5$ *and* $[\mathbf{m}]_3 + [\mathbf{m}]_4 = 5$. *Thus, the state space can be represented in two dimensions (Fig. 2.8). Given a configuration* $\mathcal{C}_i$, $\mathbf{m}_q$ *is an equilibrium marking of the i-th mode if it is a solution of:*

$$\begin{bmatrix} \mathbf{C}\boldsymbol{\Lambda}\boldsymbol{\Pi}_i \\ \mathbf{B}_y^T \end{bmatrix} \mathbf{m}_q = \begin{bmatrix} \mathbf{0} \\ \mathbf{B}_y^T \mathbf{m}_0 \end{bmatrix} \tag{2.11}$$

and, it is contained in the corresponding region, $\mathbf{m}_q \in \mathcal{R}_i$. *In other words, not all the solutions of (2.11) are equilibrium markings and, therefore, not all the regions contain equilibria. Solutions can be:*

- *Admissible: As in* $\mathcal{C}_a = \{(p_1, t_1), (p_2, t_2), (p_4, t_3)\}$, *where* $\mathbf{m}_{q1} = [30/7\ 5/7\ 20/7\ 15/7]^T$ *is the solution of (2.11) and is contained in* $\mathcal{R}_a$ *(represented as a red square in Fig. 2.8). In other words,* $\mathbf{m}_{q1}$ *is an equilibrium marking of the system.*
- *Virtual: As in* $\mathcal{C}_c = \{(p_1, t_1), (p_3, t_2), (p_4, t_3)\}$, *where* $\mathbf{m}_{v3} = [6\ -1\ 2\ 3]^T$ *is the solution of (2.11), however, is not contained in* $\mathcal{R}_c$ *(it is not even reachable). Then,* $E_c = \emptyset$. *Notice that* $\mathbf{m}_{v3}$ *influence the dynamics of that region even though it lies outside of it (the phase portrait in region c is oriented towards* $\mathbf{m}_{v3}$*).*
- *Boundary: As in* $\mathcal{C}_d = \{(p_1, t_1), (p_3, t_2), (p_3, t_3)\}$ *where* $\mathbf{m}_{q4} = [0\ 5\ 0\ 5]^T$ *is the solution of (2.11), and it lies in the boundary between* $\mathcal{R}_c$ *and* $\mathcal{R}_e$, *i.e., it is a solution in both regions.*

For the forced case, the analysis of equilibria is carried out in a similar manner. Nevertheless, in this case, more equilibria can be induced by means of an adequate control input. A way of characterizing the sets of equilibrium markings was introduced in the literature, by using a *generator* of equilibrium markings, defined as follows:

Definition 2.16. *[Vázquez et al., 2014] A full column rank matrix* $\mathbf{G}_i$ *is called* Generator *of* $E_i \neq \emptyset$ *if it fulfills the following:*

- $\forall \mathbf{m}_1, \mathbf{m}_2 \in E_i$, *the vector* $(\mathbf{m}_2 - \mathbf{m}_1)$ *is in the range of* $\mathbf{G}_i$ *(it is a linear combination of the columns of* $\mathbf{G}_i$*).*

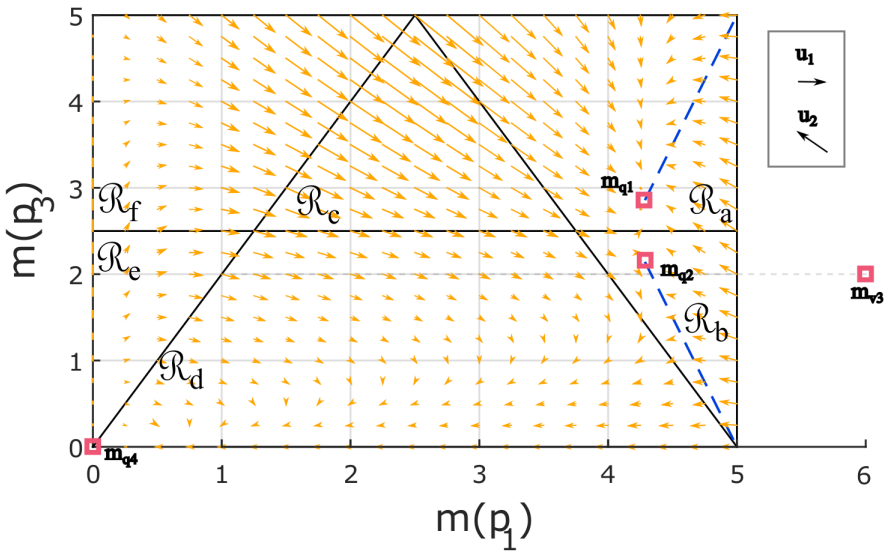

Figure 2.8. Phase portrait of the system with $\boldsymbol{\lambda} = [1\ 3\ 1]$. The equilibrium markings of the unforced system, $\mathbf{m}_{q1}$ and $\mathbf{m}_{q2}$ are depicted as red squares. The equilibrium markings of the forced system with $T_c = \{t_1\}$ are depicted as a dashed blue lines. Clearly, $\mathbb{E}^*$ is not connected.

- $\mathbf{G}_i$ *is minimal (if one of its columns is removed, then the previous statement is false)*

A generator $\mathbf{G}_i$ is a kind of basis of $E_i \neq \emptyset$ (formally speaking, it is not a basis because E_i is not a vector space). By definition, the columns of $\mathbf{G}_i$ are linear combinations of those of $\mathbf{C}$, the incidence matrix, since the span of $\mathbf{G}_i$ is a subspace of the span of $\mathbf{C}$. Algorithm 1 in Vázquez et al. [2014] can be used to compute $\mathbf{G}_i$, given a region.

Example 2.6. *Consider again the TCPN system of Figure 2.7, focusing on the forced case. We can compute the equilibrium markings for this case by using the previous concept. For configuration $\mathcal{C}_a$ a generator for the equilibrium markings in $\mathcal{R}_a$, E_a, can be computed as $\mathbf{G}_a = [-1\ 1\ -3\ 3]^T$ (see Alg. 1 in Vázquez et al. [2014]). In other words, for any pair $\mathbf{m}_1, \mathbf{m}_2 \in E_a$, $(\mathbf{m}_2 - \mathbf{m}_1) \in Img(\mathbf{G}_a)$,* i.e., *all the equilibrium markings lie on one line in the state space (represented by a blue dashed line in Figure 2.8).*

A similar analysis can be done for the b-th region, in which the blue dashed line represents the equilibrium set of the region.

Remark 2.1. *In the literature, it was conjectured that the connectivity of $\mathbb{E}^*$ was always fulfilled [Vázquez et al., 2014]. Unfortunately, as can be seen in the previous counterexample, connectivity of $\mathbb{E}^*$ is not always fulfilled.*

2.5 — Controllability in linear-time invariant systems

As shown in the previous section, each configuration of the TCPN describes a linear system. Thus, some basic concepts that will be useful through this work will be briefly recalled. More detailed information on the subject can be found in Chen [1998].

A linear time invariant system (LTI) $\Sigma(\mathbf{A}, \mathbf{B}, \mathbf{C})$ is represented by

$$\begin{aligned} \dot{\mathbf{x}}(\tau) &= \mathbf{A}\mathbf{x}(\tau) + \mathbf{B}\mathbf{u}(\tau) \\ \mathbf{y}(\tau) &= \mathbf{C}\mathbf{x}(\tau) \end{aligned} \tag{2.12}$$

where $\mathbf{x} \in \mathbb{R}^n$ is the state vector, $\mathbf{u} \in \mathbb{R}^p$ is the control input, $\mathbf{y} \in \mathbb{R}^q$ the output signal, and, $\mathbf{A}$, $\mathbf{B}$ and $\mathbf{C}$ are constant matrices of appropriate dimensions.

Definition 2.17. *A state equation is fully controllable if there exists an input such that for any two states $\mathbf{x}_1$ and $\mathbf{x}_2$ of the state space, it is possible to transfer the state from $\mathbf{x}_1$ to $\mathbf{x}_2$ in finite time.*

Controllability in LTI systems can be decided in a simple way:

Theorem 2.1. *Chen [1998] Given an n-dimensional LTI system (2.12), it is controllable iff any of the following equivalent conditions is satisfied.*

1. *all rows of $e^{\mathbf{A}\tau}\mathbf{B}$ are linearly independent on $[0, \infty)$ over $\mathbb{C}$, the field of complex numbers.*
2. *all rows of $(s\mathbf{I} - \mathbf{A})^{-1}\mathbf{B}$ are linearly independent over $\mathbb{C}$.*
3. *the controllability matrix $Cont(\mathbf{A}, \mathbf{B}) = [\mathbf{B}, \mathbf{AB}, \cdots, \mathbf{A}^{n-1}\mathbf{B}]$ has rank n.*
4. *for every eigenvalue s of $\mathbf{A}$, the complex matrix $[sI - \mathbf{A}, \mathbf{B}]$ has rank n.*

From the linear algebra theory, it is known that a subspace is a vector space that is a subset of some other higher dimension vector space. Furthermore, the dimension of a vector space is equal to the number of linearly independent vectors needed to generate it (i.e., the number of vectors in its basis).

A subspace $\mathcal{V}$ is named A-invariant iff $\mathbf{A}\mathcal{V} \subseteq \mathcal{V}$. A particular case of subspaces are those of dimension one, generated by the eigenvectors. An eigenvector is a non-zero vector $\mathbf{v}$ satisfying

$$\mathbf{A}\mathbf{v} = \beta\mathbf{v} \tag{2.13}$$

i.e., the eigenvector generates an A-invariant subspace of dimension one. The vector $\mathbf{v}$ is said to be an eigenvector of $\mathbf{A}$ associated to the eigenvalue β. Particularly, if $\forall \mathbf{v} \in \mathcal{V}$ it holds that $\mathbf{Av} = \mathbf{0}$, then $\mathcal{V}$ is known as the kernel (or null space) of $\mathbf{A}$, $ker(\mathbf{A})$. In this case, all vectors $\mathbf{v} \in \mathbf{V}$ are eigenvectors associated with the eigenvalue 0.

The next theorem characterizes controllability of a LTI system by means of the eigenvectors of the dynamical matrix.

Theorem 2.2. *[Chen, 1998]* ***Popov-Belevitch-Huatus-(PBH) eigenvector test*** *A pair* $\{\mathbf{A}, \mathbf{B}\}$ *will be non-controllable iff there exist a vector* $\mathbf{q} \neq 0$ *such that*

$$\mathbf{q}^T\mathbf{A} = \lambda\mathbf{q}^T, \quad \mathbf{q}^T\mathbf{B} = \mathbf{0}.$$

In other words, $\{\mathbf{A}, \mathbf{B}\}$ *will be controllable iff there is no left eigenvector of* $\mathbf{A}$ *that is orthogonal to* $\mathbf{B}$*.*

This theorem will be important during the structural characterization of controllability in further chapters.

2.6 — State of the art: Controllability in TCPN systems

Controllability is one of the most important properties of any dynamical system since, in order to impose a particular behavior on the system by means of a control action, we must ensure that it is *controllable*.

The analysis of controllability of TCPNs, however, it is not trivial. It is well-known that checking certain controllability properties, even for very simple piecewise linear systems (the general class of hybrid systems to which TCPNs belong) are undecidable problems [Blondel and Tsitsiklis, 1999, Xu and Xie, 2005]. Despite these pessimistic results, the controllability analysis for these types of systems has received considerable attention. For the particular case of PWA systems, a wide variety of works dealing with this subject can be found in the literature, *e.g.*, Bemporad et al. [2000] and Habets et al. [2006]. The approach from Bemporad et al. [2000] requires the solution of a Mixed-Integer Linear Programming problem (MILP) to determine the controllability of a PWA system; Habets et al. [2006] provided sufficient conditions for *reachability* in PWA systems based on the reachability inside the different polyhedral regions of a system, which can be extended to controllability. These results, however, can only be applied to TCPNs with a small number of state variables since the solution of MILPs is a computationally complex problem and the number of polyhedral regions composing a TCPN grows exponentially in the size of the PN [Silva et al., 2011]. Hence, these results do not provide useful information in general TCPNs.

To deal with that, the study of the controllability for the particular case of TCPNs under ISS has been largely addressed in the literature: Jiménez et al. [2005] where the controllability was studied for Join-Free systems (fully described by a single linear system); Mahulea et al. [2008b] where it was stated that TCPN systems are frequently not controllable in the sense of continuous-state systems due to the existence of state invariants, related to marking conservation laws imposed by P-flows; Vázquez et al. [2014] where controllability was studied for general systems; among others. These works take advantage of the continuous control theory in conjunction with the Petri net theory, thus, obtaining more adequate results for the problem under consideration.

For the particular case of TCPNs, since the state evolution is restricted to $Class(\mathbf{m}_0)$ and the input must be bounded, the classical LTI systems controllability definition cannot be applied. Particularly, the controllability for TCPN systems under ISS has been defined as:

Definition 2.18. *[Vázquez et al., 2014] A TCPN system is bounded input controllable (BIC) over a set of markings $S \subseteq Class(\mathbf{m}_0)$ if, for any $\mathbf{m}_1, \mathbf{m}_2 \in S$, there exists a SB $\mathbf{u}(\tau)$ that transfers the system from $\mathbf{m}_1$ to $\mathbf{m}_2$ in finite or infinite time, and maintains this marking.*

As in any dynamic system, this property is dependent on its parameters, particularly, on *the set of controllable transitions* T_c. Therefore, different cases may arise. In the following sections, we discuss the most recent advances in this subject.

2.6.1. Controllability when all the transitions are controllable

In the case where all the transitions are controllable, the controllability is easily characterized by the following theorem.

Theorem 2.3. *[Vázquez et al., 2014] Let $\langle \mathcal{N}, \boldsymbol{\lambda}, \mathbf{m}_0 \rangle$ be a TCPN system in which all the transitions are controllable. The system is BIC over $Class(\mathbf{m}_0)$ iff the net is consistent and there are no unmarked siphons at any marking in $Class(\mathbf{m}_0)$*

For this case, BIC is independent of the timing and can be verified in polynomial time (Algorithm 2 in Vázquez et al. [2014]). Notice also that in this case the controllability can be seen as "global" since there exists an input that transfers the system between any pair $\mathbf{m}_1, \mathbf{m}_2 \in Class(\mathbf{m}_0)$.

Nevertheless, it is worth noticing that this result is restrictive in the sense that it considers that *all* the transitions are controllable (*i.e.*, that the speed with which all events occur can be reduced). In practice, it is often found that there are events that cannot be controlled. Therefore, we are interested in the general case, where there exist uncontrollable transitions.

2.6.2. Controllability with the presence of uncontrollable transitions

The controllability analysis for this case is generally much more complex. It is well known that controllability over the entire $Class(\mathbf{m}_0)$ cannot be achieved [Vázquez et al., 2014]. The commonly adopted goal for this case is to study controllability over the set of equilibrium markings of the system, which represent the stationary operating points of the modeled plant. This set will be referred to as the *controllability set* of the system.

In other words, when $T_c \subset T$, we are interested in controlling the system over the markings that can be reached and maintained indefinitely by an appropriate input, rather than over the markings that can only be reached in a transitory way. From a practical point of view, this approach is interesting since controllers are frequently designed to drive a system towards a desired operating point, maintaining it indefinitely.

As it will become apparent in the following, this *controllability set* is composed of the equilibrium markings of the system and corresponds to the set $\mathbb{E}^*$. It depends heavily on the set of controllable transitions. Ideally, it would be possible to control the system over all of the equilibrium markings in $\mathbb{E}^*$. However, since TCPN systems are, in general, nonlinear systems with a potentially exponential number of linear modes, the computation of $\mathbb{E}^*$ is not trivial. Hence, dealing with the characterization of controllability directly over $S = \mathbb{E}^*$ is challenging. In the following, we present different approaches to deal with this problem.

Controllability within a single region (Local Controllability)

One way to deal with this problem is by using the approach used in Vázquez et al. [2014], i.e., by characterizing the controllability over the equilibrium markings at each given region ($S = E_i^*$), where the system behaves linearly, in terms of the controllability matrices of the different linear modes.

Definition 2.19. *Given the TCPN, $\langle \mathcal{N}, \boldsymbol{\lambda} \rangle$, and a set T_c, the controllability matrix at configuration $\mathcal{C}_i$ is:*

$$\mathbb{C}_i = [\mathbf{CS}_c \ \mathbf{C\Lambda\Pi}_i\mathbf{CS}_c \ ... \ (\mathbf{C\Lambda\Pi}_i)^{|P|-1}\mathbf{CS}_c] \tag{2.14}$$

Theorem 2.4. *[Vázquez et al., 2014] Let $\langle \mathcal{N}, \boldsymbol{\lambda}, \mathbf{m}_0 \rangle$ be a TCPN system. Consider a region $\mathcal{R}_i$ s.t. $E_i^* \neq \emptyset$ and let $\mathbf{G}_i$ be a generator of E_i^*. The system is BIC over E_i^* iff the columns of $\mathbf{G}_i$ are in the image[3] of $\mathbb{C}_i$.*

The previous theorem characterizes the controllability of the system within a single region.

Definition 2.20. *(Local Controllability) Given a TCPN system, $\langle \mathcal{N}, \boldsymbol{\lambda}, \mathbf{m}_0 \rangle$, it is said to be* locally controllable *at configuration $\mathcal{C}_i$ if it is BIC over E_i^**

[3]The image of a matrix $\mathbf{A}$, $Img(\mathbf{A})$ is the set of all possible linear combinations of its columns.

The main drawback with this approach is that we lose the "global" view of controllability, in which we want to transfer the system between operations points belonging to different regions.

Clearly, local controllability in each region is necessary if we want to extend it to controllability between multiple regions. However, it is not a sufficient condition. As an example, consider the system in Fig. 2.7, from example 2.6. In that system, the only regions where $E_i^* \neq \emptyset$ are $\mathcal{R}_a$ and $\mathcal{R}_b$, corresponding to the configurations $\mathcal{C}_a = \{(p_1, t_1), (p_2, t_2), (p_4, t_3)\}$ and $\mathcal{C}_b = \{(p_1, t_1), (p_2, t_2), (p_3, t_3)\}$ (the other equilibrium markings, such as $\mathbf{m}_{q4}$, are deadlocks and therefore not included in $\mathbb{E}^*$). The corresponding sets, E_a^* and E_b^*, are depicted in Fig. 2.8 by dashed lines. By analyzing the linear modes corresponding to those regions, it can be easily verified that the system fulfills the conditions of Theorem 2.4 and, therefore, is locally controllable in both regions (i.e., it is *locally controllable* in all the regions that contain equilibria). However, the system is not globally controllable since there does not exist a SB input that drives the system from any $\mathbf{m}_a^q \in E_a^*$ to any $\mathbf{m}_b^q \in E_b^*$. This can be observed from Fig. 2.8. The arrow $\mathbf{u}_1$, illustrates the direction in which the phase portrait may be reoriented by means of a SB control input in t_1. Then, it can be seen that any trajectory starting in $\mathcal{R}_a$ stays within the region (cannot be steered), meaning that controllability between both regions is not possible.

Controllability between multiple regions

Fortunately, if the equilibrium sets of multiple regions are *connected*, it is possible to extend the concept of local controllability to *controllability between multiple regions*:

Proposition 2.1. *[Vázquez et al., 2014] Let $\langle \mathcal{N}, \boldsymbol{\lambda}, \mathbf{m}_0 \rangle$ be a TCPN system. Consider some equilibrium sets E_1^*, E_2^*,..., E_j^*, related to different regions $\mathcal{R}_1$, $\mathcal{R}_2$,..., $\mathcal{R}_j$. If the system is BIC over each one and their union is connected, then, the system is BIC over the union.*

Consider the same system of Fig. 2.7 but with $T_c = \{t_2\}$. For this case, Fig. 2.9 depicts in blue dashed lines the different equilibrium sets (controllability set) of the system. In this case, there are equilibrium sets with positive flow in almost all of the regions. Clearly, $\mathbb{E}^*$ can be divided in two connected subsets: $c_1 = E_a^* \cup E_c^* \cup E_f^*$ and $c_2 = E_b^* \cup E_d^*$. It can be easily verified that the system is locally controllable in each region. Then, by proposition 2.1, the system will be controllable over c_1 and c_2, respectively. Let us formalize this:

Definition 2.21. *Let $\langle \mathcal{N}, \boldsymbol{\lambda}, \mathbf{m}_0 \rangle$ be a TCPN system where $\mathbb{E}^*$ is its controllability set. Let ε be the number of* maximal connected subsets[4] *of $\mathbb{E}^*$, $c_1 \cup ... \cup c_\varepsilon = \mathbb{E}^*$. The union of regions of the system, $\mathcal{R}_i \cup \cdots \cup \mathcal{R}_k$, that collectively contain the β-th connected subset, c_β, will be denoted as the β-th* Macro-Region *($\mathcal{MR}_\beta$) of the system.*

To illustrate the previous definition, let's focus on the example of Fig. 2.9. The system in that case has two macro-regions $\mathcal{MR}_1 = \mathcal{R}_a \cup \mathcal{R}_c \cup \mathcal{R}_f$ and $\mathcal{MR}_2 = \mathcal{R}_b \cup \mathcal{R}_d$. The previous

[4]They correspond to the subsets of $\mathbb{E}^*$ that cannot be divided into two disjoint non-empty open subsets.

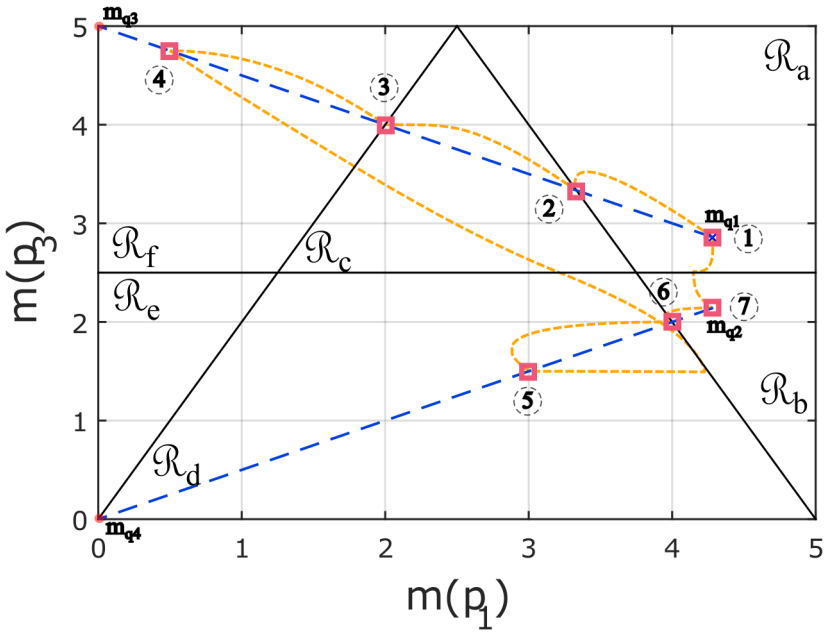

Figure 2.9. Phase plane of the system in Fig. 2.7. The equilibrium sets for the case where $T_c = \{t_2\}$ are depicted as blue dashed lines. Moreover, a particular trajectory of the forced system is depicted as a yellow dashed line. The system is globally controllable.

information can be represented as a graph $\langle V, E\rangle$, where there is a vertex for each configuration whose corresponding region contains equilibria and there is an edge between two vertices if its corresponding sets of equilibrium markings are connected. Let us formally define this.

Definition 2.22. *Let $\langle \mathcal{N}, \boldsymbol{\lambda}, \boldsymbol{\mu}\rangle$ be a TCPN system. Its* connectivity graph *is defined as a graph (V, E) where:*

- *There is a vertex in V, labeled as $\mathcal{R}_i$, if $E_i^* \neq 0$.*
- *There is an edge between vertices $\mathcal{R}_i$ and $\mathcal{R}_j$ if $E_i^* \cap E_j^* \neq \emptyset$.*

Clearly, the strongly connected components of a given connectivity graph represent the macro-regions of the system.

Regarding the controllability of the system and given a macro-region, $\mathcal{MR}_i$, if the system is locally controllable in each region of $\mathcal{MR}_i$, then it is also BIC over the equilibria of the macro-region [Vázquez et al., 2014] (For the given example, with $T_c = \{t_2\}$, the system is BIC over the equilibria in each macro-region).

It is important to note, however, that *connectivity is only a sufficient condition for controllability between different regions.* For instance, in the system of Fig. 2.7, Proposition 2.1 only ensures that the system will be BIC over $\mathcal{MR}_1$ and over $\mathcal{MR}_2$, but not the union. However, in this particular case, the system is also BIC over the union since it is possible to transfer the system from an equilibrium marking in $\mathcal{R}_f$ to another in $\mathcal{R}_d$ (two regions that do not belong

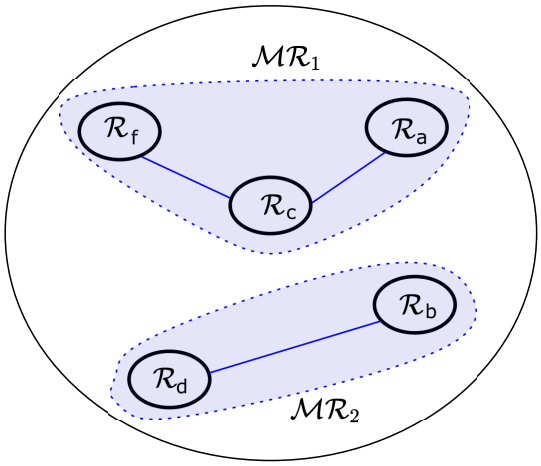

Figure 2.10. Connectivity graph: The partition induced by the connected components of the controllability set of the system in Fig. 2.7.

to the same macro-region). Nevertheless, this is only possible since the dynamics of the system are s.t. its unforced trajectories[5] allow to reach $\mathcal{R}_d$ from an initial condition within $\mathcal{R}_f$ (in Fig. 2.9, this corresponds to the system going from the point 4, to the point 5). In general systems, this is usually not possible for any arbitrary pair of regions (for instance, in the case depicted in Fig. 2.8, where it is not possible to transfer the system from any marking in $\mathcal{R}_a$ to any marking in $\mathcal{R}_b$).

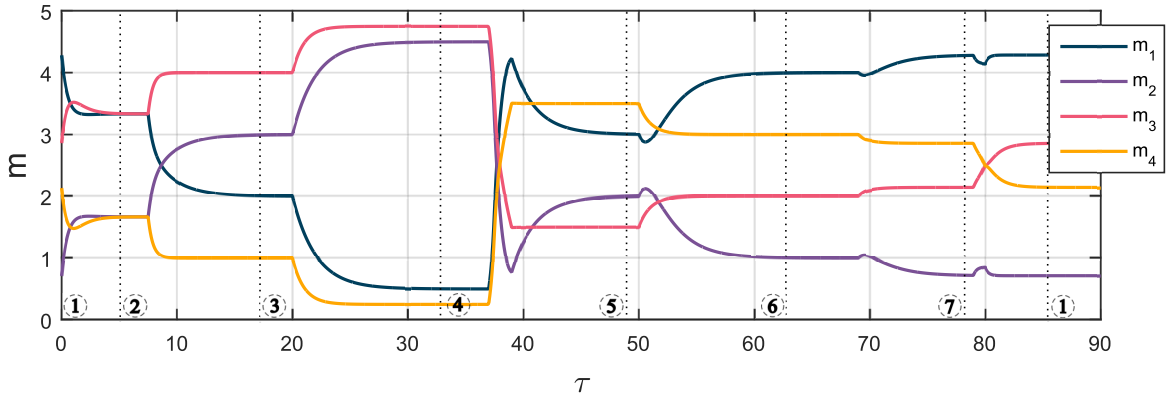

Figure 2.11. The marking trajectory of the system in Fig. 2.7, depicted in the phase plane of Fig. 2.9.

Therefore, although connectivity of $\mathbb{E}^*$ is not necessary for controllability between all the regions with equilibria, it is a desirable property. This is due to the fact that characterizing controllability without considering connectivity of the equilibrium sets is difficult to generalize to general systems. Moreover, it will require a complex analysis of the trajectories of the system,

[5]In the sense of dynamical systems, where a *trajectory* is the set of points in the phase portrait that correspond to the evolution of the system, resulting from a given initial state.

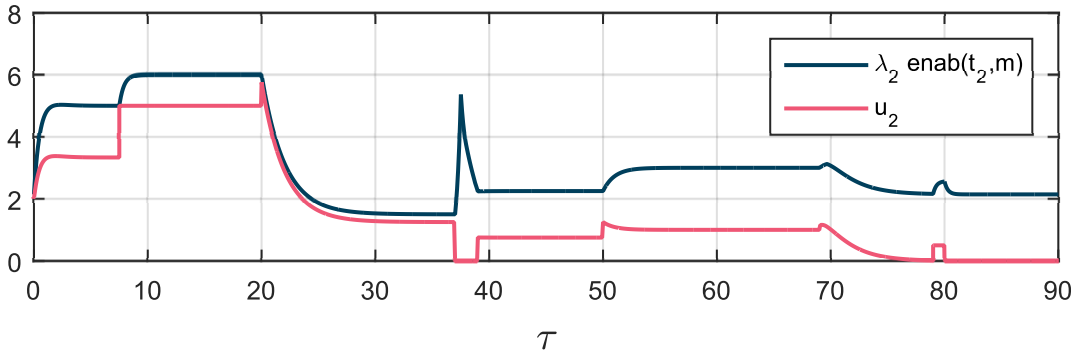

Figure 2.12. The control input, in t_2, applied to the system in Fig. 2.7 to obtain the marking trajectory depicted in the phase plane of Fig. 2.9. Notice that right before the time unit 40, the control input is exactly 0 (unforced) meaning that the trajectory is that of the unforced system.

considering the evolution within multiple regions, whose number can grow exponentially (it can only be performed efficiently in simple examples, with few regions and state variables such as the one in Fig. 2.9). Therefore, we will be working under the following assumption.

Assumption 2.1. *When dealing with the characterization of BIC within multiple regions, the connectivity of the equilibrium sets in the considered regions will be assumed, i.e., controllability will be studied only over the equilibria of each macro-Region in the system (considering all marking trajectories in the macro-Region).*

2.7 — Main objectives

As it has been seen in the previous sections, the current techniques found in the literature for the analysis of the controllability in TCPNs require the study of each of the linear modes of the system, whose number *grow exponentially* with respect to the number of join of transitions in the net (See Def. 2.8). Due to the potentially exponential number of configurations, the complexity of the controllability analysis, from this perspective, also grows exponentially. Therefore, the following topics should be addressed:

• First, a different approach to characterize the controllability in each of the regions should be proposed. In particular, a structural approach to deal with this problem is interesting since the connection between the controllability property and the net structure is not completely understood for systems with uncontrollable transitions. This would help to avoid the analysis by configurations.

• Secondly, in the literature, it was conjectured that the connectivity of the sets of equilibrium markings, within the different regions of the system, was fulfilled for the general case.

However, we have previously demonstrated, by means of a counterexample, that it is not the case. Then, since this is an important property for the controllability analysis over the union of different regions, efficient techniques for the analysis of the connectivity of the controllability sets within multiple regions is required.

• Finally, the control synthesis for systems with uncontrollable transitions should be addressed since the number of works addressing this problem is quite limited.

Taking this into consideration, we propose to address the problem of controllability by using the following approaches:

1. First, it is necessary guarantee that local controllability is fulfilled in all the regions: In order to do this, in the following chapter, we propose a new property named the *net rank-controllability* (NRC), a *structural property* of the TCPN that indicates that the controllability matrices of all the linear modes of the system have the largest possible rank. Then, the relation between NRC and controllability will be studied. More importantly, we will show that this new property can be characterized in terms of *global structural objects* of the net, thus avoiding the analysis by configurations. We will derive conditions for NRC (and, therefore, for BIC) in terms of the structure of the PN.

2. Secondly, it is necessary to provide tools for the computation of the connectivity graph of a given system: we will provide different tools for the analysis and computation of the connectivity graph of a given system, achieving a better performance than the brute force methods used in the literature. This will provide useful information for the analysis of controllability and synthesis of controllers in general TCPN systems with uncontrollable transitions. For instance, to obtain the different regions under which it is possible to operate the system (macro-regions).

3. Finally, we propose a control scheme to optimize the behavior of TCPN systems with the presence of uncontrollable transitions. The scheme is based on an On-Off type control over the firing speed at the controllable transitions that reduce the marking error, i.e., the difference between the desired and actual state of the system. The proposed control law can be computed easily online, despite the complexity of a given system. The effectiveness of the proposed control scheme is studied using simulation results and its use in different case studies.

The first point will be developed in chapters 3 and 4, while the second objective will be developed in chapter 5. Finally, chapter 6 includes the proposal of a control law for the case of systems with uncontrollable transitions. Moreover, we will introduce different case studies to showcase the applicability of the results presented in previous chapters.

Chapter 3

Net Rank-Controllability: A structural approach

3.1 — Introduction

The main contribution of this chapter is presenting a novel property called *net-rank controllability*, which can be related to the study of controllability in TCPNs. We look for its relation with the controllability considering the case of *controllability between multiple regions* and the effects of *liveness* of the TCPN in the study of NRC. In particular, it is shown that NRC is a *sufficient* condition for controllability in *live* TCPN systems.

Moreover, we introduce some preliminary results on how this property is closely related and can be studied from the structure of the Petri net. This chapter, in a way, helps to build the intuition for the structural approach herein developed.

3.2 — Net rank-controllability and its relation to controllability

This section explores the property of *net rank-controllability*, to be used in the structural characterization of controllability. First, let us formally introduce it.

Definition 3.1. *A TCPN is rank-controllable (RC) at configuration $\mathcal{C}_i$ if, given T_c, $rank(\mathbb{C}_i) = |P| - rank(\mathbf{B}_y)$. Moreover, it is net rank-controllable (NRC) if it is RC in every configuration.*

According to (2.14), $rank(\mathbb{C}_i) \leq rank(\mathbf{C}) = |P| - rank(\mathbf{B}_y^T)$. Therefore, NRC is a net level property that indicates that the controllability matrices of all the configurations have the largest possible rank. If a net is NRC, the image of any $\mathbb{C}_i$ is equal to the image of $\mathbf{C}$, thus, $Img(\mathbb{C}_i)$ *includes the difference of any pair of reachable markings.*

Considering the previous, the next proposition states that *under some assumptions, rank-*

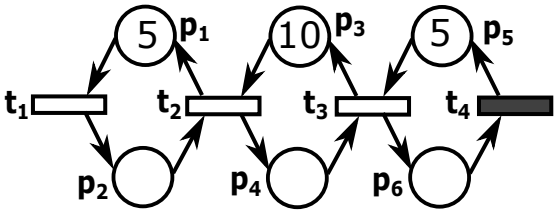

Figure 3.1. Live and bounded TCPN system (thus $\mathcal{N}$ is Cv and Ct) that is BIC over its equilibrium markings but is not NRC.

controllability implies BIC in a single region.

Proposition 3.1. *Let $\langle \mathcal{N}, \boldsymbol{\lambda}, \mathbf{m}_0 \rangle$ be a TCPN system. Consider any region $\mathcal{R}_i$ s.t. $E_i^* \neq \emptyset$. If $\langle \mathcal{N}, \boldsymbol{\lambda} \rangle$ is RC at $\mathcal{C}_i$, then, $\langle \mathcal{N}, \boldsymbol{\lambda}, \mathbf{m}_0 \rangle$ is BIC over E_i^*.*

Proof. Under these assumptions, Theorem 5.6 in Vázquez et al. [2014] states that a *TCPN* is controllable over E_i^* if, for any pair of equilibrium markings $\mathbf{m}_1, \mathbf{m}_2 \in E_i^*$, it is true that $\mathbf{m}_2 - \mathbf{m}_1 \in \text{Img}(\mathbb{C}_i)$. Now, consider any $\mathbf{m}_0, \mathbf{m}_1 \in E_i^*$. From (2.2), any reachable marking $\mathbf{m}_1 - \mathbf{m}_0 \in \text{Img}(\mathbf{C})$. Assuming that the *TCPN* is rank-controllable at $\mathcal{C}_i$, then $\text{Img}(\mathbb{C}_i) = \text{Img}(\mathbf{C})$, therefore $\mathbf{m}_1 - \mathbf{m}_0 \in \text{Img}(\mathbb{C}_i)$, then controllability follows. □

On the contrary, given a $\mathcal{C}_i$, it is not necessary that $\mathbb{C}_i$ has its maximum possible rank for the system to be BIC. Thus, *RC is not a necessary condition for BIC*. The following example illustrates this.

Example 3.1. *Consider the system in Fig. 3.1 with $T_c = \{t_4\}$ and $\boldsymbol{\lambda} = [1\ 1\ 1\ 2]^T$. The net has four configurations. Let us focus on $\mathcal{C}_1 = \{(p_1, t_1), (p_2, t_2), (p_4, t_3), (p_6, t_4)\}$. In this case, the timed net is not NRC at $\mathcal{C}_1$. Moreover, a basis for the equilibrium markings in $\mathcal{R}_1$, E_1^*, can be computed as $\mathbf{G}_1 = [0\ 0\ 0\ 0\ 1\ -1]^T$ (see Alg. 1 in Vázquez et al. [2014]). In other words, for any pair $\mathbf{m}_1^q, \mathbf{m}_2^q \in E_1^*$, $(\mathbf{m}_2^q - \mathbf{m}_1^q) \in Img(\mathbf{G}_1)$, i.e., all the equilibrium markings lie on one line in the state space. Thus, even if $\mathbb{C}_1$ does not cover all the directions ($rank(\mathbb{C}_1) < rank(\mathbf{C})$), it does include $\mathbf{G}_1$ and thus the system is BIC over E_1^* (but not over $\mathcal{R}_1$).*

It is important to note that NRC presents some limitations that must be considered for its use in the study of controllability. Let us explain this by looking at the parallelism with LTI systems. It is well known that a LTI system is controllable (i.e., the system can be driven to any location in the state space) *iff* its controllability matrix has full rank (see, for example, Chen [1998]). Nevertheless, the fact that a TCPN system is RC at $\mathcal{C}_i$ does not imply the reachability of all the markings in $\mathcal{R}_i$ through a SB $\mathbf{u}(\tau)$ (See Example 5.11 in Vázquez et al. [2014]). This is due to the fact that NRC does not considers that, at a given state, the input cannot be chosen arbitrarily (it must be non-negative and upper bounded). Therefore, it is not always possible to guarantee controllability by means of NRC. In particular, in *non-live systems*, *NRC is not a necessary nor sufficient condition for BIC*.

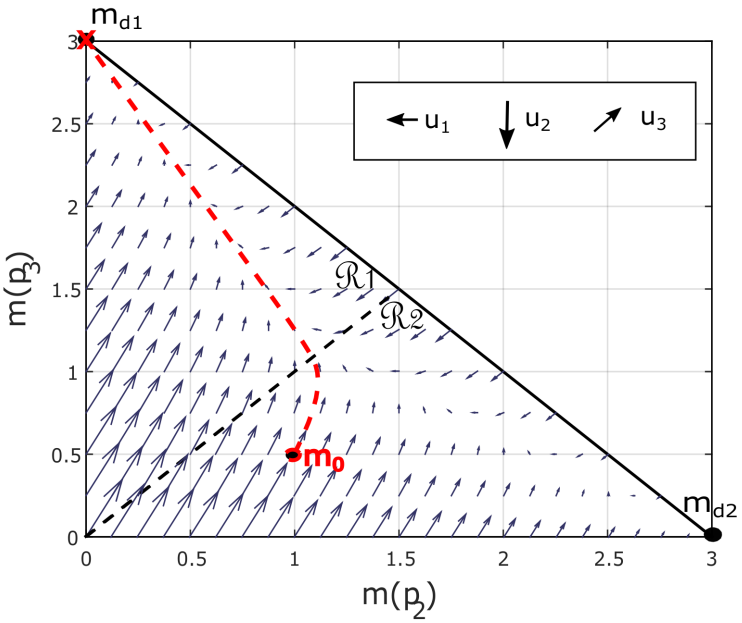

Figure 3.2. Phase portrait of the unforced system in Fig. 2.5, with timing $\boldsymbol{\lambda} = [1\ 2\ 1]^T$. For any initial condition in $Class(\mathbf{m}_0) \setminus \{\mathbf{m}_{d2}\}$, it always reaches the deadlock $\mathbf{m}_{d1}$. As forced, each arrow u_i represent the direction in which the phase portrait may be reoriented by controlling t_i.

Example 3.2. *Consider the Cv and Ct TCPN system in Fig. 2.5 with* $\boldsymbol{\lambda} = [1\ 2\ 1]^T$ *and* $T_c = \{t_1\}$. *The existence of the P-semiflow* $\mathbf{y} = [1\ 1\ 1]^T$ *leads to the marking invariant* $[\mathbf{m}(\tau)]_1 + [\mathbf{m}(\tau)]_2 + [\mathbf{m}(\tau)]_3 = 3$, *thus, its* $Class(\mathbf{m}_0)$ *can be represented in two dimensions (Fig. 3.2).*
The phase portrait of the unforced system ($\mathbf{u} = \mathbf{0}$*) is also shown in the Fig. 3.2. In this case,* $\mathbb{E} = \{\mathbf{m}_{d1}, \mathbf{m}_{d2}\}$ *and it is not timed-live since it always reaches* $\mathbf{m}_{d1}$ *for any initial condition different from* $\mathbf{m}_{d2}$.
Consider the system as forced. For $T_c = \{t_1\}$, *it is NRC. However, due to the constraints on* $\mathbf{u}(\tau)$ *(it has a maximum possible magnitude at each state and it must be non-negative), it is not possible to prevent the system from reaching* $\mathbf{m}_{d1}$ *by controlling* t_1 *(See Fig. 3.2). Moreover, once the system reaches* $\mathbf{m}_{d1}$, *it is not possible to transfer it to any other state through a SB* $\mathbf{u}(\tau)$. *In conclusion, since liveness does not hold, NRC cannot guarantee BIC.*

Nevertheless, for the most interesting case in which the TCPN is live as untimed (timed-live for any $\boldsymbol{\lambda}$), the controllability can be approached using this property as follows:

Theorem 3.1. *Let* $\langle \mathcal{N}, \mathbf{m}_0 \rangle$ *be a live and bounded CPN system. Let* $\boldsymbol{\lambda}$ *be s.t. the timed unforced system reaches the steady state* $\mathbf{m}_{ss}$. *Given* T_c, *if* $\langle \mathcal{N}, \boldsymbol{\lambda} \rangle$ *is NRC, then,* $\langle \mathcal{N}, \boldsymbol{\lambda}, \mathbf{m}_0 \rangle$ *is BIC over* $\mathbb{E}^*_{ss}$, *where* $\mathbb{E}^*_{ss}$ *is the largest connected subset of* $\mathbb{E}^*$ *that contains* $\mathbf{m}_{ss}$.

Proof. Assume that $\mathbf{m}_{ss} \in \mathcal{R}_i$. Since $\langle \mathcal{N}, \mathbf{m}_0 \rangle$ is live, $\mathbf{m}_{ss}$ is a live equilibrium marking, *i.e.*,

$\mathbf{m}_{ss} \in E_i^*$. Moreover, since $\langle \mathcal{N}, \boldsymbol{\lambda} \rangle$ is NRC, the system is BIC over E_i^* (Prop. 3.1). Additionally, if the set E_i^* reaches the border of some other region $\mathcal{R}_j$, the system is also BIC over the union $E_i^* \cup E_j^*$ (Prop. 6.1 in Vázquez et al. [2014]). The same reasoning can be applied until the sets of equilibrium markings reach the border of $Class(\mathbf{m}_0)$ or no new region is reached. Thus, BIC holds over the set of all the equilibrium markings that are connected to $\mathbf{m}_{ss}$. □

It is worth noticing that theorem 3.1 does not guarantee BIC over the entire controllability set, $\mathbb{E}^*$, as connectivity of $\mathbb{E}^*$ in general systems is not always fulfilled. Consequently, the characterization of the equilibrium markings is also required for a complete characterization of BIC in TCPN systems. This will be formally addressed in chapter 5.

Up to this point, the analysis by configurations of BIC has not been avoided. However, in the following we will show that *it is possible to verify NRC without enumerating configurations*, i.e., conditions for BIC can be analyzed without studying all the configurations. Particularly, in the next section, we will introduce the first necessary structural condition for NRC, known as the *influence of controllable transitions*. This property helps to build intuition regarding the connection between the structure of the Petri net and the properties of NRC and controllability.

3.3 — Influence of the controllable transitions

This section is devoted to the analysis of the *influence of the controllable transitions*, a purely structural property of a PN that is closely related to the concept of net rank controllability.

In simpler terms, a node is said to be influenced by the controllable transitions if, regardless of the active configuration, *its marking or flow can be affected by the variations in the effective flow of the controllable transitions*. In order to build some intuition, consider the place transition sequence (Fig. 3.3) with $T_c = \{t_1\}$. Then, the $TCPN$ represented by this sequence becomes rank-controllable. In detail, for $\boldsymbol{\lambda} = [\lambda_1, ..., \lambda_n]^T$, its dynamic equation is described by:

$$\dot{\mathbf{m}} = \begin{bmatrix} -\lambda_1 & 0 & ... & 0 \\ \lambda_1 & -\lambda_2 & ... & 0 \\ \vdots & \vdots & & \vdots \\ 0 & 0 & \lambda_{n-1} & -\lambda_n \end{bmatrix} \mathbf{m} + \begin{bmatrix} -1 \\ 1 \\ \vdots \\ 0 \end{bmatrix} \mathbf{u} \tag{3.1}$$

and it can be easily verified that the rank of its controllability matrix is equal to the rank of the token-flow matrix.

This observation suggests that if a transition is controllable, then its control action *influences* over the marking of the places downstream in a sequence. However, the presence of join transitions or other structural objects may stop the influence propagation in some configurations. See, for instance, the net depicted in Fig. 3.4.a). In this system, if $T_c = \{t_1\}$, then the

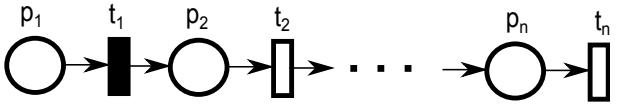

Figure 3.3. Place transition sequence.

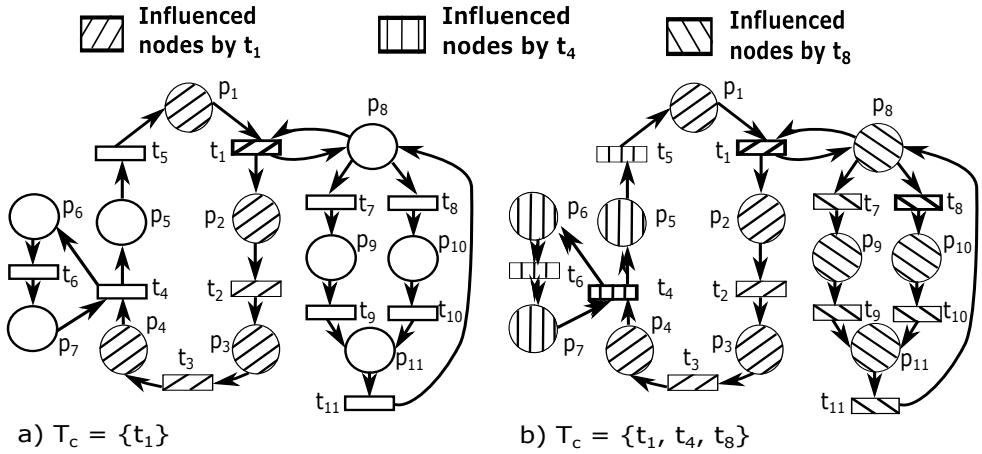

Figure 3.4. Influence of the controllable transitions: a) Influence of t_1 is stopped at the join transition t_4 and the self-loop place p_8. b) In this case, influence of $\{t_1, t_4, t_8\}$ is total.

markings in p_1, p_2, p_3 and p_4 can be influenced. For instance, the marking at p_2 is described by $\dot{m}_2 = w_1 - \lambda_2 m_2$, where w_1 is the effective (controlled) flow of transition t_1. Thus m_2 can be controlled by means of w_1. Moreover, the flow at t_2 is given by $f_2 = \lambda_2 m_2$, thus f_2 can be controlled by means of controlling m_2. The same occurs for p_1, p_3 and p_4. Now, the flow at transition t_4 and the marking in place p_5 cannot be influenced if p_7 constrains the flow of t_4 since, in such case, the flow at t_4 is given by $f_4 = \lambda_4 m_7$. A similar reasoning is applied to every join transition. Moreover, the marking in place p_8 cannot be influenced since its marking is described by $\dot{m}_8 = f_{11} - (\lambda_7 + \lambda_8)m_8 + (w_1 - w_1) = f_{11} - (\lambda_7 + \lambda_8)m_8$, i.e., any control action in t_1 will not affect its marking evolution since it's only connected through a balanced self-loop.

In other words, a place (transition) is said to be influenced by the control actions if it is always possible to state its marking evolution (its flow) in terms of some control action, in any of the configurations.

3.3.1. Influence definition

Let us formally define this property. First, we present some useful definitions.

Definition 3.2. *Given a net, $\mathcal{N}$, and a configuration, $\mathcal{C}_i$, a* $\mathcal{C}_i$-path, *$\omega = (p_a, t_a, ..., p_s, t_s, p_{s+1})$, is defined as a* directed path *of $\mathcal{N}$ s.t. for any pair of consecutive nodes p_j, t_j in ω, $(p_j, t_j) \in \mathcal{C}_i$.*

Consider again the net in Fig. 3.1 at configuration $\mathcal{C}_1 = \{(p_1, t_1), (p_2, t_2), (p_4, t_3), (p_6, t_4)\}$. Then, $\omega_a = (p_1, t_1, p_2, t_2, p_4)$ and $\omega_b = (p_6, t_4, p_5, t_3, p_3)$ are paths of $\mathcal{N}$ but only ω_a is a $\mathcal{C}_1$-path since in ω_b, the arc $(p_5, t_3) \notin \mathcal{C}_1$.

Influence is a basic structural property of a CPN that is related to NRC. Intuitively, a place (resp. a transition) is *influenced* by T_c if the control may modify its marking (resp. its flow) in any configuration. It depends on the structure of the net, as the following definition indicates.

Definition 3.3. *Let $\mathcal{N}$ be a CPN. Given T_c, a place p_α is* influenced by T_c, *in any configuration, if it is contained in one of the following sets:*

- $A = \{p_\alpha | \exists t_\beta \in ({}^\bullet p_\alpha \cup p_\alpha{}^\bullet),\ t_\beta \in T_c \wedge [\mathbf{C}]_{\alpha,\beta} \neq 0\}$
- $B = \{p_\alpha | \forall t_\beta \in ({}^\bullet p_\alpha \cup p_\alpha{}^\bullet),\ t_\beta \in T_c \wedge [\mathbf{C}]_{\alpha,\beta} = 0\}$ *(balanced self-loops)*
- $C = \{p_\alpha | \forall \mathcal{C}_i$, *there is a $\mathcal{C}_i$-path ω_i from a $p_c \in A$ to p_α, s.t. for any pair of consecutive nodes in ω_i, t_j and p_k,* $[\mathbf{C}]_{k,j} \neq 0\}$.

A transition t is influenced *if $t \in T_c$ or $\forall p \in {}^\bullet t$, p is being influenced. The* set of places (transitions) influenced *by T_c is denoted as P_I (T_I). Influence is* total *if $P_I = P$.*

Example 3.3. *Fig. 3.4 illustrate these notions. First, consider the net in Figure 3.4.a) where $T_c = \{t_1\}$. In that case, $A = \{p_1, p_2\}$ and $C = \{p_3, p_4\}$ (since the $\mathcal{C}_i$-path $\omega = (p_2, t_2, p_3, t_3, p_4)$ exists in all the configurations). Consider any $\mathcal{C}_i$ s.t. p_7 constrains t_4 (*i.e. *$(p_4, t_4) \notin \mathcal{C}_i$). Then, it is not possible to find a $\mathcal{C}_i$-path from any place in A to p_5 in those configurations. Therefore, p_5 is not influenced. Similarly for p_6, p_7. Place p_8 is a self-loop with t_1, thus its marking does not change when the control variations are applied to t_1, stopping the propagation of influence at p_8,* i.e. *it is not transmitted to the rest of the nodes. Then, the only nodes that are influenced in all the configurations are $P_I = \{p_1, p_2, p_3, p_4\}$ and $T_I = \{t_1, t_2, t_3\}$. Clearly, influence depends on T_c. For instance, in the net of Fig. 3.4.b), if $T_c = \{t_1, t_4, t_8\}$, then $P_I = A \cup C = \{p_1, p_2, p_4, p_5, p_6, p_7, p_8, p_{10}\} \cup \{p_3, p_9, p_{11}\}$ and $T_I = T$. Therefore, influence is total.*

Remark 3.1. *Places in sets A and C are influenced by T_c in the sense that the flow variations due to the control are captured as marking variations in these places. Places in set B are added because, although their marking cannot be modified by control variations (they correspond to P-semiflows), they do not stop the propagation of influence since controllable transitions are connected to them.*

3.3.2. Influence verification

The sets of influenced nodes, P_I and T_I, can be computed in polynomial time by using Algorithm 1 . Starting from the nodes that are "directly influenced" by the input, $T_I := T_c$ and $P_I := A \cup B$,

Alg. 1 iteratively constructs P_I and T_I. At each step, a new place p_j (resp. transition t_k) is added to P_I (resp. T_I) if there is a $t_k \in T_I$ such that $[\mathbf{C}]_{j,k} \neq 0$ (resp. if all the input places to t_k are already in P_I). The above procedure is equivalent to verifying the existence of $\mathcal{C}_i$-paths to all nodes in the resulting P_I and T_I, regardless of the configuration. The algorithm ends when no new nodes are discovered (a fixed point is found). The following proposition formalizes this.

Proposition 3.2. *Let $\mathcal{N}$ be a CPN and T_c the set of controllable transitions. Then, Algorithm 1 computes, in polynomial time, the sets of influenced nodes, P_I and T_I, in all the configurations.*

Proof. Notice that the loop of Alg. 1 ends, at most, after $|P| - 1$ iterations. Moreover, the operations from the loop are performed in polynomial time. Then, the previous algorithm computes P_I and T_I in polynomial time. □

Algorithm 1 Sets of influenced nodes by T_c, $\forall \mathcal{C}_i$.

Inputs: **Pre**, **Post** and the set T_c,
Outputs: The sets of influenced nodes, P_I and T_I.

1: **Initialize:** $T_I := T_c$.
2: **compute** $P_I := A \cup B$.
3: **repeat**
4: $\quad T_A := T_I; P_A := P_I;$
5: $\quad T_I := T_A \cup \{t \in P_A{}^\bullet \mid t \notin T_A \wedge {}^\bullet t \subseteq P_A\}$
6: $\quad P_I := P_A \cup {}^\bullet(T_I \setminus T_A) \cup (T_I \setminus T_A)^\bullet$
7: **until** $P_I = P_A$.
8: **return** P_I and T_I.

3.3.3. Influence as a necessary condition for NRC

As a consequence of its definition, if influence is not total, then there exists at least one place p and one configuration $\mathcal{C}_i$ in which the control actions of T_c cannot modify the marking of p. Then, the timed net cannot be NRC. This is formalized in the following proposition.

Proposition 3.3. *Let $\langle \mathcal{N}, \boldsymbol{\lambda} \rangle$ be a TCPN. Given T_c, if $\langle \mathcal{N}, \boldsymbol{\lambda} \rangle$ is NRC, then,* influence is total.

The converse of Prop. 3.3 does not hold. It is because total influence only guarantees that marking variations can be produced by the control inputs in all the places, but it does not ensure that these variations are linearly independent from each other. Next example shows a TCPN where influence is total but NRC is not fulfilled.

Example 3.4. *Consider the TCPN of Fig. 3.4.b). If $T_c = \{t_1, t_4, t_8\}$, influence is total. However, this does not imply NRC. For example, with $\boldsymbol{\lambda} = [1, ..., 1]^T$, $\langle \mathcal{N}, \boldsymbol{\lambda} \rangle$ is not RC at some configurations. For instance, at $\mathcal{C}_a = \{(p_1, t_1), (p_2, t_2), (p_3, t_3), (p_4, t_4), (p_5, t_5), (p_6, t_6), (p_8, t_7), (p_8, t_8), (p_9, t_9), (p_{10}, t_{10}), (p_{11}, t_{11})\}$, where $rank(\mathbb{C}_a) = |P| - rank(\mathbf{B}_y^T) - 1 < rank(\mathbf{C})$,* i.e., $\exists \boldsymbol{v}$

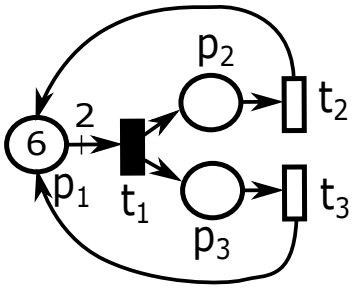

Figure 3.5. Join Free TCPN system with $T_c = \{t_1\}$. Influence of t_1 is total, however, the influence over p_2 and p_3 is not *independent* since it influence its marking evolution in the exact same amount.

s.t. $\boldsymbol{v}^T\mathbb{C}_a = \mathbf{0}$ *that is not a P-semiflow. For this particular case,* $\boldsymbol{v} = [0\ 0\ 0\ 0\ -1\ 1\ 0\ 0\ 0\ 0\ 0]^T$. *In other words,* $[\mathbf{m}(\tau)]_5 = [\mathbf{m}(\tau)]_6$ *is an* uncontrollable marking invariant *(that only appear in the system as timed); thus, the timed net is not RC at* $\mathcal{C}_a$.

Let us consider a simpler example to visualize the effects of a *non-independent influence* over the marking evolution of the system.

Example 3.5. *Consider the Join Free TCPN of Fig. 3.5 (only one configuration,* $\mathcal{C}_1$*). The only P-semiflow of the system leads to the token conservation law* $[\mathbf{m}(\tau)]_1 + [\mathbf{m}(\tau)]_2 + [\mathbf{m}(\tau)]_3 = 6$*, therefore, the marking of the system, as untimed, can only evolve in two dimensions. If* $T_c = \{t_1\}$*, influence is total. However, considering the timing* $\boldsymbol{\lambda} = [2, 1, 1]^T$*,* $\langle \mathcal{N}, \boldsymbol{\lambda} \rangle$ *it is not NRC. By verifying its unique controllability matrix, we can see that* $\exists \boldsymbol{v}$ *s.t.* $\boldsymbol{v}^T\mathbb{C}_1 = \mathbf{0}$ *that is not a P-semiflow. For this particular case,* $\boldsymbol{v} = [0\ -1\ 1]^T$*. In other words,* $[\mathbf{m}(\tau)]_2 = [\mathbf{m}(\tau)]_3$ *is an* uncontrollable marking invariant*. This can be visualized in Fig. 3.6. The flow of* t_1 *is being controlled in an arbitrary way (figure on the right). However, the marking evolution of places* p_2 *and* p_3 *(depicted in the figure on the left) is being influenced by the control of* t_1 *in the exact same way, i.e., the influence over those places is not independent. In fact, the loss of controllability becomes apparent as the evolution of the system's state is restricted to the invariant* $[\mathbf{m}(\tau)]_2 = [\mathbf{m}(\tau)]_3$.

Nevertheless, Alg. 1 can still be used as a quick preliminary step in the NRC analysis. Since the contrapositive of Prop. 3.3 indicates that *if influence is not total, then the net is not NRC*. Alg. 1 may easily discard a large number of non NRC TCPNs. In the following, we will assume that the next condition is fulfilled:

Assumption 3.1. ***Structural Condition 1 (SC1)****: Given* $\mathcal{N}$*, the influence of* T_c *is total.*

The linear dependence between marking variations in different places can be explained by the existence of circuits and some other structural objects that may introduce uncontrollable marking invariants. The next chapter focuses on characterizing their existence polynomially.

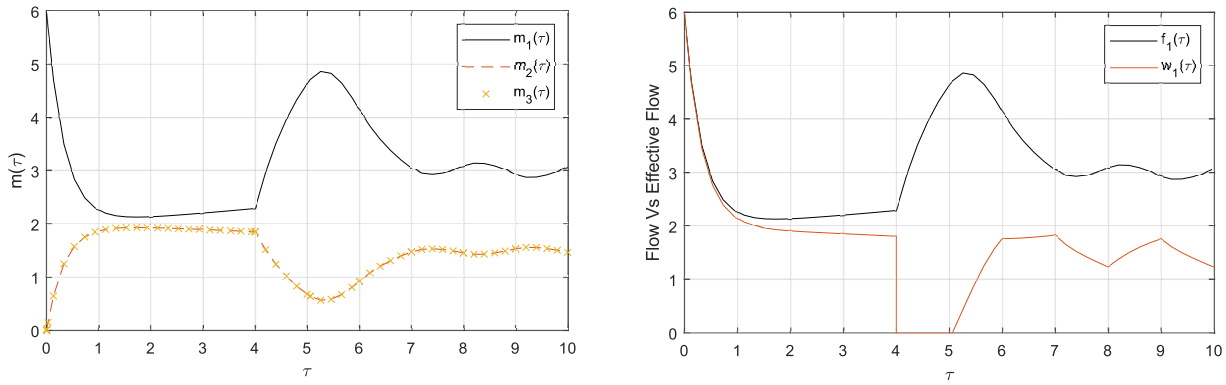

Figure 3.6. In the left, the marking evolution of the forced TCPN in Fig. 3.5 is shown. On the right, the effective (controlled) flow of t_1, $w_1(\tau) = f_1(t) - u(t)$ is shown. Notice that, regarding of the control input variations, the influence over m_2 and m_3 is exaclty the same, i.e., is not independent.

Finally, the next proposition adds an additional result related to influence of the controllable transitions. It states that if influence is total, then all of the conservative components of the system must contain at least one controllable transition.

Proposition 3.4. *Let $\mathcal{N}$ be a conservative CPN. Let P_I be the set of places influenced by T_c and $\mathbf{y}$ be any P-semiflow of $\mathcal{N}$. If $P_I = P$, then, the P-subnet $\mathcal{N}'$, generated by the set $||\mathbf{y}||$, contains at least one controllable transition.*

Proof. Assume that there exists a P-subnet $\mathcal{N}'$ without controllable transitions, generated by a minimal P-semiflow $\mathbf{y}$ of $\mathcal{N}$. Consider any configuration $\mathcal{C}_i$ s.t. $\forall t' \in \mathcal{N}'$, t' is being constrained by a place in $\mathcal{N}'$. Since no transition in $\mathcal{N}'$ is controllable, any direct path from an influenced place to a particular place $p' \in \mathcal{N}'$ contains an arc (p, t) where $t \in \mathcal{N}'$ and $p \notin \mathcal{N}'$, hence, $(p, t) \notin \mathcal{C}_i$. This means that p' is not influenced by T_c (see definition 3.3). Therefore, P_I is a proper subset of P, i.e., $P_I \neq P$, a contradiction. □

The converse of proposition 3.4 does not hold in general nets. See, for instance, the TCPN depicted in Fig. 3.7. It is conservative and it includes a unique minimal P-semiflow, whose associated P-subnet includes a controllable transition, $T_c = \{t_4\}$. However, as seen previously, in such case $P_I = \{p_4, p_5\}$.

3.4 — Concluding remarks

In this chapter, it has been stated that *Bounded Input Controllability* (BIC) *analysis* in TCPN systems, under infinite server semantics, can be studied through the structural property of *net*

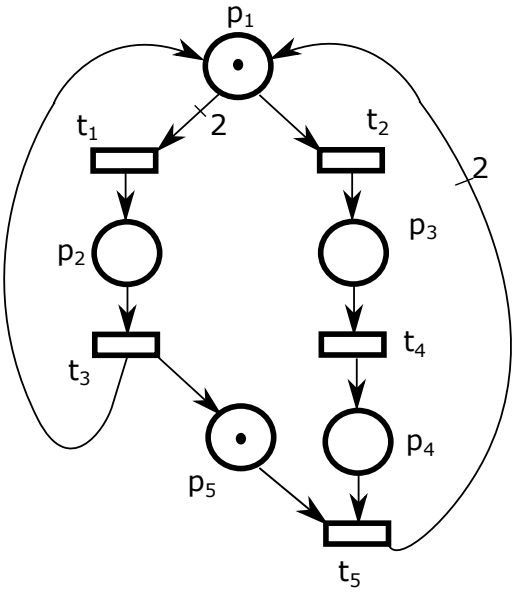

Figure 3.7. Conservative and consistent TCPN with $T_c = \{t_4\}$

rank-controllability (NRC), a *global structural property.*

A relation between NRC and BIC was introduced: *if the system is live as untimed, then, NRC is a sufficient condition for BIC over multiple regions* (Thm. 3.1). Moreover, it has been pointed out that *in non-live systems NRC is not sufficient nor necessary for BIC.*

Then, a first necessary structural condition for *full rank-controllability*, was derived: the control actions must *influence* the marking at all the nodes of the net. This can be verified from the net structure for all the configurations in *polynomial* time.

However, it was established that influence is not a sufficient condition since, even if influence is fulfilled, there might exist a linear dependence between marking variations in different places. This, as will be shown in the next chapter, can be explained by the existence of circuits and some other structural objects that may introduce uncontrollable marking invariants. The next chapter focuses on characterizing their existence polynomially.

Chapter 4

Structural characterization of NRC

4.1 — Introduction

This chapter presents a structural-based approach for analyzing net rank-controllability. The goal is to obtain structural conditions, depending only on the information given by the structure of the net, that guarantee that this property is fulfilled.

In the previous chapter, preliminary results of structural controllability had already been presented, using the concept of influence. However, it has been noted that this property is only a necessary condition for rank-controllability. As explained previously by means of an example, if the TCPN is a place-transition chain and the control has influence over all the nodes, then, it is rank-controllable. However, if circuits and other structural objects are found, marking and flow invariants may be introduced. This may affect the controllability. In such case, the influence is not *independent* on each place, thus it does not imply rank-controllability.

Example 4.1. *Consider the net of Fig. 4.1. In this case,* $P_I = P$ *and* $T_I = T$*. However, this does not imply net rank-controllability. For example, with* $\boldsymbol{\lambda} = [1, ..., 1]^T$*,* $\langle \mathcal{N}, \boldsymbol{\lambda} \rangle$ *is not rank-controllable at some configurations. For instance,* $\mathcal{C}_a = \{(p_{11}, t_1), (p_2, t_2), (p_{13}, t_3), (p_4, t_4), (p_{13}, t_5), (p_7, t_6), (p_{11}, t_7), (p_9, t_8), (p_5, t_9)\}$*, where* $rank(\mathbb{C}_a) = |P| - rank(\mathbf{B}_y^T) - 1$*, i.e.,* $\exists \boldsymbol{v}$ *s.t.* $\boldsymbol{v}^T \mathbb{C}_a = \mathbf{0}$ *and* $\boldsymbol{v} \notin Img(\mathbf{B}_y)$*.*

For this particular case:

$$\boldsymbol{v} = \begin{bmatrix} -2 & 0 & 0 & 0 & -1 & 1 & 0 & -1 & 0 & 0 & 1 & 0 & 0 \end{bmatrix}^T \tag{4.1}$$

In other words, there exists a loss of rank-controllability, and it is related to the marking of the places in $||\boldsymbol{v}|| = \{p_1, p_5, p_6, p_8, p_{11}\}$*.*

From classical control theory, we know that the loss rank-controllability is due to the existence of *uncontrollable marking invariants* (they correspond to the *uncontrollable invariant subspaces* of the system (2.9) [Wonham, 1985]). However, the existence of these invariants cannot be easily associated with any structural object of the net such as P-semiflows, T-

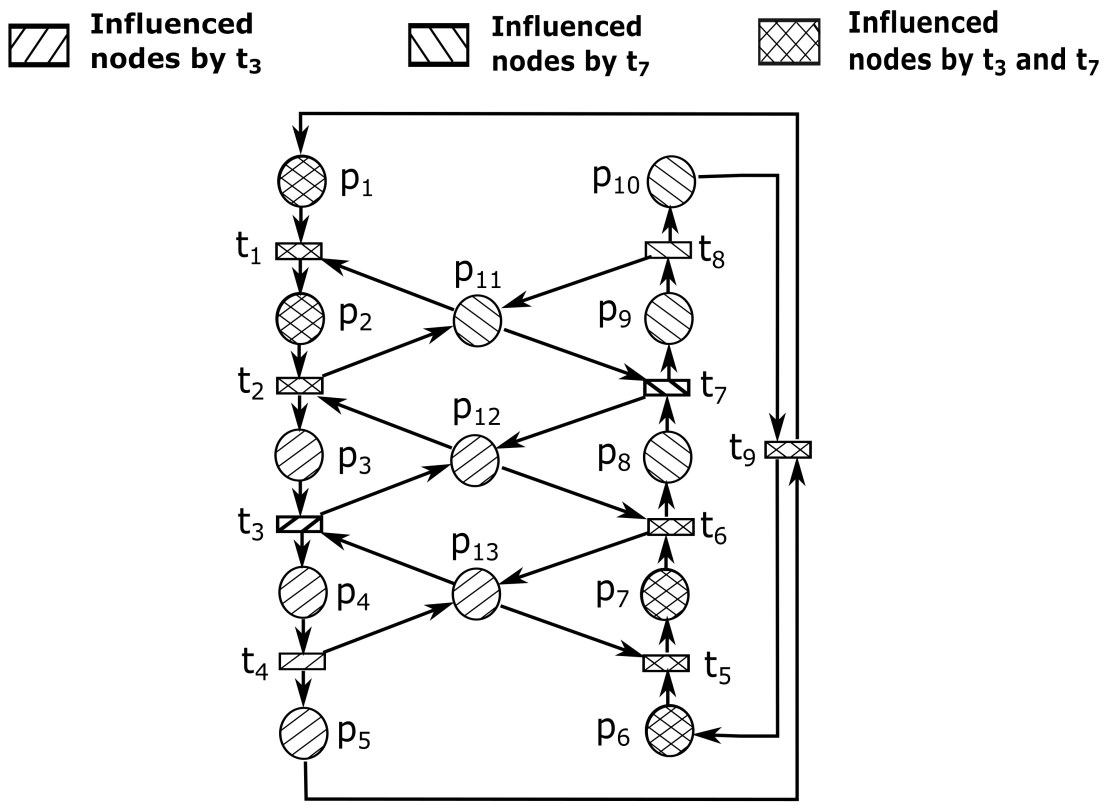

Figure 4.1. Influenced nodes when $T_c = \{t_3, t_7\}$: $P_I = P$ and $T_I = T$.

semiflows, traps, etcetera (as the one in example 4.1, that is not NRC and the uncontrollable marking invariant, involving the marking of places $\{p_1, p_5, p_6, p_8, p_{11}\}$, cannot be associated to any particular structural object of the Petri net).

Nevertheless, as it will be shown in this chapter, the loss of NRC can be explained by the existence of *uncontrollable invariants subspaces* in the *effective flow system* (EFS) (2.10). This concept is considered in this chapter by analyzing the controllability of the EFS by means of its controllability matrix:

$$\mathbb{W}_i = [\mathbf{S}_c \ (\mathbf{\Lambda\Pi}_i\mathbf{C})\mathbf{S}_c \ ... \ (\mathbf{\Lambda\Pi}_i\mathbf{C})^{|T|-1}\mathbf{S}_c] \tag{4.2}$$

Definition 4.1. *Given a TCPN, the corresponding EFS (2.10) is* flow controllable (FC) *at* $\mathcal{C}_i$ *if* $rank(\mathbb{W}_i) = |T|$ *and* net flow-controllable (NFC)*, if it is FC* $\forall \mathcal{C}_i$.

In the forthcoming sections, the existence of uncontrollable invariants subspaces of the EFS will be associated with net structural objects such as P-flows or choice places, among others, thus facilitating the characterization of NFC. Finally, as it will be shown in Theorem 4.2, NFC is a sufficient condition for the NRC (the relation lies in the similarity of the structure of the respective controllability matrices, (2.14) and (4.2)).

4.2 — Uncontrollable invariant subpsaces

Definition 4.2. *Let $\langle \mathcal{N}, \boldsymbol{\lambda} \rangle$ be a TCPN. Consider the EFS at $\mathcal{C}_i$ represented by Eq. (2.10). Given T_c, an* uncontrollable flow invariant (UFI)*, appearing at $\mathcal{C}_i$, is a left eigenvector of the dynamic matrix $\mathbf{\Lambda\Pi}_i\mathbf{C}$ that is orthogonal to $\mathbf{S}_c$. UFIs corresponds to $\boldsymbol{\alpha}$, $\boldsymbol{\beta}$ and $\boldsymbol{\delta}$ in one of the three following disjoint cases:*
(1) $\boldsymbol{\alpha}^T\mathbf{\Lambda\Pi}_i = \mathbf{0} \wedge \boldsymbol{\alpha}^T\mathbf{S}_c = \mathbf{0}$
(2) $\boldsymbol{\beta}^T\mathbf{\Lambda\Pi}_i \neq \mathbf{0} \wedge \boldsymbol{\beta}^T\mathbf{\Lambda\Pi}_i\mathbf{C} = \mathbf{0} \wedge \boldsymbol{\beta}^T\mathbf{S}_c = \mathbf{0}$
(3) $\boldsymbol{\delta}^T\mathbf{\Lambda\Pi}_i\mathbf{C} = \gamma\boldsymbol{\delta}^T$, *where* $\gamma \neq 0 \wedge \boldsymbol{\delta}^T\mathbf{S}_c = \mathbf{0}$

Here, the Popov-Belevitch-Hautus controllability test (PBH test) is used for the characterization of NFC.

Proposition 4.1. *[Chen, 1998] A LTI system $\dot{\mathbf{x}}(\tau) = \mathbf{A}\mathbf{x}(\tau) + \mathbf{B}\mathbf{u}(\tau)$ is controllable iff there is no left eigenvector of $\mathbf{A}$ that is orthogonal to $\mathbf{B}$.*

By definition, any UFI appearing at $\mathcal{C}_i$ is a left eigenvector of the dynamic matrix, $\mathbf{\Lambda\Pi}_i\mathbf{C}$, that is orthogonal to $\mathbf{S}_c$, (cases (1) and (2) are the ones associated to the eigenvalues 0, and case (3) are the ones associated to the non-zero eigenvalues). Thus, in accordance with the PBH test, its existence leads to a loss of FC. For example, consider a system evolving in region $\mathcal{R}_i$, in which it exhibits an UFI of case (1), $\boldsymbol{\alpha}$. By premultiplying the effective flow by $\boldsymbol{\alpha}$ we obtain $\boldsymbol{\alpha}^T\boldsymbol{w}(\tau) = \boldsymbol{\alpha}^T\mathbf{\Lambda\Pi}_i\mathbf{m}(\tau) - \boldsymbol{\alpha}^T\mathbf{S}_c\mathbf{u}(\tau) = \mathbf{0}$, which can be interpreted as that the weighted sum of the effective flow in some transitions remain constant while the system evolves in $\mathcal{R}_i$, regardless of the control actions. Thus the flow of these transitions cannot be independently controlled.

UFIs can be classified into two different categories, depending on the conditions for their existence:
• Since $\mathbf{\Lambda}$ is a diagonal matrix (thus, it has full rank), the existence of the UFIs of cases (1) and (2) depends only on T_c and on the kernels of matrices $\mathbf{\Pi}_i$ and $\mathbf{\Pi}_i\mathbf{C}$, respectively, *i.e.* purely structural conditions. Therefore, the UFIs corresponding to these cases are named *uncontrollable structural flow invariants* (USFIs).
• In case (3) the existence of the invariant depends also on the value $\mathbf{\Lambda}$, i.e., they depend on the timing of the net. Then, UFIs corresponding to case (3) are named *uncontrollable timed flow invariants* (UTFIs).
In the following, conditions that will guarantee the non-existence of UFIs in any configuration are stated in terms of some structural objects of the net.

4.3 — Structural characterization of UFIs

In this section we stablish structural conditions (in terms of the Petri net structure) for the non-existence of UFIs of the EFS. First, for the case of structural UFIs and then for the case of timed UFIs.

4.3.1. Uncontrollable structural flow invariants

First, let us show that the existence of choice places may generate USFIs of case (1). An USFI of case (1), $\boldsymbol{\alpha}$, is said to be generated by the choice place, p_c, if $||\boldsymbol{\alpha}|| \subseteq p_c^\bullet$.

Example 4.2. *In the TCPN of Fig. 4.1, with $T_c = \{t_3, t_7\}$, it can be seen that, in any configuration s.t. $(p_{12}, t_2), (p_{12}, t_6) \in \mathcal{C}_i$, $\exists \boldsymbol{\alpha}$ s.t. $\boldsymbol{\alpha}^T \boldsymbol{\Lambda}\boldsymbol{\Pi}_i = \mathbf{0}$ and $\boldsymbol{\alpha}^T \mathbf{S}_c = 0$,* i.e., *an UFI of case (1) : $\boldsymbol{\alpha} = [0\ 1/\lambda_2\ 0\ 0\ 0\ -1/\lambda_6\ 0\ 0\ 0]^T$. This is due to the fact that, in any of those configurations, p_{12} constrains the uncontrollable transitions t_2 and t_6, thus, $[\boldsymbol{w}(\tau)]_2 = \lambda_2[\mathbf{m}(\tau)]_{12}$ and $[\boldsymbol{w}(\tau)]_6 = \lambda_6[\mathbf{m}(\tau)]_{12} \rightarrow [\boldsymbol{w}(\tau)]_2/\lambda_2 - [\boldsymbol{w}(\tau)]_6/\lambda_6 = 0$,* i.e., *the weighted sum of the effective flow in t_2 and t_6 remains constant as long as the system evolves in $\mathcal{R}_i$, regardless of the control actions. Next proposition formalizes this.*

Proposition 4.2. *Let $\langle \mathcal{N}, \boldsymbol{\lambda} \rangle$ be a TCPN. Let $\mathcal{C}_i$ be the active configuration and p_c be a choice place. There exists at least one USFI of case (1) at $\mathcal{C}_i$, generated by p_c, iff p_c constrains the flow of more than one of its uncontrollable output transitions at $\mathcal{C}_i$.*

Proof. ($\leftarrow$) Rename transitions and places in such a way that $\{t_1, \ldots, t_k\}$ are the output transitions of p_c, that are being constrained by the choice place at $\mathcal{C}_i$, and that p_c is the first place appearing in the token-flow matrix. Hence:

$$\boldsymbol{\Pi}_i = \left[\begin{array}{c|ccc} 1/[\mathbf{Pre}]_{1,1} & 0 & \ldots & 0 \\ \vdots & \vdots & \ddots & \vdots \\ 1/[\mathbf{Pre}]_{1,k} & 0 & \ldots & 0 \\ \hline \mathbf{0} & \multicolumn{3}{c}{\boldsymbol{\Pi}'} \end{array}\right] \tag{4.3}$$

Then, the vectors $\mathbf{a}_1 = [[\mathbf{Pre}]_{1,1}\ -[\mathbf{Pre}]_{1,2}\ 0\ ...\ 0]^T$, ..., $\mathbf{a}_{k-1} = [[\mathbf{Pre}]_{1,1}\ 0 ...\ 0\ -[[\mathbf{Pre}]_{1,k}\ 0\ ...\ 0]^T$ are left annulers of $\boldsymbol{\Pi}_i$. Since $\boldsymbol{\Lambda}$ is a full rank matrix, the system $\boldsymbol{\alpha}_j^T \boldsymbol{\Lambda} = \mathbf{a}_j^T$, $j \in \{1, ..., k-1\}$, has solution. Then $\boldsymbol{\alpha}_j^T \boldsymbol{\Lambda}\boldsymbol{\Pi}_i = 0$. Without loss of generality, consider that t_1 and t_2 are two of the uncontrollable output transitions of p_c (by hypothesis, there are at least two). Then, $\boldsymbol{\alpha}_1^T \boldsymbol{\Lambda}\boldsymbol{\Pi}_i = 0$ and, by definition of $\mathbf{S}_c$, $\boldsymbol{\alpha}_1^T \mathbf{S}_c = \mathbf{0}$. Thus, it follows that there exists at least one $USFI$s of case (1).

($\rightarrow$) Assume that there is an USFI of case (1) at $\mathcal{C}_i$, $\boldsymbol{\alpha}$, generated by p_c. By definition, $\boldsymbol{\alpha}^T \boldsymbol{\Lambda}\boldsymbol{\Pi}_i = \mathbf{0}$ and $\boldsymbol{\alpha}^T \mathbf{S}_c = \mathbf{0}$. Thus, $||\boldsymbol{\alpha}|| \subseteq T_{nc}$ and, since it is generated by p_c, then $||\boldsymbol{\alpha}|| \subseteq p_c^\bullet$.

Since $\mathbf{\Lambda}$ is a full rank matrix, then the left null space of $\mathbf{\Pi}_i$ is not empty. Moreover, by construction (See Eq. (2.6)), the only way that $\mathbf{\Pi}_i$ is not a full row rank matrix is that there exists a place constraining more than one of its output transitions at $\mathcal{C}_i$. Then, $||\boldsymbol{\alpha}||$ contains, at least two elements, *i.e.*, p_c constrains more than one of its uncontrollable transitions at $\mathcal{C}_i$. □

Now, it is shown that USFIs of case (2) are generated when all the places in the support of a P-flow are constraining one of their uncontrollable output transitions.

Example 4.3. *Consider the TCPN in Fig. 4.1.a), where* $T_c = \{t_3, t_7\}$. *Clearly,* $||\mathbf{y}|| = \{p_2, p_9, p_{11}\}$ *is the support of a P-semiflow (*i.e., $[\mathbf{m}(\tau)]_2 + [\mathbf{m}(\tau)]_9 + [\mathbf{m}(\tau)]_{11} =$ *constant holds* $\forall m \in Class(\mathbf{m}_0)$*). Consider any configuration s.t.* $(p_{11}, t_1), (p_2, t_2), (p_9, t_8) \in \mathcal{C}_i$. *Thus all the places in* $||\mathbf{y}||$ *constrain one of their uncontrollable output transition. It can be seen that, in any of those configurations,* $\exists \boldsymbol{\beta}$ *s.t.* $\boldsymbol{\beta}^T \mathbf{\Lambda\Pi}_i \mathbf{C} = \mathbf{0}$, $\boldsymbol{\beta}^T \mathbf{\Lambda\Pi}_i \neq \mathbf{0}$ *and* $\boldsymbol{\beta}^T \mathbf{S}_c = 0$, i.e., *an UFI of case (2):* $\boldsymbol{\beta} = [1/\lambda_1 \ 1/\lambda_2 \ 0 \ 0 \ 0 \ 0 \ 0 \ 1/\lambda_8 \ 0]^T$. *This is due to the fact that, in those configurations,* $[\boldsymbol{w}(\tau)]_1 = \lambda_1 [\mathbf{m}(\tau)]_{11}$, $[\boldsymbol{w}(\tau)]_2 = \lambda_2 [\mathbf{m}(\tau)]_2$ *and* $[\boldsymbol{w}(\tau)]_8 = \lambda_8 [\mathbf{m}(\tau)]_9$. *Thus, the marking invariant can be written as the flow invariant* $[\boldsymbol{w}(\tau)]_1/\lambda_1 + [\boldsymbol{w}(\tau)]_2/\lambda_2 + [\boldsymbol{w}(\tau)]_8/\lambda_8 =$ *constant. The following proposition formalizes this.*

Proposition 4.3. *Let* $\langle \mathcal{N}, \boldsymbol{\lambda} \rangle$ *be a TCPN. Let* $\mathcal{C}_i$ *be the active configuration and* $\mathbf{y}$ *be a P-flow of* $\mathcal{N}$. *There exists at least one USFI of case (2) at* $\mathcal{C}_i$, *generated by* $\mathbf{y}$, *iff* $\forall p \in ||\mathbf{y}||$, p *constrains at least one uncontrollable transition.*

Proof. ($\leftarrow$) Assume that a P-flow $\mathbf{y}_j = \begin{bmatrix} y_1 \cdots y_n \end{bmatrix}^T$ is s.t. $||\mathbf{y}_j|| \subseteq \mathcal{TC}_i$. If $y_k \neq 0$ then the place p_k is constraining the flow of at least one transition in $\mathcal{C}_i$. Without loss of generality name these transitions as $t_a, t_b, ..., t_l \in T_{nc}$. Thus $\pi_{a,k}, \pi_{b,k}, ...\pi_{l,k} \neq 0$ (the entries of matrix $\mathbf{\Pi}_i$). Moreover, at $\mathcal{C}_i$, each transition is constrained by only one place, thus rows of $\mathbf{\Pi}_i$ have only one non-null entry. Hence, there exists scalars $b_1, ..., b_m$ such that

$$[b_1 \ ... \ b_m]\mathbf{\Pi}_i = {\mathbf{y}_j}^T \tag{4.4}$$

Since ${\mathbf{y}_j}^T \mathbf{C} = \mathbf{0}$, then $\mathbf{b}_j = [b_1 \ ... \ b_m]$ is a left annuler of $\mathbf{\Pi}_i \mathbf{C}$. Moreover, matrix $\mathbf{\Lambda}$ has full rank, then

$$\boldsymbol{\beta}_j^T = \mathbf{b}_j^T \mathbf{\Lambda}^{-1} \tag{4.5}$$

is a left annuler of the matrix $\mathbf{\Lambda\Pi}_i \mathbf{C}$ generated by the P-flow $\mathbf{y}_j$. Moreover, by definition of $\mathbf{S}_c$, $\boldsymbol{\beta}_j^T$ is s.t. $\boldsymbol{\beta}_j^T \mathbf{S}_c = \mathbf{0}$. Thus, there exists at least one USFI of case (2) generated by $\mathbf{y}_j$.
($\rightarrow$) By definition, an USFI of case (2) is a vector $\boldsymbol{\beta}^T \mathbf{\Lambda\Pi}_i \mathbf{C} = \mathbf{0}$ s.t. $||\boldsymbol{\beta}|| \subseteq T_{nc}$ and $\boldsymbol{\beta}^T \mathbf{\Lambda\Pi}_i \neq \mathbf{0}$, *i.e.*, $\boldsymbol{\beta}^T \mathbf{\Lambda\Pi}_i = \mathbf{y}^T > \mathbf{0}$, where $\mathbf{y}$ is a P-flow of $\mathcal{N}$. Moreover, $\forall p_j \in ||\mathbf{y}||$, $[\mathbf{y}]_j \neq 0$, which is true iff $\boldsymbol{\beta}^T \mathbf{\Lambda} [\mathbf{\Pi}_i]_{\bullet,j} \neq 0$. More specifically, it is true if $\exists t_k \in T_{nc} \cap p_j^\bullet$ s.t. $[\boldsymbol{\beta}]_k [\mathbf{\Lambda}]_{k,k} [\mathbf{\Pi}_i]_{k,j} \neq 0$. Since $[\mathbf{\Lambda}]_{k,k} \neq 0$, then $[\mathbf{\Pi}_i]_{k,j} \neq \mathbf{0}$, which means that p_j constrains $t_k \in T_{nc}$ at $\mathcal{C}_i$. Since this is true $\forall p_j \in ||\mathbf{y}||$, the results follows. □

Assumption 4.1. • ***Structural Condition 2 (SC2)****: Given $\mathcal{N}$, for all choice place, $p_c \in \{p \in P || p^\bullet| > 1\}$, $p_c^\bullet \subseteq T_c$.*

According to Prop. 4.2, SC2 guarantees the non-existence of USFIs of case (1) in any $\mathcal{C}_i$. Moreover, the following proposition states that, if SC1 also holds, the system will not exhibit USFIs of case (2).

Proposition 4.4. *Let $\langle \mathcal{N}, \boldsymbol{\lambda} \rangle$ be a TCPN. Given T_c, if SC1 and SC2 are fulfilled, then, $\langle \mathcal{N}, \boldsymbol{\lambda} \rangle$ will not exhibit USFIs of case (2) in any configuration.*

Proof. Assume that there is an USFI of case (2) at some $\mathcal{C}_i$. Then, $\exists \mathbf{y}$ of $\mathcal{N}$, s.t. $\forall p \in ||\mathbf{y}||$, p constrains one of its uncontrollable output transitions at $\mathcal{C}_i$. Let $P_y = ||\mathbf{y}||$. P_y contains no choice place, otherwise SC2 is not true, a contradiction. Thus, $\forall p \in P_y$, p constrains its only uncontrollable output transition at $\mathcal{C}_i$. Then, any $\mathcal{C}_i$-path from an influenced place to a place $p \in P_y$ contains an arc (p', t) where $p' \notin P_y$ and $t \in P_y^\bullet$. Therefore, $\forall p \in P_y$, p is not influenced by T_c in all the configurations (see Def. 3.3), which is a contradiction (SC1). □

4.3.2. Uncontrollable timed flow invariants

This section deals with invariants that depend on the net's structure and timing. Let us first introduce an example of this type of invariants.

Example 4.4. *Consider the Join-Free net of Fig. 4.2 with $\boldsymbol{\lambda} = [1\ 1\ 1\ 2\ 3]^T$, where $T_c = \{t_1\}$. It can be easily verified that SC1 and SC2 hold. However, by analyzing the dynamic matrix of the EFS, $\mathbf{\Lambda \Pi}_a \mathbf{C}$, it can be seen that $\exists \boldsymbol{\delta}$ s.t. $\boldsymbol{\delta}^T \mathbf{\Lambda \Pi}_a \mathbf{C} = -\boldsymbol{\delta}^T$ and $\boldsymbol{\delta}^T \mathbf{S}_c = \mathbf{0}$,* i.e.*, an UTFI (case (3)): $\boldsymbol{\delta} = [0\ -1\ 1\ 0\ 0]^T$, meaning that the control input affects the effective flow in t_2 and t_3 in the same proportion, regardless of the initial conditions.*

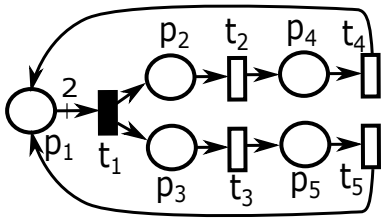

Figure 4.2. A Join-Free TCPN with $T_c = \{t_1\}$. Its only configuration is $\mathcal{C}_a = \{(p_1, t_1), (p_2, t_2), (p_3, t_3), (p_4, t_4), (p_5, t_5)$.

The existence of this type of invariant is difficult to characterize. This section introduces some conditions for the non existence of these flow invariants. First, a necessary condition for the existence of these flow invariants is introduced.

Proposition 4.5. *Let $\langle \mathcal{N}, \boldsymbol{\lambda} \rangle$ be a TCPN. If there exist a configuration $\mathcal{C}_i$ in which an UTFI appears, then, $\mathbf{CS}_c$ has left annulers $\boldsymbol{v}$ s.t. $\boldsymbol{v}^T\mathbf{C} \neq \mathbf{0}$.*

Proof. Assume that there exist a configuration $\mathcal{C}_i$ in which an UTFI appear. Then, $\exists \boldsymbol{\delta}$ s.t. $\boldsymbol{\delta}^T \boldsymbol{\Lambda}\boldsymbol{\Pi}_i\mathbf{C} = \gamma\boldsymbol{\delta}^T$, with $\gamma \neq 0$, and $\boldsymbol{\delta}^T\mathbf{S}_c = \mathbf{0}$. Thus, $\boldsymbol{\delta} = \mathbf{C}^T(\boldsymbol{\Pi}_i^T\boldsymbol{\Lambda}\boldsymbol{\delta})(1/\gamma)$, i.e. $\boldsymbol{\delta} \in \mathrm{Img}(\mathbf{C}^T)$. Hence, $\exists \boldsymbol{v}$ s.t. $\mathbf{C}^T\boldsymbol{v} = \boldsymbol{\delta}$, and ${\mathbf{S}_c}^T\mathbf{C}^T\boldsymbol{v} = 0$. Thus $\boldsymbol{v}^T\mathbf{C}\mathbf{S}_c = \mathbf{0}$, i.e., $\boldsymbol{v}$ is a left annuler. □

According to Prop. 4.5, a necessary condition for the existence of UTFIs is that there exist a left annuler, $\boldsymbol{v}$, of matrix $\mathbf{CS}_c$, s.t., $\boldsymbol{v}^T\mathbf{C} \neq \mathbf{0}$. In other words, the nonexistence of UTFIs can be guaranteed if $ker(\mathbf{C}^T) = ker(\mathbf{S}_c^T\mathbf{C}^T)$, i.e., $rank(\mathbf{C}) = rank(\mathbf{CS}_c)$. Structurally speaking, this condition is equivalent to stating that there is, at most, one uncontrollable transition in each of the minimal T-semiflows of the system. For instance, in MTS-systems, it will be equivalent to state that there is only one uncontrollable transition. This condition, however, might be restrictive in the general case. Therefore, it is necessary to further investigate these invariants from a structural point of view.

In order to do this, under the assumptions SC1 and SC2, a structural sufficient condition that guarantees the non-existence of UTFIs can be stated. Lets consider again the system in example 4.4. In that case, UTFIs appear because there are different *branches* that are affected/influenced by the control in a particular proportion (*branches* are the different directed paths starting in a particular node, as in Fig. 4.3). Then, depending on $\boldsymbol{\lambda}$, UTFIs may appear. This can also be observed from matrix $\mathbb{W}_i$ since the influence of T_c in a particular $\mathcal{C}_i$ (i.e., the influence over the $\mathcal{C}_i$-paths of the configuration) is captured in its columns. For instance, in the previous example, t_1 influences the branches $\omega_1 = (p_1, t_1, p_2, t_2, p_4, t_4)$ and $\omega_2 = (p_1, t_1, p_3, t_3, p_5, t_5)$ and this is captured in the columns generated by the expansion of the control in t_1:

$$\begin{aligned}\mathbb{W}_a &= \begin{bmatrix} \mathbf{S}_c & \mathbf{A}_a\mathbf{S}_c & \mathbf{A}_a^2\mathbf{S}_c & \mathbf{A}_a^3\mathbf{S}_c & \cdots \end{bmatrix} \\ &= \begin{bmatrix} 1 & -\lambda_1 & \lambda_1^2 & * & \\ 0 & \lambda_2 & -\lambda_2(\lambda_1+\lambda_2) & \lambda_2(\lambda_1^2+\lambda_1\lambda_2+\lambda_2^2) & \\ 0 & \lambda_3 & -\lambda_3(\lambda_1+\lambda_3) & \lambda_3(\lambda_1^2+\lambda_1\lambda_3+\lambda_2^3) & \cdots \\ 0 & 0 & \lambda_2\lambda_4 & -\lambda_2\lambda_4(\lambda_1+\lambda_2+\lambda_4) & \\ 0 & 0 & \lambda_3\lambda_5 & -\lambda_3\lambda_5(\lambda_1+\lambda_3+\lambda_5) & \end{bmatrix}\end{aligned} \tag{4.6}$$

where $\mathbf{A}_a = \boldsymbol{\Lambda}\boldsymbol{\Pi}_a\mathbf{C}$ and $*$ represents a non-zero entry.

In the first column, the only non-zero entry is in the 1-st position, meaning that t_1 is the first affected transition, by T_c, in ω_1 or ω_2. At the next expansion, entries 2 and 3 are non-zero since t_2 and t_3 are the next affected/influenced transitions in ω_1 and ω_2. The same reasoning applies to the next expansion, where entries 4 and 5 are non-zero. However, even if all of the nodes are influenced, it can be seen that in the controllability matrix (Eq. (4.6)), rows 2 and 3

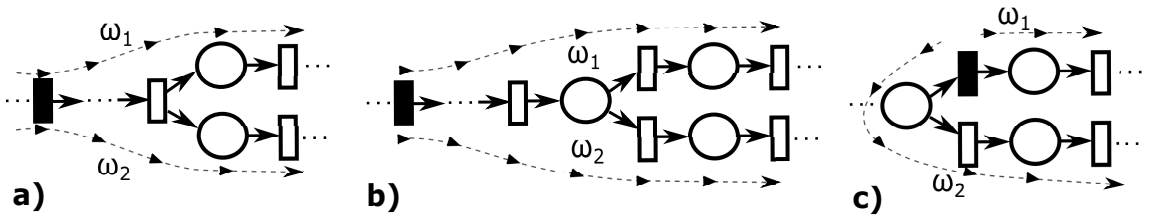

Figure 4.3. The 3 main structures that cause multiple branches to be influenced by T_c in the same proportion.

are linearly dependent (in fact, equal) if $\lambda_2 = \lambda_3$. This means that the control actions will affect the dynamic of the effective flow in t_2 and t_3 in the same proportion, generating the UTFI, $\boldsymbol{\delta}$.

In general, when $\mathbb{W}_i$ is being computed, if a column generates new non-zero entries w.r.t. the previous columns (*i.e.*, if it contains an *innovation*), then it is sure that the rank of $\mathbb{W}_i$ is increased by one. Let us formalize this.

Definition 4.3. *Given a matrix* $\mathbf{X}$*, it is said that a vector* $\mathbf{v}$ *includes* innovation in the information *w.r.t* $\mathbf{X}$ *if* $\exists j$ *s.t.* $[\mathbf{v}]_j \neq 0$ *and* $[\mathbf{X}]_{j,\bullet} = \mathbf{0}$*. The* degree of innovation *of* $\mathbf{v}$ *w.r.t.* $\mathbf{X}$*,* $dI(\mathbf{X}, \mathbf{v})$*, is a function that returns the number of non-zero entries in* $\mathbf{v}$ *that are zero rows in* $\mathbf{X}$*.*

For instance, in Eq. (4.6), $dI(\mathbf{S}_c, \mathbf{A}_a\mathbf{S}_c) = 2$ and $dI([\mathbf{S}_c\ \mathbf{A}_a\mathbf{S}_c], \mathbf{A}_a^2\mathbf{S}_c) = 2$. Then, it is clear that $rank([\mathbf{S}_c,\ \mathbf{A}_a\mathbf{S}_c,\ \mathbf{A}_a^2\mathbf{S}_c]) = 3$. However, since $dI([\mathbf{S}_c\ \mathbf{A}_a\mathbf{S}_c\ \mathbf{A}_a^2\mathbf{S}_c],\ \mathbf{A}_a^3\mathbf{S}_c) = 0$, it is not clear if the rank of $\mathbb{W}_a$ increases by adding the column $\mathbf{A}_a^3\mathbf{S}_c$ since it could be a linear combination of the previous ones.

Structurally speaking, branches affected in the same proportion appear when:

a) T_c influences a fork transition t_f s.t. $|\{t_f{}^\bullet\}^\bullet \cap T_{nc}| \geq 2$.

b) T_c influences an input transition to a choice place with two or more output uncontrollable transitions.

c) There is a controllable output transition, t_c, of a choice place that has at least one uncontrollable output transition and $|\{t_c{}^\bullet\}^\bullet \cap T_{nc}| \geq 1$.

These basic cases are shown in Fig. 4.3. To avoid these structures, an easily verifiable condition that ensures that case **a)** cannot occur is stated below.

Assumption 4.2. • ***Structural Condition 3 (SC3)****: Given* $\mathcal{N}$*, let* $T_F = \{t \in T || t^\bullet| > 1\}$ *be the set of fork transitions. For all* $t_f \in T_F$*, we assume that* $|\{t_f^\bullet\}^\bullet \cap T_{nc}| \leq 1$*.*

Cases **b)** and **c)** are avoided when SC1 and SC2 are fulfilled. Next Lemma states an intermediate result useful to conclude on the rank of matrix $\mathbb{W}_i$, in any $\mathcal{C}_i$.

Lemma 4.1. *Let $\langle \mathcal{N}, \boldsymbol{\lambda} \rangle$ be a TCPN and let $\mathcal{C}_i$ be any configuration. Let T_c be s.t. SC1, SC2 and SC3 are fulfilled. Given a matrix $\mathbf{X}$, composed by columns of $\mathbb{W}_i$, if there is a column $[\mathbb{W}_i]_{\bullet,k}$ s.t. $dI(\mathbf{X}, [\mathbb{W}_i]_{\bullet,k}) > 0$, then there is a column $[\mathbb{W}_i]_{\bullet,j}$ s.t. $dI(\mathbf{X}, [\mathbb{W}_i]_{\bullet,j}) = 1$.*

Proof. Given a configuration $\mathcal{C}_i$, the lemma is proven by showing that it is possible to recursively construct a matrix $\mathbf{X}$ by choosing columns of $\mathbb{W}_i$ s.t. the degree of innovation of each new column, w.r.t. the previous ones, is greater than zero; that is, increase the rank of $\mathbf{X}$ by 1. This procedure is carried out by using Alg. 2 and is used in the proof of Thm. 4.1.

Algorithm 2 Compute a subset of columns of $\mathbb{W}_i$ with innovation w.r.t. each other

Inputs: $\mathbf{S}_c$, $\mathbf{\Lambda \Pi}_i \mathbf{C}$
Outputs: A matrix, $\mathbf{X}$, containing columns of $\mathbb{W}_i$ with innovation w.r.t. each other.

1: **Initialize:** A $|T_c| \times |T|$ array, $\mathbf{Q}$, whose j,k-th entry is $[\mathbf{Q}]_{j,k} = (\mathbf{\Lambda \Pi}_i \mathbf{C})^{k-1} \mathbf{s}_j$, where $\mathbf{s}_j = [\mathbf{S}_c]_{\bullet,j}$.
2: $\mathbf{X} := \mathbf{S}_c$
3: **while** $\exists j,k$ s.t. $dI(\mathbf{X}, [\mathbf{Q}]_{j,k}) > 0$ **do**
4: $\quad \mathbf{v} = \min_{j,k}(dI(\mathbf{X}, [\mathbf{Q}]_{j,k}) > 0)$
5: $\quad$ Update $\mathbf{X} := [\mathbf{X}\ \mathbf{v}]$
6: **end while**

Assume that in the first $k \geq 0$ cycles of the while loop in Alg. 2, entries in $\mathbf{Q}$ with innovation equal to 1 were found. Next, assume that for cycle $k+1$, any entry of $\mathbf{Q}$ with positive innovation is s.t. $dI(\mathbf{X}, [\mathbf{Q}]_{h,j}) \geq 2$. This can only happen if the control expansion reaches two or more branches in the net, *i.e.*, due to the presence of fork transitions or choice places. Without loss of generality, let us consider the case of 2 branches, *i.e.*, two new uncontrollable transitions, t_a and t_b, are discovered in the expansion (the argument is easily extended to the case of n branches). Some cases arise (See Fig. 4.3): **(a)** t_a and t_b are immediate successors of a fork transition. By SC3, this is a contradiction. **(b)** t_a and t_b are immediate successors of a choice place. By SC2, this is a contradiction. **(c)** t_a is the uncontrollable output transition of a choice place p_c and t_b is an immediate successor of one of the controllable output transitions of p_c. By SC2, this is a contradiction. □

Finally, the following theorem generalizes the previous ideas to state *a sufficient structural condition for the non-existence of UTFIs in any configuration.*

Theorem 4.1. *Let $\langle \mathcal{N}, \boldsymbol{\lambda} \rangle$ be a TCPN. Given T_c, if SC1, SC2 and SC3 are fulfilled, then $\langle \mathcal{N}, \boldsymbol{\lambda} \rangle$ will not exhibit UTFIs in any configuration.*

Proof. Let us show that, under these assumptions, $\forall \mathcal{C}_i$, $\mathbb{W}_i$ is a full row rank matrix, *i.e.*, s.t. $\langle \mathcal{N}, \boldsymbol{\lambda} \rangle$ will not exhibit UTFIs in any $\mathcal{C}_i$. Consider any $\mathcal{C}_i$ and the matrix $\mathbf{X} := \mathbf{S}_c$. If $T_c = T$, $rank(\mathbf{X}) = |T| \rightarrow rank(\mathbb{W}_i) = |T| = m$ and the result follows. Otherwise,

$rank(\mathbf{X}) = |T_c| < |T|$ and $\mathbf{X}$ contains $m - |T_c|$ zero rows. By Lemma 4.1, if there is a column $[\mathbb{W}_i]_{\bullet,k}$ having innovation w.r.t. $\mathbf{X}$, then there is at least one column $\mathbf{w}_j = [\mathbb{W}_i]_{\bullet,j}$ s.t. $dI(\mathbf{X}, \mathbf{w}_j) = 1$. Then, $X := [\mathbf{X}\ \mathbf{w}_j]$ and $rank(\mathbf{X}) = |T_c| + 1$. This can be done recursively until no new column can be added to $\mathbf{X}$. Therefore, we only need to prove that if $rank(\mathbf{X}) < m$, there is a column in $\mathbb{W}_i$ that has innovation w.r.t. $\mathbf{X}$. Assume that is not true. Then, there is a set of transitions that cannot be discovered by adding more columns of $\mathbb{W}_i$, *i.e.* there are no $\mathcal{C}_i$-paths from an influenced place to any transition in that set and $T_I \subset T$, a contradiction. Thus, it is possible to form a matrix $\mathbf{X}$ s.t. $rank(\mathbf{X}) = |T|$, and the result follows. □

Example 4.5. *Consider the net of example 4.4 (Fig. 4.2), but with $T_c = \{t_1, t_2\}$. Thus, SC1,...,SC3 are fulfilled. Then, by Thm. 4.1, it does not exhibit any UFI at its unique configuration,* i.e.*, it is NFC. This is because the given T_c ensures that $\mathbb{W}_a$ has full row rank: we can obtain a square matrix, $\mathbf{X}$, composed by columns of $\mathbb{W}_a$, s.t. each column has innovation equal to 1 w.r.t. the previous one:*

$$\begin{aligned}\mathbf{X} &= \begin{bmatrix} \mathbf{S}_c & \mathbf{A}_a\mathbf{s}_{c1} & \mathbf{A}_a\mathbf{s}_{c2} & \mathbf{A}_a^2\mathbf{s}_{c1} \end{bmatrix} \\ &= \begin{bmatrix} 1 & 0 & -\lambda_1 & 0 & \lambda_1^2 \\ 0 & 1 & \lambda_2 & -\lambda_2 & -\lambda_2(\lambda_1+\lambda_2) \\ 0 & 0 & \lambda_3 & 0 & -\lambda_3(\lambda_1+\lambda_3) \\ 0 & 0 & 0 & \lambda_4 & \lambda_2\lambda_4 \\ 0 & 0 & 0 & 0 & \lambda_3\lambda_5 \end{bmatrix}\end{aligned} \tag{4.7}$$

where $\mathbf{s}_{cj} = [\mathbf{S}_c]_{\bullet,j}$. Clearly, $rank(\mathbf{X}) = |T| = 5 \rightarrow rank(\mathbb{W}_a) = |T|$, thus, the timed net cannot exhibit UFIs.

The converse of Thm. 4.1 does not hold. This can be seen from Example 4.4 (Fig. 4.2) in which $T_c = \{t_1\}$ is s.t. SC3 is not fulfilled. However, $\forall \boldsymbol{\lambda}$ s.t. $\lambda_2 \neq \lambda_3$ and $\lambda_4 \neq \lambda_5$, the TCPN does not exhibit UTFIs.

Nevertheless, the advantage of this new approach is that the proposed conditions guarantee the non-existence of UFIs, regardless of the timing, without analyzing any configuration.

4.4 — Structural conditions for net rank-controllability

This subsection relates the structural conditions established in the previous sections with NRC. Up until this point, we have been studying the controllability of the effective flow system (net flow-controllability) by analyzing the existence of its uncontrollable invariant subspaces (UFIs). As will be shown, the controllability of the EFS can be related to the controllability of the TCPN system, establishing in this way a structural approach to characterize the property of NRC. In order to obtain the main result of the section, let us first introduce some intermediate results.

First, the following Lemma establishes the relation between NFC and the previously established structural conditions.

Lemma 4.2. *Let $\langle \mathcal{N}, \boldsymbol{\lambda} \rangle$ be a TCPN. Given T_c, if SC1, SC2 and SC3 are fulfilled, then $\langle \mathcal{N}, \boldsymbol{\lambda} \rangle$ is NFC.*

Proof. Consider any $\mathcal{C}_i$ of $\langle \mathcal{N}, \boldsymbol{\lambda} \rangle$. Since SC1, SC2, and SC3 are fulfilled, by Prop. 4.4 and Thm. 4.1, there are no UFIs at $\mathcal{C}_i$. Now, let us demonstrate that if there are no UFIs in $\mathcal{C}_i$ then, it is FC at the configuration, i.e., $rank(\mathbb{W}_i) = |T|$. Proceeding by contradiction, suppose that there are no UFIs but $rank(\mathbb{W}_i) < |T|$, then there exists $\boldsymbol{v}$ s.t. $\boldsymbol{v}^T \mathbf{S}_c = \mathbf{0}$ and $\boldsymbol{v}^T \mathbb{W}_i = \mathbf{0}$. This last equality means that the flow state equation (2.10) is uncontrollable. Thus, by the PBH test (Proposition 4.1) it follows that $\boldsymbol{v}$ is a left eigenvector of $\boldsymbol{\Lambda\Pi}_i\mathbf{C}$. Moreover, $\boldsymbol{v}^T \mathbf{S}_c = \mathbf{0}$ means that $\boldsymbol{v}$ is orthogonal to the selector of controllable transitions, which implies $||\boldsymbol{v}|| \subset T_{nc}$, then $\boldsymbol{v}$ is an UFI, which is a contradiction. Since this is valid for any configuration, the results follows □

Next, the following proposition states a relation between the rank of the controllability matrix of the TCPN system and the controllability matrix of the effective flow system.

Proposition 4.6. *Let $\langle \mathcal{N}, \boldsymbol{\lambda} \rangle$ be a TCPN. Given a configuration $\mathcal{C}_i$, let*

$$\mathbb{C}_i = \mathbf{C}\boldsymbol{\Psi}_i = \mathbf{C}[\mathbf{S}_c \ \boldsymbol{\Lambda\Pi}_i\mathbf{C}\mathbf{S}_c \ \cdots \ (\boldsymbol{\Lambda\Pi}_i\mathbf{C})^{|P|-1}\mathbf{S}_c]$$

and

$$\mathbb{W}_i = [\mathbf{S}_c \ (\boldsymbol{\Lambda\Pi}_i\mathbf{C})\mathbf{S}_c \ ... \ (\boldsymbol{\Lambda\Pi}_i\mathbf{C})^{|T|-1}\mathbf{S}_c]$$

be the corresponding controllability matrices of the TCPN system and the effective flow system, respectively. Then $rank(\boldsymbol{\Psi}_i) = rank(\mathbb{W}_i)$

Proof. Let us show that $rank(\boldsymbol{\Psi}_i) = rank(\mathbb{W})$, despite the difference in the length of the expansions. First, if $|P| > |T|$ then $\boldsymbol{\Psi}_i$ has more columns than $\mathbb{W}$, but, by the Caley-Hamilton theorem, the columns of $\boldsymbol{\Psi}_i$ associated to the terms with exponents $k > |T|$ are linearly dependent of those columns of $\mathbb{W}$, thus both matrices have the same rank. On the other hand, if $|T| > |P|$, $\mathbb{W}$ has more columns than $\boldsymbol{\Psi}_i$, however, by construction $rank(\boldsymbol{\Lambda\Pi}_i\mathbf{C}) \leq |P|$, then the columns of $\mathbb{W}$ associated to the terms with exponents $k > |P|$ are linearly dependent of those columns in $\boldsymbol{\Psi}_i$, thus both matrices have the same rank. □

Finally, the following theorem relates the derived structural conditions with the NRC of the TCPN.

Theorem 4.2. *Let $\langle \mathcal{N}, \boldsymbol{\lambda} \rangle$ be a TCPN. Given T_c, if SC1, SC2 and SC3 are fulfilled, then $\langle \mathcal{N}, \boldsymbol{\lambda} \rangle$ is NRC.*

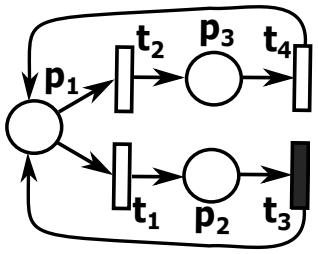

Figure 4.4. Join-Free TCPN with $T_c = \{t_3\}$. It exhibits an USFI of case (1) and it is NRC.

Proof. Consider any $\mathcal{C}_i$. Since SC1,...,SC3 are fulfilled, by Lemma. 4.2, $rank(\mathbb{W}_i) = |T|$ $\forall \mathcal{C}_i$. Thus, by Prop. 4.6, $rank(\mathbf{\Psi}_i) = |T|$. Therefore, since $\mathbb{C}_i = \mathbf{C}\mathbf{\Psi}_i$ and $\mathbf{\Psi}_i$ has full row rank, then rank($\mathbb{C}_i$) = rank($\mathbf{C}$), *i.e.*, the TCPN is RC in $\mathcal{C}_i$. Since this holds $\forall \mathcal{C}_i$, then the TCPN is NRC. □

It is worth noticing that the converse of Thm. 4.2 is not true. We can prove this by means of the following example:

Example 4.6. *Consider the timed net in Fig. 4.4 with* $\boldsymbol{\lambda} = [1 \ \cdots \ 1]^T$ *and* $T_c = \{t_3\}$. *It can be verified that it is NRC. However, SC2 does not hold and there is an USFI of case (1) generated by* p_1*:* $\boldsymbol{\alpha}_1 = [1 \ -1 \ 0 \ 0]^T$.

4.5 — Net rank-controllability verification

In order to guarantee NRC, conditions of Thm. 4.2 must be tested. Algorithm 3 verifies these in polynomial time.

Proposition 4.7. *Let* $\langle \mathcal{N}, \boldsymbol{\lambda} \rangle$ *be a TCPN. Given* T_c*, algorithm 3 verifies if the TCPN is NRC in polynomial time.*

Proof. Line 5 verifies SC1 by means of Alg. 1 in at most $|P| - 1$ steps (Prop. 3.2). *Line 6* checks SC2 by analyzing each choice place in P_C, *i.e.*, in at most $|P_C|$ steps. *Line 7* verifies SC3 by checking each fork transition in T_F, *i.e.*, in at most $|T_F|$ steps. Then, the conditions are verified in, at most, $|P| - 1 + |P_C| + |T_F|$ steps. Since the Algorithm fixes $Flag := 1$ when all the conditions of Thm. 4.2 are verified, then it correctly determines when the TCPN is NRC. □

If algorithm 3 gives $Flag = 0$ as a result, then, it is not possible to conclude if the TCPN is NCR since it tests only sufficient conditions.

Algorithm 3 Test for NRC.

Input: **Pre**, **Post** and T_c.
Output: Variable $Flag = 1$ if the timed net is NRC.
Initialize: $Flag := 0$, $\mathbf{C} := \mathbf{Post} - \mathbf{Pre}$.
Compute the set of fork transitions, T_F; the set of Choice places, P_C.
If given T_c, $P_I = P$ (Alg. 1) **then** (SC1)
  If $\forall p_c \in P_C$, $p_c^\bullet \subseteq T_c$ **then** (SC2)
    If $\forall t_f \in T_F$, $|\{t_f^\bullet\}^\bullet \setminus T_c| \leq 1$ **then** (SC3)
      $Flag := 1$
end of algorithm

4.6 — Illustrative example: A Flexible Manufacturing System

To illustrate the relevance of 4.2 on practical systems, we provide an example of a flexible manufacturing system consisting of two workflows that are attended by a pool of three machines (see Fig. 4.5) [Silva et al., 2014]. A TCPN that models the system is presented in Fig. 4.6.

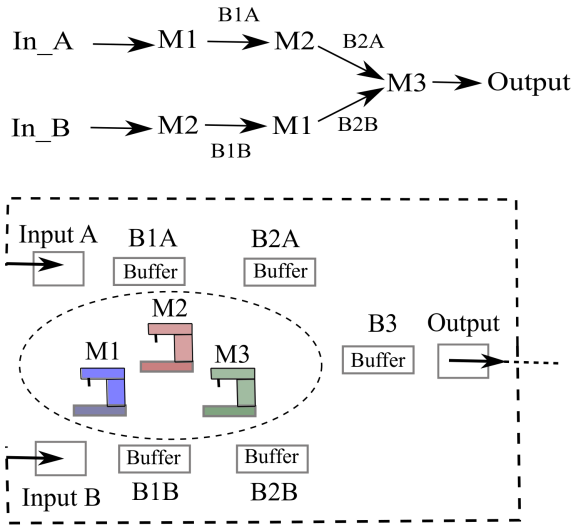

Figure 4.5. Production process of a manufacturing system.

It has 216 configurations and 11 transitions, each one representing one of the following events:

1. Loading of material to the machines $(t_1, t_3, t_5, t_7, t_9)$.
2. Unloading of the processed material to be stored in a buffer $(t_2, t_4, t_6, t_8, t_{10})$.
3. Removing parts from the system output (t_{11}).

Assuming that the machines are always working at their nominal speed (they are released/unloaded as soon as the material is processed), then, $T_{nc} = \{t_2, t_4, t_6, t_8, t_{10}\}$. The rest

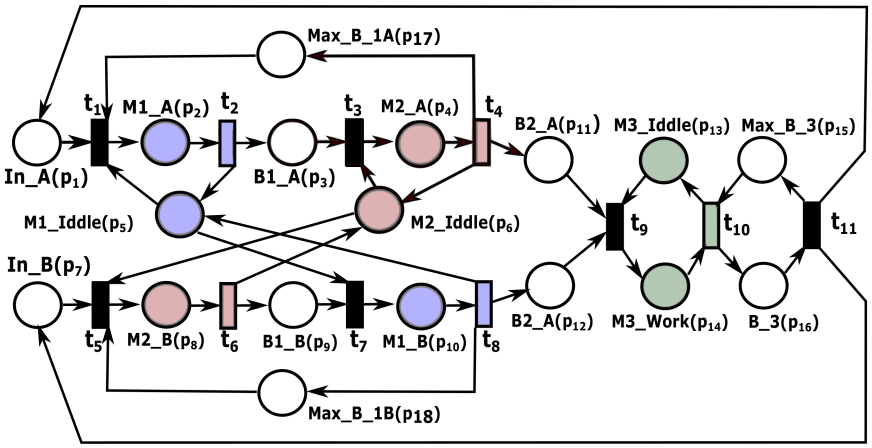

Figure 4.6. TCPN that models the flexible system in Fig. 4.5. The controllable events transitions are depicted in black.

of the events can be controlled since, during the process, it is possible to decide the number of parts to introduce on an available machine and the output buffer can always be emptied, *i.e.*, $T_c = \{t_1, t_3, t_5, t_7, t_9, t_{11}\}$.

It is easy to see that T_c fulfills SC1, SC2, and SC3, then, by Thm. 4.2, it ensures the NRC of the TCPN.

Notice that the previous results are derived *only from information given by the structure of the net, even if the number of configurations grows exponentially.*

Moreover, even though the sets of equilibrium markings of a TCPN system depend on the initial marking, $\mathbf{m}_0$ is not considered here. Nevertheless, by using the presented approach we can conclude that $\forall \mathbf{m}_0$ that marks the support of all the P-semiflows, the system is controllable $\forall \mathcal{C}_i$, over the corresponding sets E_i^* (Thm. 3.1). In contrast, the study of this property by enumerating configurations means that, for each different $\mathbf{m}_0$, a new analysis must be carried out by studying each configuration of the system, which, in general, TCPNs, may become intractable.

4.7 — Concluding remarks

Bounded Input Controllability (BIC) *analysis* in TCPN systems under infinite server semantics with the presence of uncontrollable transitions is a relevant topic from a practical point of view. The current analysis techniques for this property require the study of all the *configurations* of the system, whose number *grows exponentially.* To cope with this, the problem is addressed by studying *net rank-controllability* (NRC), a *global structural property.*

It was demonstrated that *if total influence holds and there are no UFIs, NRC is guaranteed*

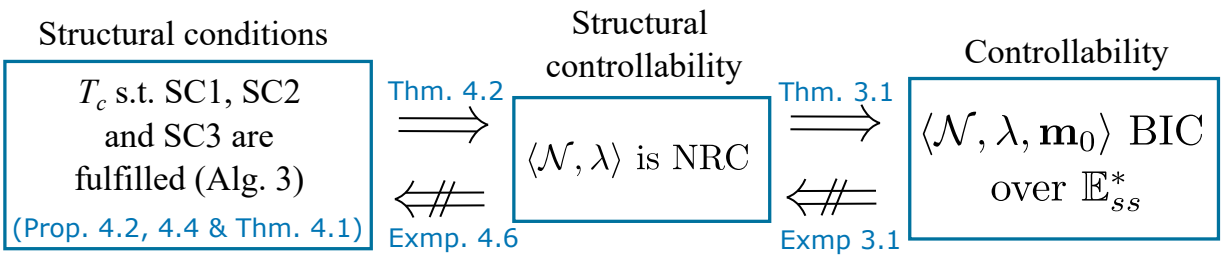

Figure 4.7. Relationships between BIC and the structural controllability concepts in live and bounded TCPN systems.

(Thm. 4.2). Moreover, polynomial-time algorithms for the verification of NRC, and therefore, for the verification of BIC, are provided. These results are summarized in Fig. 4.7.

Chapter 5

Characterization of the controllability sets

As discussed in Chapter 3, the two main problems when addressing controllability in TCPNs are related to the analysis of the rank condition of the controllability matrix of each linear mode and the analysis of the equilibrium markings in the corresponding regions. The former can be addressed by following the structural theory developed in Chapters 4 and 5. On the other hand, this chapter introduces some relevant results to to address the latter.

While analyzing the equilibrium markings of a given system may not always be a prerequisite in the analysis of controllability (according to Thm. 3.1, NRC implies controllability over the different connected sets of equilibrium markings, regardless of the knowledge of these sets) it remains a valuable aspect to explore. Understanding the properties of these equilibrium sets can help in developing control strategies and gaining insights into the particular regions where the system might be controllable. Additionally, ensuring that these equilibrium sets are connected is vital for achieving global controllability (controllability over all of the sets of equilibrium markings).

In order to do this, in this chapter we first deal with the characterization of equilibrium sets and the verification of connectivity for general net systems. In general, a structural approach is difficult to establish since the equilibrium sets depend explicitly on the initial marking distribution (not only on the information of the structure, since, for a particular structure and timing, having a different token load on the system, will generate a different equilibrium set). Nevertheless, we have found that the number of regions to analyze in order to characterize connectivity can be reduced, in general. We show the proposed method in this chapter and we showcase its effectiveness by analyzing different benchmark nets found in the literature.

Moreover, in the second section of the chapter, we particularize some results for subclasses of nets, in which a structural approach can be proposed. We show that in the particular subclasses of nets, connectivity is always fulfilled.

In the sequel we will distinguish between results for a given initial condition $\langle \mathcal{N}, \boldsymbol{\lambda}, \mathbf{m}_0 \rangle$, and results for any initial condition contained in a particular $Class(\mathbf{m}_0)$, denoted as $\langle \mathcal{N}, \boldsymbol{\lambda}, \boldsymbol{\mu} \rangle$,

holding for any $\boldsymbol{\mu} \in Class(\mathbf{m}_0)$. In other words, $\boldsymbol{\mu}$ represents any marking that preserves the same load in the P-semiflows as $\mathbf{m}_0$ (not necessarily the same initial marking of each place). The former represents a single trajectory of the system while the latter considers all the possible trajectories of the system. Let us first introduce the following useful definition.

Definition 5.1. *Given a system* $\langle \mathcal{N}, \boldsymbol{\lambda}, \mathbf{m}_0 \rangle$, $\boldsymbol{\mu} \in Class(\mathbf{m}_0)$ *represents any initial marking that preserves the same token load in the P-semiflows as* $\mathbf{m}_0$. *Therefore, in non-trivial cases,* $\langle \mathcal{N}, \boldsymbol{\lambda}, \boldsymbol{\mu} \rangle$ *represents an infinite set of systems.*

5.1 — Characterization of the controllability set

The main focus of this section will be to provide tools for the computation of the connectivity graph of a given TCPN system. This will provide useful information for the analysis of controllability and synthesis of controllers in general TCPN systems with uncontrollable transitions. For instance, to obtain the different regions under which it is possible to operate the system (macro-regions). Moreover, the connectivity information of the equilibrium sets will be useful for efficiently designing control strategies.

5.1.1. Reducing the number of regions to analyze

The connectivity graph of a given system can be computed by following the naive approach of analyzing all the configurations of the TCPN (*brute force*). The biggest challenge, however, is that the number of regions may grow exponentially as a function of the number of synchronizations of the net. The first contribution of this section is a set of tools and strategies that allow reducing the computational cost of verifying the connectivity of the equilibrium markings in TCPNs.

Let us denote the set of all the configurations of a TCPN as $\mathbb{K}$, and the cardinality of this set by $K = |\mathbb{K}|$. Following the naive approach of analyzing all the configurations to compute the connectivity graph, it is necessary to perform a pairwise analysis of all the elements of $\mathbb{K}$. Therefore, it is necessary to analyze

$$\frac{(K-1)K}{2}$$

pairs.

However, in our experience, we have found that, given an arbitrary TCPN system, the number of regions with equilibria is commonly much smaller than the total number of regions, even in complex systems. Moreover, as will be shown in the rest of the chapter, there is theoretical evidence that indicates that this is very common in subclasses of systems such as TEC-TCPNs. Then, if the number of configurations composing the TCPN under study is

reduced, the complexity of the connectivity analysis can be reduced. Here, by focusing only on a reduced set of configurations associated with the regions with equilibria of the system, we will show that it is possible to reduce the number of pairs to analyze during the verification of connectivity.

Removing implicit arcs

The number of configurations to be analyzed can be reduced by removing the *implicit arcs* of the net. The existence of this kind of object has been studied in the literature (e.g. Recalde et al. [2006]). Let us formally define this object.

Definition 5.2. *Given a CPN system,* $\langle \mathcal{N}, \mathbf{m}_0 \rangle$*, an arc* (p_j, t_k) *of* $\mathcal{N}$ *is named* implicit *if for any* $\mathbf{m} \in Class(\mathbf{m}_0)$*:*

$$\frac{[\mathbf{m}]_j}{[\mathbf{Pre}]_{j,k}} \geq \frac{[\mathbf{m}]_l}{[\mathbf{Pre}]_{l,k}},\ \forall p_l \in {}^\bullet t_k \setminus \{p_j\}$$

From the previous definition and the definition of the configurations in TCPNs, if the arc (p_j, t_k) is implicit, then, for any reachable marking, the place p_j will never be the only place constraining t_k. Let $\mathbb{J} \subseteq \mathbb{K}$ be the set of configurations of the TCPN system that do not contain any implicit arc. Clearly, only the configurations in $\mathbb{J}$ should be considered to compute the connectivity graph since:
1) Any reachable marking that activates a configuration $\mathcal{C}_i$ containing (p_j, t_k) lies on the border of region $\mathcal{R}_i$ with another region $\mathcal{R}_j$ whose corresponding configuration does not contain (p_j, t_k). In other words, it is enough to analyze $\mathcal{C}_j$ and $\mathcal{C}_i$ can be eliminated.
2) Or, no reachable marking activates any configuration containing (p_j, t_k)

Fortunately, it is possible to compute all of the implicit arcs of a given a TCPN system in polynomial time. Algorithm 4 (taken from Recalde et al. [2006]) can be used to compute the implicit arcs of a TCPN.

Algorithm 4 [Recalde et al., 2006] Given a CPN $\langle \mathcal{N}, \mathbf{m}_0 \rangle$, LPP to test if an arc $(p, t) \in \mathcal{N}$ is implicit.

Input: $\langle \mathcal{N}, \mathbf{m}_0 \rangle$ and a particular arc $(p_i, t_j) \in \mathcal{N}$:
Define: $P' = P \setminus \{p_i\}$.
Solve the following LPP:
$z = \min\ \mathbf{y}^T [\mathbf{m}_0]_{P'}$ s.t.
$\mathbf{y}^T [\mathbf{C}]_{P',T} \leq [\mathbf{C}]_{\{p_i\},T}$
$\mathbf{y}^T [\mathbf{Pre}]_{P',\{t_j\}} \geq [\mathbf{Pre}]_{i,j}$
$\mathbf{y}^T \geq \mathbf{0}$
If $[\mathbf{m}_0]_i \geq z \longrightarrow (p_i, t_j)$ is implicit.

Notice that, by definition, if there is at least one implicit arc in the net, the number of configurations in $\mathbb{J}$ is considerably reduced w.r.t. the ones in $\mathbb{K}$. For instance, consider a system

that contains 16 join transitions, each one with only two input places. Thus, it has $2^{16} = 65536$ configurations. Then, if at least one of the input arcs to the join transitions is implicit, the number of configurations in $\mathbb{J}$ will be $2^{15} = 32768$. In other words, the number of configurations to analyze reduces exponentially.

This reduction does not generate a problem while computing the connectivity graph since 1) the regions associated with the eliminated configurations cannot contain equilibria or, 2) said equilibria lie on the border with another region whose corresponding configuration has not been eliminated. Finally, it is important to note that this analysis is performed on the untimed net, i.e., it holds for TCPNs under any timing.

Classification of regions with equilibria

Now, let us make a classification between the configurations that contain equilibria and those that do not. This can be computed by means of Algorithm 5. It includes solving a linear programming problem. If the LPP has a valid solution, then, the configuration contains equilibria.

Algorithm 5 Computing the subset of configurations that contain equilibria.

Input: A TCPN system, $\langle \mathcal{N}, \boldsymbol{\lambda}, \mathbf{m}_0 \rangle$.
Output: A set, $\mathbb{J}'$, containing only the configurations with equilibria.
Initialize: $\mathbb{J}' := \emptyset$.
Compute a positive basis for the P-semiflows of the net, $\mathbf{B}_y$, and the set of all configurations $\mathbb{J}$ with no implicit arc (if there are none, $\mathbb{J} = \mathbb{K}$).
for each $\mathcal{C}_i \in \mathbb{J}$ **do** solve the following LPP
    max ε s.t.
        $\mathbf{B}_y^T(\mathbf{m}_q - \mathbf{m}_0) = \mathbf{0}$
        $\mathbf{C}\boldsymbol{\Lambda}\boldsymbol{\Pi}_i\mathbf{m}_q = \mathbf{C}\mathbf{u}_q$
        $\mathbf{R}_i\mathbf{m}_q \leq \mathbf{0}$
        $\boldsymbol{\Lambda}\boldsymbol{\Pi}_i\mathbf{m}_q - \mathbf{u}_q \geq \varepsilon\mathbf{1}$
        $\mathbf{u}_q[j] \geq \varepsilon$, $\forall t_j \in T_c$
        $\mathbf{u}_q[j] = 0$, $\forall t_j \in T_{nc}$
        $\mathbf{m}_q$, $\mathbf{u}_q$, $\varepsilon \geq \mathbf{0}$
    If there is a $\varepsilon > 0$ **then** $\mathbb{J}' := \mathbb{J}' \cup \{\mathcal{C}_i\}$
end for

As notation: $\mathbf{R}_i$ is the matricial representation of all of the inequalities that define the region $\mathcal{R}_i$. That is, given a join transition of the net, t_j, and the place that constrains t_j at $\mathcal{C}_i$, $(p_k, t_j) \in \mathcal{C}_i$, there are $|{}^\bullet t| - 1$ inequalities that must be fulfilled for any marking in the region:

$$[\mathbf{m}]_k/[\mathbf{Pre}]_{k,j} - [\mathbf{m}]_l/[\mathbf{Pre}]_{l,j} \leq 0,\ \forall p_l \in {}^\bullet t_j \setminus \{p_k\}$$

Each one of the inequalities is expressed in a row of $\mathbf{R}_i$. Clearly, the size of $\mathbf{R}_i$ is $r \times |P|$, where $r = \sum_{\forall t \text{ s.t. } |{}^\bullet t|>1} (|{}^\bullet t| - 1)$.

After using Algorithm 5, we obtain a reduced set $\mathbb{J}'$ of the configurations that contain equilibria ($\mathbb{J}' \subseteq \mathbb{J}$). The cardinality of $\mathbb{J}'$ is potentially smaller than J.

5.1.2. Connectivity verification of the controllability sets

Once the set of configurations with equilibria, $\mathbb{J}'$, has been obtained, we can compute the connectivity of the equilibrium sets over this reduced set. Given a particular configuration $\mathcal{C}_i \in \mathbb{J}'$, it is easy to verify if connectivity is fulfilled with the equilibrium set of a neighboring region, $\mathcal{C}_j \in \mathbb{J}'$, by analyzing if there is an equilibrium point lying in the border of both regions:

Algorithm 6 [Vázquez et al., 2014] Connectivity test between regions $\mathcal{R}_i$ and $\mathcal{R}_j$.

Solve the following LPP
max ε s.t.
  $\mathbf{B}_y^T(\mathbf{m}_q - \mathbf{m}_0) = \mathbf{0}$
  $\mathbf{C}\mathbf{\Lambda}\mathbf{\Pi}_i\mathbf{m}_q = \mathbf{C}\mathbf{u}_q$
  $\mathbf{\Pi}_i\mathbf{m}_q = \mathbf{\Pi}_j\mathbf{m}_q$
  $\mathbf{R}_i\mathbf{m}_q \leq \mathbf{0}$
  $\mathbf{\Lambda}\mathbf{\Pi}_i\mathbf{m}_q - \mathbf{u}_q \geq \varepsilon\mathbf{1}$
  $\mathbf{u}_q[k] \geq \varepsilon$, $\forall t_k \in T_c$
  $\mathbf{u}_q[k] = 0$, $\forall t_k \in T_{nc}$
  $\mathbf{m}_q$, $\mathbf{u}_q$, $\varepsilon \geq \mathbf{0}$
If there is a $\varepsilon > 0$ **then** $E_i^* \cap E_j^* \neq \emptyset$

Based on this, we can establish a procedure to analyze the connectivity of the set of equilibrium markings of the system, $\mathbb{E}^*$. This can be done by representing the information of the connectivity as a graph $\langle V, E\rangle$, where there is a vertex for each configuration in $\mathbb{J}'$ and there is an edge between two vertices if its corresponding sets of equilibrium markings are connected (definition 3.5).

Then, the resulting graph can be analyzed to obtain two possible conclusions:

- If $\langle V, E\rangle$ is strongly connected, then, the set of all of the equilibrium markings is connected.
- If $\langle V, E\rangle$ is not strongly connected, the strongly connected components can be obtained. In this case, even though global controllability (over $\mathbb{E}^*$) is not guaranteed, the system may be controllable between multiple regions. This information is encoded in the strongly connected components of $\langle V, E\rangle$.

The previous analysis can be performed by means of the Algorithm 7. The complexity of the analysis of connectivity is polynomial on the cardinality of $\mathbb{J}'$ (only $(|J'| - 1)|J'|/2$ pairs are analyzed).

Algorithm 7 Graph of connectivity.

Input: A TCPN system, $\langle \mathcal{N}, \boldsymbol{\lambda}, \mathbf{m}_0 \rangle$ and the set $\mathbb{J}'$.
Output: The graph, $\langle V, E \rangle$, of equilibrium connectivity.
Initialize: $E := \emptyset$ and V as a set of nodes, c_i, one per each $\mathcal{C}_i \in \mathbb{J}'$ (with the same label as the corresponding configuration).
repeat
    Take first configuration $\mathcal{C}_i \in \mathbb{J}'$
    Remove $\mathcal{C}_i$ from $\mathbb{J}'$
    for all $\mathcal{C}_j \in \mathbb{J}'$ **do**
        If $E_i^* \cap E_j^* \neq \emptyset$ (Alg. 6) **then**
            Add the edge (c_i, c_j) to E
    end for
until $\mathbb{J}' = \emptyset$

5.1.3. Results and Discussion

To assess the efficacy of our method in reducing the number of configurations to be analyzed during the verification of connectivity, we conducted tests on various TCPN systems representing real-world applications. Tests were carried out with different benchmark systems from the literature [1] (Figures 5.1 and 5.2), The results are summarized in Table 5.1.

Table 5.1

System	K	J	J'	Size of LPP	$(K-1)K/2$	$(J'-1)J'/2$	$\mathbb{E}^*$ connected?
Σ_1 (L&B MTS)	216		55	57 ×30	23220	1485	✓
Σ_2 (L&B CF)	96		40	58 × 32	4560	780	✓
Σ_3 (L&B MTS)	128		8	43 × 23	8128	28	✓
Σ_4 (L&B MTS)	1536		18	61 × 32	1178880	153	✓
Σ_5 (L&B GS^{3}PR)	256	16	3	52 × 27	32640	3	✓
Σ_6 (L&B S^{3}PR)	64	16	4	38 × 20	2016	6	✓
Σ_7 (L&B MTS)	8	4	1	20 × 11	28	0	✓
Σ_8 (L&B SimpleN)	16		4	50 × 29	120	6	✓
Σ_9 (L&B SimpleN)	32	16	12	55 × 31	496	66	✓
Σ_{10} (L&B DSSP)	256	128	34	71 × 40	32640	561	✓
Σ_{11} (L&B DSSP2)	64	32	20	39 × 21	2016	190	✓
Σ_{12} (L&B MTS)	6		5	15 × 8	15	10	×

The 2nd column denotes the number of configurations of the system. The 3rd and the 4th columns represent the number of configurations to be analyzed after removing implicit arcs and the classification of regions with equilibria, respectively. The 6th column represents the number of pairs to analyze to verify connectivity by means of brute force. The 7th column represents the number of pairs to analyze to verify connectivity by using the proposed method.

[1] Σ_1 from Silva et al. [2014], Σ_2 from Teruel et al. [1997], Σ_3, Flexible Manufacturing System from Fig. 4.1, Σ_4 from Navarro-Gutiérrez et al. [2020], Σ_5 from Liu and Barkaoui [2016], Σ_6 from Abdul-Hussin [2015], Σ_8 and Σ_9 from Rodríguez et al. [2020], Σ_{10} from Recalde et al. [1998], Σ_{11} from Souissi and Beldiceanu [1988], and Σ_{12} is the net from Fig. 2.7.

It can be noted that, in general, the reduction is significant, achieving a reduction of at least 80% of the pairs to analyze, in most cases.

Clearly, the complexity of the method is still heavily influenced by the initial number of configurations of the TCPN system. Nevertheless, the substantial reduction in the number of pairs to analyze when using the proposed method is a promising development. This reduction not only accelerates the analysis process but also enhances its efficiency by minimizing the computational resources required. It demonstrates the practicality and effectiveness of the proposed approach in tackling complex real-life benchmarks.

5.2 — Structural characterization of connectivity in subclasses

As was stated in the previous section, developing a structural approach for computing the equilibrium sets in general systems is not an easy task due to its dependence on the initial token distribution of a system: Given a simple TCPN structure and timing, depending on the token distribution, the equilibrium sets can be completely different.

Nevertheless, in this section, we explore the relation between the structure of the net and its equilibrium sets for different subclasses of nets. We analyze and derive some properties, related to the structure and the configurations

In particular, in this section, qualitative properties of the equilibrium sets in some subclasses of nets are studied by using a structural approach, i.e., by taking advantage of the information provided by the Petri net weighted graph to avoid the enumeration of all the linear modes. Moreover, the connectivity of the equilibrium sets will be proven for this subclass of systems.

5.2.1. Equilibrium markings and structural components in CF-TCPN systems

Usually, in TCPN systems, not all the regions contain equilibrium markings. Since we are interested in the ones that do contain equilibria, the aim of this section is to derive some properties that are fulfilled in the configurations corresponding to those regions. In particular, we will show that $\forall \mathcal{C}_i$ s.t. $E_i \neq \emptyset$, the places contained in the "*slowest parts*" of the system are always included, in some sense, in the corresponding T-coverture. This allows us to define a structural object that will be useful to state some qualitative properties of the equilibrium sets in CF-TCPNs. Later the results will be extended to TEC-TCPNs.

Definition 5.3. *Let $\Sigma = \langle \mathcal{N}, \boldsymbol{\lambda}, \boldsymbol{\mu} \rangle$ represent a Cv and Ct CF-TCPN system and $\mathbf{y}_k$ be a min-*

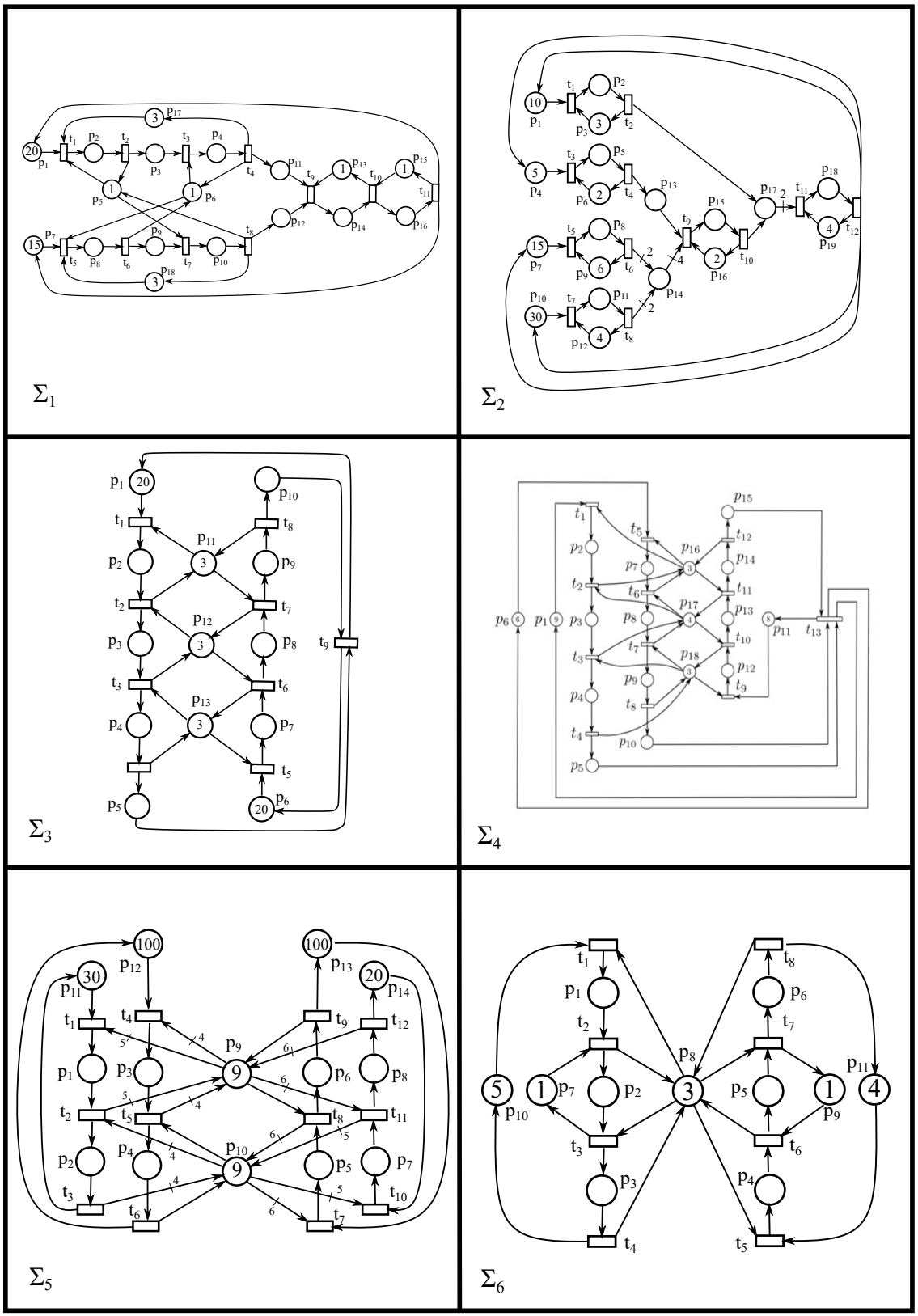

Figure 5.1. Benchmark nets

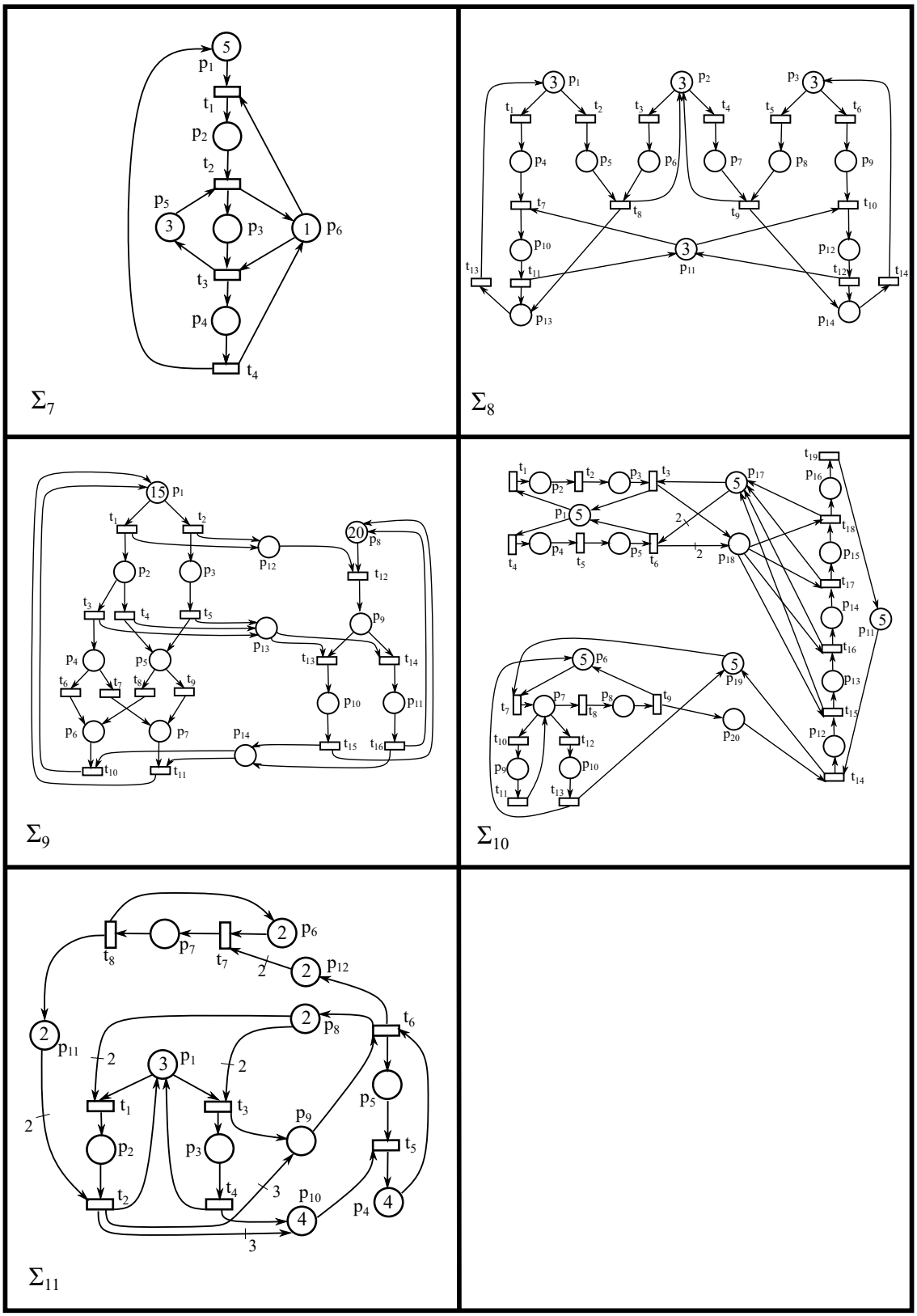

Figure 5.2. Benchmark nets

imal P-semiflow of $\mathcal{N}$. *The* Cv-subsystem, Σ_k, *induced by* $\mathbf{y}_k$, *is defined as* $\Sigma_k = \langle \mathcal{N}_k, \boldsymbol{\lambda}_k, \boldsymbol{\mu}_k \rangle$, *where* $\mathcal{N}_k$ *is the corresponding Cv-component,* $\boldsymbol{\lambda}_k = \boldsymbol{\lambda}[T_k]$ *and* $\boldsymbol{\mu}_k = \boldsymbol{\mu}[P_k]$.

Throughout this work, the concept of *speed of a Cv-subsystem* will be used. Since any Σ_k induced by a minimal P-semiflow of $\mathcal{N}$ is a Cv and Ct FA-TCPN [Teruel et al., 1997], then Σ_k has a unique equilibrium marking $\boldsymbol{\mu}_k^q$ (Corollary 24 in Mahulea et al. [2008b]), and $\boldsymbol{\varphi}_k^q = \alpha_k \mathbf{x}[T_k]$ is its corresponding equilibrium flow, where $\mathbf{x}$ is the unique minimal T-semiflow of $\mathcal{N}$ (Teruel et al. [1997]).

Definition 5.4. *Let* Σ_k *be a Cv-subsystem of* $\langle \mathcal{N}, \boldsymbol{\lambda}, \boldsymbol{\mu} \rangle$ *and let* $\boldsymbol{\varphi}_k^q = \alpha_k \mathbf{x}[T_k]$ *be its corresponding equilibrium flow. The constant* α_k *is named the* speed *of* Σ_k.

The Cv-subsystems of a CF system can be classified according to their speed α. In this work we are interested in the slowest ones (those with the smaller value of α).

Definition 5.5. *Let* $\Sigma = \langle \mathcal{N}, \boldsymbol{\lambda}, \boldsymbol{\mu} \rangle$ *represent a Cv and Ct CF-TCPN system. The set of minimal P-semiflows associated with the slowest Cv-subsystems of* Σ *is:*

$$\mathcal{Y}_s = \{\mathbf{y}_k \text{ of } \mathcal{N} | \alpha_k \leq \alpha_j \ \forall \Sigma_j \text{ associated to a minimal P-semiflow } \mathbf{y}_j \text{ of } \mathcal{N}\}$$

Example 5.1. *Consider the system of Fig. 5.3 with the depicted initial marking and* $\boldsymbol{\lambda} = \begin{bmatrix} 1 & 1 & 1 & 1 \end{bmatrix}^T$. *The support of the minimal P-semiflows of* $\mathcal{N}$ *are* $||\mathbf{y}_1|| = \{p_1, p_2\}$, $||\mathbf{y}_2|| = \{p_3, p_4\}$ *and* $||\mathbf{y}_3|| = \{p_5, p_6\}$. *Clearly, the equilibrium marking and the speed for the Cv-subsystems* Σ_1 *and* Σ_3 *are* $\boldsymbol{\mu}_1^q = \boldsymbol{\mu}_3^q = [2.5 \ \ 2.5]^T$ *and* $\alpha_1 = \alpha_3 = 2.5$, *respectively. Moreover, the equilibrium marking and speed of* Σ_2 *are* $\boldsymbol{\mu}_2^q = [5 \ \ 5]^T$ *and* $\alpha_2 = 5$. *Then,* $\mathcal{Y}_s = \{\mathbf{y}_1, \mathbf{y}_3\}$.

The previous classification may be carried out using the naive approach of enumerating all the minimal P-semiflows of $\mathcal{N}$ (this number may be an exponential) and computing the corresponding speeds. Instead of that, this work characterizes some properties of CF-TCPNs allowing to derive an efficient algorithm to compute the slowest part of the system. The following proposition states that the T-covertures corresponding to regions that include equilibria must always contain the support of the P-semiflows in $\mathcal{Y}_s$.

Proposition 5.1. *Let* $\Sigma = \langle \mathcal{N}, \boldsymbol{\lambda}, \boldsymbol{\mu} \rangle$ *represent an unforced Cv and Ct CF-TCPN. Let* $\mathbf{m}^q$ *be an equilibrium marking and* $\mathcal{Y}_s$ *be the set of minimal P-semiflows associated to the slowest Cv-subsystems of* Σ. *If* $\mathbf{m}^q \in E_1 \cap ... \cap E_r$, *then,* $\forall \mathcal{TC}_i$, $i \in [1, ..., r]$, $\exists \mathbf{y}_s \in \mathcal{Y}_s$, *such that* $||\mathbf{y}_s|| \subseteq \mathcal{TC}_i$.

Proof. Since the system is a Cv and Ct CF-TCPN, the equilibrium throughput at $\forall \mathbf{m}^q \in E_i$ is $\mathbf{f}^q = \alpha_l \mathbf{x}$, for some constant value α_l (Theorem 21 in Mahulea et al. [2008b]). Also, consider the flow $\mathbf{f}_s = \alpha_s \mathbf{x}$, where α_s is the speed of the slowest Cv-subsystems of Σ.

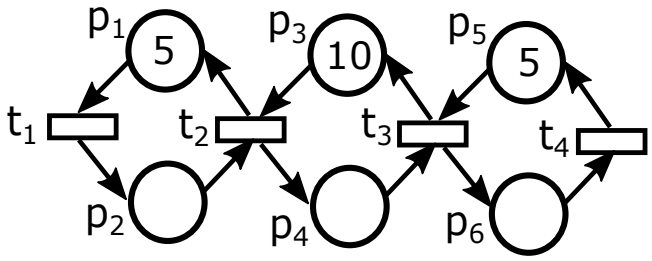

Figure 5.3. TCPN system.

Suppose that $\exists \mathcal{TC}_i,\ i \in [1,...,r]$ s.t. $\forall \mathbf{y}_s \in \mathcal{Y}_s,\ ||\mathbf{y}_s|| \not\subset \mathcal{TC}_i$, and that $\mathbf{m}^q \in \mathcal{R}_i$. Since every T-coverture of a Cv and Ct CF net contains the support of a P-semiflow [Teruel et al., 1997], then, $\exists \mathbf{y}_l \notin \mathcal{Y}_s$ s.t. $||\mathbf{y}_l|| \subseteq \mathcal{TC}_i$. Consider any $\mathbf{y}_s \in \mathcal{Y}_s$. Then, $\exists p_k \in ||\mathbf{y}_s||$, s.t. $p_k \notin \mathcal{TC}_i$. Let t be the output transition of p_k. Then, $\exists p' \notin ||\mathbf{y}_s||$ that is constraining t. Thus, $\mathbf{m}^q[p']/\mathbf{Pre}[p',t] \leq \mathbf{m}^q[p_k]/\mathbf{Pre}[p_k,t]$. Then, p' imposes an equilibrium flow at t and two cases arise:
(a) If $\alpha_l \mathbf{x}[t] \leq \alpha_s \mathbf{x}[t]$, hence $\forall t_w,\ \mathbf{f}^q[t_w] = \alpha_l \mathbf{x}[w] \leq \alpha_s \mathbf{x}[w]$, i.e. the Cv-subsystem induced by $\mathbf{y}_l$ is equally or slower than Cv-subsystems induced by the P-semiflows in $\mathcal{Y}_s$, a contradiction.
(b) If $\alpha_l \mathbf{x}[t] > \alpha_s \mathbf{x}[t]$, then $\alpha_l > \alpha_s$, and $\mathbf{m}^q[p_k]/\mathbf{Pre}[p_k,t] \geq \mathbf{m}^q[p']/\mathbf{Pre}[p',t] = \alpha_l \mathbf{x}[t]/\boldsymbol{\lambda}[t] > \alpha_s \mathbf{x}[t]/\boldsymbol{\lambda}[t] = \mathbf{m}_s[p_k]/\mathbf{Pre}[p_k,t]$, i.e., p_k has more tokens at $\mathbf{m}^q$ than in $\mathbf{m}_s$. Then, $\exists p'' \in ||\mathbf{y}_s|| \setminus \{p_k\}$ that have less tokens at $\mathbf{m}^q$ than in $\mathbf{m}_s$ (in order to fulfill conservativity). Thus, the flow at its output transitions cannot be bigger at $\mathbf{m}^q$ than at $\mathbf{m}_s$. Said differently, if $t'' \in p''^{\bullet}$, then $\mathbf{f}^q[t''] < \mathbf{f}_s[t'']$, i.e. $\alpha_s > \alpha_l$, a contradiction.

Since both cases lead to a contradiction, the T-covertures corresponding to the regions that include an equilibrium marking $\mathbf{m}^q$ must contain the support of a $\mathbf{y}_s \in \mathcal{Y}_s$. □

The following corollary states that, at every equilibrium state of the system, the corresponding equilibrium flow is the same, and it is limited by the speed of the slowest Cv-subsystems. Moreover, the token distribution in the places of any slow Cv-subsystem is unique for any equilibrium marking and is equal to its corresponding $\boldsymbol{\mu}_k^q$, even if they are not constraining its output transition.

Corollary 5.1. *Let $\langle \mathcal{N}, \boldsymbol{\lambda}, \boldsymbol{\mu} \rangle$ represent an unforced Cv and Ct CF-TCPN system. Then, $\forall \mathbf{m}^q \in \mathbb{E}$, $\mathbf{f}^q = \alpha_s \mathbf{x}$, where α_s is the speed of the slowest Cv-subsystems. Moreover, $\forall \mathcal{N}_k$ induced by some $\mathbf{y}_k \in \mathcal{Y}_s$, $\mathbf{m}^q[P_k] = \boldsymbol{\mu}_k^q$.*

Proof. From proof of Prop. 5.1 it follows that the equilibrium flow $\forall \mathbf{m}^q \in E_i$ is $\mathbf{f}^q = \alpha_s \mathbf{x}$.

Moreover, since the equilibrium flow of the system is $\mathbf{f}^q = \alpha_s \mathbf{x}$, the flow in the output transitions of any slowest Cv-subsystem Σ_k must be $\mathbf{f}^q = \alpha_s \mathbf{x}[T_k]$, even if the corresponding $\mathbf{y}_k \notin \mathcal{TC}_i$. However, since $\alpha_k = \alpha_s$, the only marking distribution in the places of P_k that guarantees such throughput is the equilibrium marking of Σ_k, then, $\boldsymbol{\mu}_k^q = \mathbf{m}^q[P_k]$. Finally,

since the previous is valid $\forall \mathcal{R}_i$ s.t. $E_i \neq \emptyset$, it must be valid $\forall \mathbf{m}^q \in \mathbb{E}$. □

Remark 5.1. *The converse of proposition 5.1 is not true. See for instance the TCPN system depicted in Fig. 5.4. Consider the case where* $\lambda_7 = 1$. *The depicted* $\mathbf{m}$ *corresponds to the unique equilibrium marking in* $Class(\mathbf{m})$ *and the active configuration at* $\mathbf{m}$ *is* $\mathcal{C}_1 = \{(p_1,t_1),(p_2,t_2),(p_3,t_3),(p_4,t_4),(p_5,t_5),(p_6,t_6),(p_7,t_7)\}$.
It holds that the only minimal P-semiflow whose support is contained in $\mathcal{TC}_1$ *is the slowest one,* $||\mathbf{y}_1|| = \{p_1,p_2\}$ *(Prop 5.1). Nevertheless, consider* $\mathcal{C}_2$ *in which the only difference with respect to* $\mathcal{C}_1$ *is that* p_8 *constraints* t_3. *Notice that* $\mathcal{TC}_2$ *also contains the support of the slowest minimal P-semiflows, nonetheless,* $E_2 = \emptyset$.

Definition 5.6. *Let* $\Sigma = \langle \mathbf{m}, \boldsymbol{\lambda}, \boldsymbol{\mu} \rangle$ *represent a Cv and Ct CF-TCPN system where* $\mathcal{N}_k$ *is the Cv-component induced by a* $\mathbf{y}_k \in \mathcal{Y}_s$. *The* Maximal Limiting Subnet *(MLS) of* Σ *is* $\mathcal{N}_M = \langle P_M, T_M, \mathbf{Pre}_M, \mathbf{Post}_M \rangle = \bigcup_{\mathbf{y}_k \in \mathcal{Y}_s} \mathcal{N}_k$.

Example 5.2. *Let us consider the system of Fig. 5.3 with the depicted initial marking for two different timings. First, if* $\boldsymbol{\lambda} = [1\ 1\ 1\ 1]^T$, *as in example 5.1,* $\mathcal{Y}_s = \{\mathbf{y}_1, \mathbf{y}_3\}$. *Then,* $\mathcal{N}_M$ *is the subnet induced by* $P_M = \{p_1,p_2,p_5,p_6\}$. *Notice that* $\mathcal{N}_M$ *does not contain places* p_3 *and* p_4, *thus, is not s.c.. Finally, if* $\boldsymbol{\lambda} = \begin{bmatrix} 1 & 1 & 1 & 2 \end{bmatrix}^T$, *it can be verified that* $\mathcal{Y}_s = \{\mathbf{y}_1\}$ *and* $\mathcal{N}_M$ *is the s.c. subnet induced by* $P_M = \{p_1,p_2\}$.

Remark 5.2. *Notice that the MLS depends not only on* $\mathcal{N}$, *but also on the initial marking distribution* $\mathbf{m}_0$ *and the timing of the system. However, for a given set of systems* $\Sigma = \langle \mathcal{N}, \boldsymbol{\lambda}, \boldsymbol{\mu} \rangle$, $\boldsymbol{\mu} \in Class(\mathbf{m}_0)$, *the MLS for all the systems in* Σ *is unique and can be seen as a structural object.*

Finally, algorithm 8 takes advantage of the presented results to compute the MLS of a system, in polynomial time. It first computes the speed of the slowest Cv-subsystems, α_k, of the system (as proposed in Recalde and Silva [2001]). Based on this, it computes a set of minimal P-semiflows that contains information of all the slowest Cv-subsystems of the system. Finally, based on the obtained information, the MLS can be easily computed.

Proposition 5.2. *Let* $\Sigma = \langle \mathcal{N}, \boldsymbol{\lambda}, \boldsymbol{\mu} \rangle$ *represent a Cv and Ct CF-TCPN system. Then, the MLS of* Σ *is computed by algorithm 8 in polynomial time.*

Proof. According to Recalde and Silva [2001], given a minimal P-semiflow $\mathbf{y}$, the speed of its corresponding Cv-subsystem can be obtained with the following expression:

$$\alpha_k = (\mathbf{y}^T \mathbf{m}_0)/(\mathbf{y}^T \mathbf{Pre} \boldsymbol{\Lambda}^{-1} \mathbf{x}) \tag{5.1}$$

Then, steps 2-6 of the algorithm are used to compute the exact speed of the slowest Cv-subsystems in polynomial (LPP1 in Recalde and Silva [2001]). Next, since α_k is known and

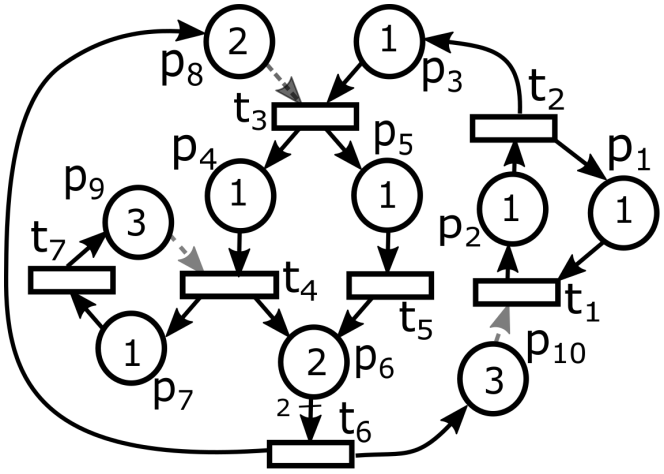

Figure 5.4. CF-TCPN with $\boldsymbol{\lambda} = [1\ 1\ 1\ 1\ 1\ 1\ \lambda_7]^T$. If $\lambda_7 = 1$, the depicted marking, $\mathbf{m}$, corresponds to the unique equilibrium marking of the system in $Class(\mathbf{m})$.

Algorithm 8 Computation of the MLS of a CF-TCPN

Inputs: Matrices **Pre**, **Post**, $\mathbf{\Lambda}$, and the initial marking $\mathbf{m}_0$.
Outputs: The MLS, $\mathcal{N}_M$, of the system.

Compute the minimal T-semiflow, $\mathbf{x}$.
$z = \mathbf{max}\ \mathbf{y}^T\mathbf{Pre}\mathbf{\Lambda}^{-1}\mathbf{x}$ subject to
    $\mathbf{y} \geq \mathbf{0}$
    $\mathbf{y}^T\mathbf{C} = \mathbf{0}$
    $\mathbf{y}^T\mathbf{m}_0 = 1$
$\alpha_k := 1/z$ // Speed of the slowest Cv-subsystems.
$Y := \mathbf{y}$
For all $p_i \in P$
    If $Y[p_i] = 0$
        min $\mathbf{y}^T\mathbf{1}$ subject to
            $\mathbf{y}^T \geq \mathbf{0}$
            $\mathbf{y}^T\mathbf{C} = \mathbf{0}$ // $\mathbf{y}$ is a P-semiflow.
            $\mathbf{y}^T(\mathbf{m}_0 - \alpha_k\mathbf{Pre}\mathbf{\Lambda}^{-1}\mathbf{x}) = \mathbf{0}$ // Eq. (5.1).
            $\mathbf{y}[p_i] = 1$ // $p_i \in ||\mathbf{y}||$.
        $Y := Y + \mathbf{y}$ and $\mathcal{Y}'_s := \mathcal{Y}'_s \cup \{\mathbf{y}\}$
    end If
end For
return the MLS, $\mathcal{N}_M$, of the system (i.e., the Cv-component induced by Y).

based on eq. (5.1), a LPP can be used to compute a set of minimal P-semiflows agreeing with the exact throughput of the system, i.e., $\mathcal{Y}'_s \subseteq \mathcal{Y}_s$ (steps 8-17). It is easy to see that if a place p is contained in the MLS of the system, then, the algorithm computes at least one P-semiflow $\mathbf{y}$ s.t. $p \in ||\mathbf{y}||$, i.e., the information of all the places in MLS is captured. Moreover, the second LPP is solved, at most, $|P|-2$ times. Finally, the MLS is easily obtained as the Cv-component of Y. □

5.2.2. Equilibria within a single region in CF-TCPNs

In this section, the relation between the set of equilibrium markings, $\mathbb{E}$, and the MLS of unforced CF-TCPN systems is considered. In particular, if the MLS is strongly connected, there is a single equilibrium point in $Class(\mathbf{m}_0)$. On the contrary, an infinite number of connected equilibrium points exist. Finally, in section 5.2.4, the presented results are extended directly to unforced TEC-TCPNs.

From corollary 5.1, we know that the token distribution of all the places contained in the MLS must remain equal for any $\mathbf{m}^q \in \mathbb{E}$. Moreover, if such marking is contained in a particular region $\mathcal{R}_i$, the token distribution of the places that constrain transitions at $\mathcal{C}_i$ also remain equal $\forall \mathbf{m}^q \in E_i$ (in order to preserve the equilibrium flow).

Definition 5.7. *Let $\langle \mathcal{N}, \boldsymbol{\lambda}, \boldsymbol{\mu} \rangle$ represent a Cv and Ct CF-TCPN system, $\mathcal{N}_M$ be its MLS and $\mathcal{C}_i$ be a configuration s.t. $E_i \neq \emptyset$. Then, $Pf_i = P_M \cup \mathcal{TC}_i$ is defined as the set of* places with fixed marking at the equilibria in $\mathcal{R}_i$. *$Pv_i = P \setminus Pf_i$ is defined as the set of* places with variable marking at the equilibria in $\mathcal{R}_i$
Based on Pf_i, a $|Pf_i| \times |P|$ matrix $\mathbb{M}_i$ is defined such that, the elementary vector e_j is a row of $\mathbb{M}_i$ if $p_j \in Pf_i$.

The following proposition states a condition that indicates whether the marking $\forall p \in Pv_i$ is fixed to a unique value due to the token conservation laws of $\mathcal{N}$, meaning that there can only be a single equilibrium within the region.

Proposition 5.3. *Let $\langle \mathcal{N}, \boldsymbol{\lambda}, \boldsymbol{\mu} \rangle$ represent an unforced Cv and Ct CF-TCPN system. Assume that $\mathcal{C}_i$ is a configuration s.t. $E_i \neq \emptyset$. If*

$$rank\left(\begin{bmatrix} \mathbb{M}_i \\ \mathbf{B}_y{}^T \end{bmatrix}\right) = |P| \tag{5.2}$$

then, there is a single equilibrium marking in $\mathcal{R}_i$.

Proof. Rename the places so that the first to appear are the ones in Pf_i. Let us denote the

marking of the places in Pf_i as $\boldsymbol{\mu} f_i$. Then, consider the following system:

$$\begin{bmatrix} \mathbb{M}_i \\ \mathbf{B}_y{}^T \end{bmatrix} \mathbf{m}^q = \begin{bmatrix} \boldsymbol{\mu} f_i \\ \mathbf{B}_y^T \mathbf{m}_0 \end{bmatrix} \tag{5.3}$$

Any solution of (5.3) is a marking that: 1) contains the fixed part of all the equilibriums, and 2) fulfills the token conservation laws of $\mathcal{N}$. Then, if (5.2) holds, (5.3) has a unique solution, i.e., $\mathcal{R}_i$ has a single equilibrium marking. □

If there exists a configuration $\mathcal{C}_i$ s.t. $E_i \neq \emptyset$ and equation (5.2) does not hold, (5.3) may have an infinite number of solutions that are within $\mathcal{R}_i$. For instance, consider the marking $\mathbf{m}_2 = \mathbf{m}^q + \beta\boldsymbol{\eta}$ where η is a vector in the kernel of $\begin{bmatrix} \mathbb{M}_i^T & \mathbf{B}_y \end{bmatrix}^T$ and $\beta \in \mathbb{R}$. If $\exists \beta \neq 0$ s.t. $\mathbf{m}_2 \in \mathcal{R}_i$, then $\mathcal{R}_i$ contains an infinite number or equilibrium markings.

Example 5.3. *Consider the system in Fig. 5.4 with $\lambda_7 = 1$. For the depicted configuration $\mathcal{C}_1$, $Pv_1 = \{p_8, p_9, p_{10}\}$ and $Pf_1 = \{p_1, p_2, p_3, p_4, p_5, p_6, p_7\}$. Notice that, $\forall p \in Pf_1$, its marking $\mathbf{m}^q[p]$ is fixed to a unique value $\forall \mathbf{m}^q \in \mathcal{R}_1$ (see definition 5.7), i.e., if there are multiple equilibria within the region, the difference must be on the markings related to places in Pv_1. In this case, however, the marking $\forall p \in Pv_1$ is fixed to a unique value from the token conservation laws:*
$\mathbf{m}^q[p_8] = 4 - (\mathbf{m}^q[p_4] + \mathbf{m}^q[p_5] + \mathbf{m}^q[p_6])/2$
$\mathbf{m}^q[p_9] = 4 - \mathbf{m}^q[p_7]$
$\mathbf{m}^q[p_{10}] = 7 - \mathbf{m}^q[p_2] - \mathbf{m}^q[p_3] - (\mathbf{m}^q[p_4] + \mathbf{m}^q[p_5] + \mathbf{m}^q[p_6])/2.$
On the other hand, (5.2) clearly holds at $\mathcal{C}_1$, i.e., $|E_1| = 1$ and we obtain the same conclusion. Now, consider the system of Fig. 5.3 with the timing $\boldsymbol{\lambda} = \begin{bmatrix} 1 & 1 & 1 & 1 \end{bmatrix}^T$ at the configuration $\mathcal{C}_2 = \{(p_1, t_1), (p_2, t_2), (p_5, t_3), (p_6, t_4)\}$. $\mathcal{C}_2$ is s.t. $E_2 \neq \emptyset$ and (5.2) does not hold. Then, the marking of the places in $Pv_i = \{p_3, p_4\}$, in the corresponding configuration, is not fixed to a unique value by the token conservation laws of the net. In fact, consider $\mathbf{m}^q = [2.5\ 2.5\ 2.5\ 7.5\ 2.5\ 2.5\ ]^T \in E_2$ and $\boldsymbol{\eta} = [0\ 0\ 1\ -1\ 0\ 0\ ]^T$ ($\boldsymbol{\eta}$ is s.t. $\begin{bmatrix} \mathbb{M}_i^T & \mathbf{B}_y \end{bmatrix}^T \boldsymbol{\eta} = \mathbf{0}$), then, $\forall \mathbf{m}_2^q = \mathbf{m}^q + \beta\boldsymbol{\eta}$ with $0 \leq \beta \leq 5$, $\mathbf{m}_2^q \in E_2$.

The following proposition relates the MLS of the system with condition (5.2).

Proposition 5.4. *Let $\Sigma = \langle \mathcal{N}, \boldsymbol{\lambda}, \boldsymbol{\mu} \rangle$ represent an unforced Cv and Ct CF-TCPN system. Let $\mathcal{C}_i$ be a configuration s.t. $E_i \neq \emptyset$ and $\mathcal{N}_M$ be the MLS of the system. $\mathcal{N}_M$ is strongly connected iff (5.2) holds.*

Proof. First, notice that a basis for the P-flows of the system always exists s.t. $\mathbf{B}_y = \begin{bmatrix} \mathbf{B}_{ys} & \mathbf{B}_{yf} \end{bmatrix}$ where $\mathbf{B}_{ys}$ is a basis that only contains information of the P-semiflows in $\mathcal{Y}_s$ and $\mathbf{B}_{yf}$ contains linearly independent vectors so that $dim(\mathbf{B}_y) = dim(\mathbf{B}_{ys}) + dim(\mathbf{B}_{yf})$. Moreover, since all the vectors in $\mathbf{B}_{ys}$ can be seen as a linear combination of the rows in $\mathbb{M}_i^T$, then, $rank([\mathbb{M}_i^T\ \mathbf{B}_y]^T) = rank([\mathbb{M}_i^T\ \mathbf{B}_{yf}]^T)$.

Sufficiency: Suppose that $\mathcal{N}_M$ is not s.c., then, it is composed by s.c. components $sc_1, ..., sc_k$, each one related to different P-semiflows of $\mathcal{Y}_s$. Then, since $\mathcal{N}$ is s.c., there exists a P-semiflow $\mathbf{y}_c \notin \mathcal{Y}_s$ s.t. its corresponding Cv-component is connecting with $sc_1, ..., sc_k$. Hence, there exist $p_a, ..., p_g \in ||\mathbf{y}_c||$ that are input places to join transitions in $sc_1, ..., sc_k$, i.e., those places do not constrain the flow of its output transition at $\mathcal{C}_i$. Since $\mathbf{y}_c \notin \mathcal{Y}_s$, its corresponding Cv-component must have extra tokens that can be distributed among the places $p_a, ..., p_g$ without violating the token conservation laws, then, there must exist more than one equilibrium marking in the same region. Thus, the marking of the variable part of $\mathbf{m}^q \in E_i$ is not fixed to a unique value and $rank([\mathbb{M}_i^T\ \mathbf{B}_{yf}]^T) < |P|$.

Necessity: Assume that $\mathcal{N}_M$ is s.c. and let P_M and T_M be their sets of places and transitions. Then, $\mathcal{N}_M$ is a Cv and Ct CF net with token flow-matrix C_M. As in any net of such kind $rank(C_M) = |P_M| - dim(\mathbf{B}_{yM}) = |T_M| - 1$. Furthermore, $\mathcal{N}_M$ is composed by the Cv-components induced by the P-semiflows in $\mathcal{Y}_s$, then, a basis $\mathbf{B}_{yM}$ can be computed as $\mathbf{B}_{yM} = \mathbf{B}_{ys}[P_M]$. Thus, the dimension of both bases is the same and $|P_M| - |T_M| = dim(\mathbf{B}_{ys}) - 1$.

Next, consider any $\mathcal{C}_i$ and it corresponding matrix $\mathbb{M}_i$. By definition, $rank(\mathbb{M}_i) = |P_{fi}|$. Then, there are $|T| - |T_M|$ transitions that are not limited by places in P_M, thus, $|P_{fi}| = |P_M| + |T| - |T_M|$ and $rank(\mathbb{M}_i) = |P_M| + |T| - |T_M| = |T| - 1 + dim(\mathbf{B}_{ys})$. Since $|T| - 1 = |P| - dim(\mathbf{B}_y)$ and $dim(\mathbf{B}_y) = dim(\mathbf{B}_{ys}) + dim(\mathbf{B}_{yf})$, then, $rank(\mathbb{M}_i) = |P| - dim(\mathbf{B}_{yf})$. Finally, $\mathbf{B}_{yf}$ contains $dim(\mathbf{B}_{yf})$ linearly independent vector to the rows in $\mathbb{M}_i$ (since each one of those P-flows contain at least one place that is not in P_{fi}), then, it follows that (5.2) holds. □

5.2.3. Equilibrium sets in Choice Free TCPN systems

The following theorem states that, whenever the MLS of the system is strongly connected, for any $\boldsymbol{\mu} \in Class(\mathbf{m}_0)$, a unique equilibrium marking exists. Notice that this is a stronger result than the ones presented in propositions 5.3 and 5.4 since they only state conditions for the existence of a unique equilibrium marking on a particular region.

Theorem 5.1. *Let $\Sigma = \langle \mathcal{N}, \boldsymbol{\lambda}, \boldsymbol{\mu} \rangle$ represent an unforced Cv and Ct CF-TCPN system. Let $\mathcal{N}_M$ be the MLS of Σ. If $\mathcal{N}_M$ is strongly connected, then, there is a single equilibrium marking on the system.*

Proof. Assume that two different equilibrium markings, $\mathbf{m}_i^q$ and $\mathbf{m}_j^q$, exist and $\mathcal{N}_M$ is s.c.. From prop. 5.4, if $E_i \neq \emptyset$ then there is a single equilibrium marking in $\mathcal{R}_i$. Thus, $\mathbf{m}_i^q$ and $\mathbf{m}_j^q$ activate two different configurations, $\mathcal{C}_i$ and $\mathcal{C}_j$, respectively. Moreover, for any $\mathbf{m}^q$, regardless of which configuration it activates, its entries related to places in P_M and places whose output transition is not-join remain equal. In other words, the difference between $\mathbf{m}_i^q$ and $\mathbf{m}_j^q$ is on the marking of places, not in P_M, which are input to join transitions. Then, there exists a join

transition $t_k \notin \mathcal{N}_M$ such that $\{p_a, p_b\} \subseteq {}^\bullet t_k$, $(p_a, t_k) \in \mathcal{C}_i$, $(p_b, t_k) \in \mathcal{C}_j$, $\mathbf{m}_i^q[p_a] \neq \mathbf{m}_j^q[p_a]$ and $\mathbf{m}_i^q[p_b] \neq \mathbf{m}_j^q[p_b]$ (i.e., the net is not evolving in the border of $\mathcal{R}_i$ and $\mathcal{R}_j$).

Let $\mathcal{P}_a$ ($\mathcal{P}_b$) be the set of all minimal P-semiflows, where the *a-th* (*b-th*) entry is different from zero. We claim that in any Cv-component induced by any $\mathbf{y} \in \mathcal{P}_a$ (resp. to any $\mathbf{y} \in \mathcal{P}_b$) there must exist at least two join transitions, t_k and another one t'_a (resp. t'_b). If it is not the case, then marking $\forall p \in ||\mathbf{y}||$ is the same in all the configurations, fixed by the equilibrium flow or the token conservation laws. Hence, the number of tokens in p_a cannot change from $\mathbf{m}_i^q$ to $\mathbf{m}_j^q$, unless it lies on the border of $\mathcal{R}_i$, $\mathcal{R}_j$, a contradiction. Thus, there exists t'_a. Moreover $t'_a \in \mathcal{N}_M$, otherwise the net is not MTS. Similarly, there exists a join transition $t'_b \in \mathcal{N}_M$ in the Cv-component induced by a P-semiflow in $\mathcal{P}_b$.

At $\mathcal{C}_j$, place p_b constrains t_k, i.e., $\mathbf{m}_j^q[p_b]$ its such that $\mathbf{f}^q[t_k] = \alpha_k \mathbf{x}[t_k]$, where α_k is the speed of the slowest Cv-components. If this marking is reduced, then the flow in transition t_k is lower than the slowest parts of the net, which it is not possible. Then $\mathbf{m}_i^q[p_b] \geq \mathbf{m}_j^q[p_b]$, and, in this case $\mathbf{m}_i^q[p_b] > \mathbf{m}_j^q[p_b]$ since the marking is not in the border of both regions.

Similarly, at $\mathbf{m}_i^q$, p_a constrains t_k in the corresponding configuration, i.e., $\mathbf{m}_i^q[p_a]$ is s.t. $\mathbf{f}^q[t_k] = \alpha_k \mathbf{x}[t_k]$. Thus, by following a similar reasoning, $\mathbf{m}_i^q[p_a] < \mathbf{m}_j^q[p_a]$. Then, in order to fulfill the token conservative laws imposed by the P-semiflows in $\mathcal{P}_a$, $\mathbf{m}_i^q[p] > \mathbf{m}_j^q[p]$ in the places $p \in {}^\bullet t'_a$. Now consider a P-semiflow $y' \in \mathcal{P}_b$ whose induced Cv-component includes place $p \in {}^\bullet t'_a$ (if such Cv-component does not exist, then, it is not connected to $\mathcal{N}_M$, a contradiction). Since the marking in p increases in $\mathbf{m}_i^q$, then the marking in $\mathbf{m}_i^q[p_b]$ must be reduced with respect to $\mathbf{m}_j^q[p_b]$, but this is not possible since $\mathbf{m}_i^q[p_b] > \mathbf{m}_j^q[p_b]$. Thus, such markings, $\mathbf{m}_i^q \neq \mathbf{m}_j^q$, cannot exists. Then, there exists a unique equilibrium marking in $Class(\mathbf{m}_0)$. □

Finally, the following theorem states that the set of equilibrium markings in Cv and Ct unforced CF systems are always connected.

Theorem 5.2. *Let $\Sigma = \langle \mathcal{N}, \boldsymbol{\lambda}, \boldsymbol{\mu} \rangle$ represent an unforced Cv and Ct CF-TCPN system. Let $\mathcal{N}_M$ be the MLS of Σ. If $\mathcal{N}_M$ is not strongly connected, then, $Class(\mathbf{m}_0)$ contains an infinite number of connected equilibrium markings.*

Proof. If $\mathcal{N}_M$ is not strongly connected, then, there is an infinite number of equilibrium markings on the system (this follows from Prop. 5.4). Now, consider any two different markings $\mathbf{m}_1^q, \mathbf{m}_2^q \in \mathbb{E}$ and let us show that they are connected by building a piecewise line segment of equilibria between them.

Let assume that $\mathbf{m}_1^q \in \mathcal{R}_1$ and $\mathbf{m}_2^q \in \mathcal{R}_2$ s.t. the corresponding configurations $\mathcal{C}_1 \neq \mathcal{C}_2$. By Prop. 5.1, we can consider that all the transitions in T_M are being constrained by the places in P_M at $\mathcal{C}_1$, thus, there are an infinite number of Eq. markings in E_1, i.e. $ker(\begin{bmatrix} \mathbb{M}_1^T & \mathbf{B}_y \end{bmatrix}^T) \neq \emptyset$. Since $\mathcal{C}_1 \neq \mathcal{C}_2$, some transitions are beign constrained by some other places $p_a, ..., p_d$ at $\mathcal{C}_2$ w.r.t. $\mathcal{C}_1$. Since the places $p_a, ..., p_d$ are not constraining its output transitions at $\mathcal{C}_1$, $\exists \eta_1 \in$

$ker(\begin{bmatrix}\mathbb{M}_1^T & \mathbf{B}_y\end{bmatrix}^T)$ s.t. the entries related to some of them are not null (since some of those places must be included in the places with variable marking at such configuration). Then, with an appropriate β, a marking $\mathbf{m}_\alpha^q = \mathbf{m}_1^q + \beta\eta_1$ can be computed so that $\mathbf{m}_\alpha^q$ lies in the border of $\mathcal{R}_1$ and $\mathcal{R}_\alpha$. Notice that the corresponding configuration $\mathcal{C}_\alpha$ must fulfill that some of the places $p_a, ..., p_d$ are constraining its output transition.

Finally, this procedure can be repeated iteratively until $\mathcal{R}_2$, and therefore $\mathbf{m}_2^q$, are reached. Then, since this procedure can be used for any pair of equilibrium markings, $\mathbb{E}$ must be connected. □

Theorem 5.2 states a condition for the existence of infinite many equilibria in Cv and Ct CF-TCPN. However, it is worth noting that, since these systems are deterministic, the equilibrium point to which the system will evolve from a particular initial condition $\boldsymbol{\mu} \in Class(\mathbf{m}_0)$ is unique.

Example 5.4. *Consider the system in Fig. 5.4 with the depicted initial marking. The support of the minimal P-semiflows of* $\mathcal{N}$ *are* $||\mathbf{y}_1|| = \{p_1, p_2\}$, $||\mathbf{y}_2|| = \{p_7, p_9\}$, $||\mathbf{y}_3|| = \{p_4, p_5, p_6, p_8\}$ *and* $||\mathbf{y}_4|| = \{p_2, p_3, p_4, p_5, p_6, p_{10}\}$. *Let us consider two different timings. First, if* $\lambda_7 = 1/3$, *by using Alg. 8 we obtain that* $\mathcal{N}_M$ *is the subnet induced by* $P_M = \{p_1, p_2, p_7, p_9\}$, *i.e.,* N_M *is not s.c.. Then, as theorem 5.2 states, the system has an infinite number of connected equilibrium markings. In fact, consider the markings*

$$\mathbf{m}_1 = \begin{bmatrix}1 & 1 & 1 & 1 & 1 & 2 & 3 & 2 & 1 & 3\end{bmatrix}^T$$

$$\mathbf{m}_2 = \begin{bmatrix}1 & 1 & 1 & 3 & 1 & 2 & 3 & 1 & 1 & 2\end{bmatrix}^T$$

$$\mathbf{m}_3 = \begin{bmatrix}1 & 1 & 2 & 3 & 1 & 2 & 3 & 1 & 1 & 1\end{bmatrix}^T$$

and the configurations

$$\mathcal{C}_a = \{(p_1, t_1), (p_2, t_2), (p_3, t_3), (p_9, t_4), (p_5, t_5), (p_6, t_6), (p_7, t_7)\}$$

and

$$\mathcal{C}_b = \{(p_1, t_1), (p_2, t_2), (p_8, t_3), (p_9, t_4), (p_5, t_5), (p_6, t_6), (p_7, t_7)\}$$

The set of equilibrium markings in regions $\mathcal{R}_a$ *and* $\mathcal{R}_b$ *are* $E_a = \overrightarrow{\mathbf{m}_1\mathbf{m}_2}$ *and* $E_b = \overrightarrow{\mathbf{m}_2\mathbf{m}_3}$, *respectively* ($\overrightarrow{ab}$ *denotes the closed line segment between a and b). Moreover,* $\mathbb{E} = E_a \cup E_b$, *which clearly is connected.*
However, if $\lambda_7 = 1$, $\mathcal{N}_M$ *is the subnet induced by* $P_M = \{p_1, p_2\}$, *i.e., it is s.c.. In this case, according to theorem 5.1, there is a single equilibrium marking for any initial condition* $\boldsymbol{\mu} \in Class(\mathbf{m}_0)$, $\mathbb{E} = \begin{bmatrix}1 & 1 & 1 & 1 & 1 & 2 & 1 & 2 & 3 & 3\end{bmatrix}^T$.

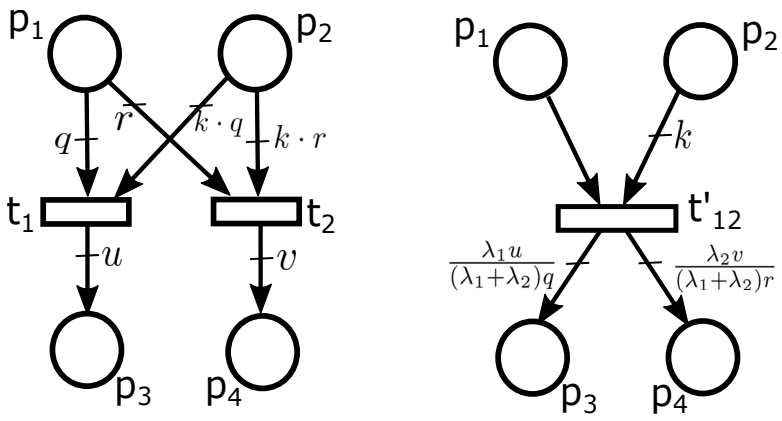

Figure 5.5. A net with transitions t_1 and t_2 (with firing rates λ_1 and λ_2) in TEC relation and its equivalent CF net with $\boldsymbol{\lambda}[t'_{12}] = \lambda_1 + \lambda_2$.

5.2.4. Equilibrium sets in TEC-TCPN systems

Let $\langle \mathcal{N}, \boldsymbol{\lambda}, \mathbf{m}_0 \rangle$ be a TEC system. It is well known that if $\mathcal{N}$ is structurally live and structurally bounded the system can be reduced to an equivalent CF system by merging the transitions in TEC relation into only one flow-equivalent transition (Fig. 5.5). The resulting CF system preserves the evolution of their input places and so, the flow associated to the output transitions. Then, the results presented in the previous sections can be extended to TEC systems.

Corollary 5.2. *Let $\Sigma_{TEC} = \langle \mathcal{N}, \boldsymbol{\lambda}, \boldsymbol{\mu} \rangle$ represent an unforced structurally live and structurally bounded TEC-TCPN system. Let $\Sigma_{CF} = \langle \mathcal{N}', \boldsymbol{\lambda}', \boldsymbol{\mu}' \rangle$ its equivalent CF system.*
• *If the MLS of $\mathcal{N}'$ is strongly connected, then, there is a single equilibrium marking on the system Σ_{TEC}.*
• *Otherwise, there is an infinite number of connected equilibrium markings on the system Σ_{TEC}.*

Proof. Since we are dealing with unforced TCPNs, the transformation is always possible. Then, $\mathcal{N}'$ is a Cv and Ct CF-TCPN. Finally, since the evolution of both systems is equivalent, the statements follow from Theorem 5.1 and Theorem 5.2, respectively. □

5.3 — Concluding remarks

In this chapter, different methods for analyzing the equilibrium sets of TCPN systems are presented.

First, a general approach to analyze the connectivity of the equilibrium sets in a given TCPN system was introduced. The idea is to reduce the complexity of the analysis, compared to the currents methods found in the literature, by means of pre-processing the TCPN information. It was tested against benchmarks of real-life systems, obtaining a significant reduction in the

complexity of the analysis. From the previous analysis, we obtain the so-called connectivity graph of the system, $\langle V, E \rangle$.

Regarding the analysis of controllability in TCPNs, the previous results complement the results presented in chapters 3 and 4 in the following manner:

- Given a TCPN system that is NRC, if $\langle V, E \rangle$ is strongly connected, then, the system is globally controllable, i.e., BIC over the set of all of the equilibrium markings.
- Given a TCPN system that is NRC, if $\langle V, E \rangle$ is not strongly connected, the system is BIC over the each of the Macro-Regions of the system.

Clearly, the complexity of the method is still heavily influenced by the initial number of configurations of the TCPN system. Nevertheless, the substantial reduction in the number of pairs to analyze when using the proposed method is a promising development.

Moreover, we addressed the analysis for net subclasses. In particular, a qualitative analysis of the equilibrium sets in Topologically Equal Conflict (TEC) systems is presented. First, for unforced conservative and consistent Choice-Free systems, with suitable $\mathbf{m}_0$, the relation between the number of equilibrium points of the system and the qualitative characteristics of its *maximal limiting subnet* (MLS) is presented. In particular, it is shown that when the MLS is strongly connected, there exists a unique equilibrium marking in the system. Otherwise, an infinite number of them exist. Moreover, it is shown that the connectivity of the equilibrium sets is always fulfilled. Finally, those results are straightforwardly extended to unforced TEC systems. This can be used to state stronger controllability results in TEC systems.

Chapter 6

Towards applications of structural controllability

This chapter is devoted to demonstrating some practical applications of the analysis techniques presented in the previous chapters. In particular, we present two case studies of real-life systems, used to demonstrate the effectiveness and applicability of the techniques in various contexts and provide a deeper understanding of their potential impact.

The first case study consists of a kanban-like flexible manufacturing system (FMS) consisting of two workflows with shared/limited resources (like machines or buffers). For the second case, we present the analysis of a *clinical pathway* of hip fracture from the "Lozano Blesa" University Hospital in Zaragoza, Spain. In both cases, we conduct a structural controllability analysis, by means of the use of the results and algorithms developed in the previous chapters.

As a part of the contributions of this thesis, these algorithms were implemented in the MATLAB toolbox, SimHPN. These tools are described in the following sections.

Additionally, we propose a control scheme to optimize the behavior of TCPN systems with the presence of uncontrollable transitions. The scheme is based on an On-Off type control over the firing speed at the controllable transitions that reduce the marking error, i.e., the difference between the desired and actual state of the system. The proposed control law can be computed easily online, despite the complexity of a given system. The proposed control scheme is implemented in the case study of the clinical pathway and its effectiveness is studied using simulation results.

6.1 — Implementation in SimHPN

SimHPN is a MATLAB-embedded software that provides support for infinite server and product semantics in both, discrete and continuous, types of transitions. This MATLAB package enables the analysis, design, and simulation of hybrid nets with these two firing semantics. For a more detailed explanation of the different functionalities of the toolbox, an interested reader may

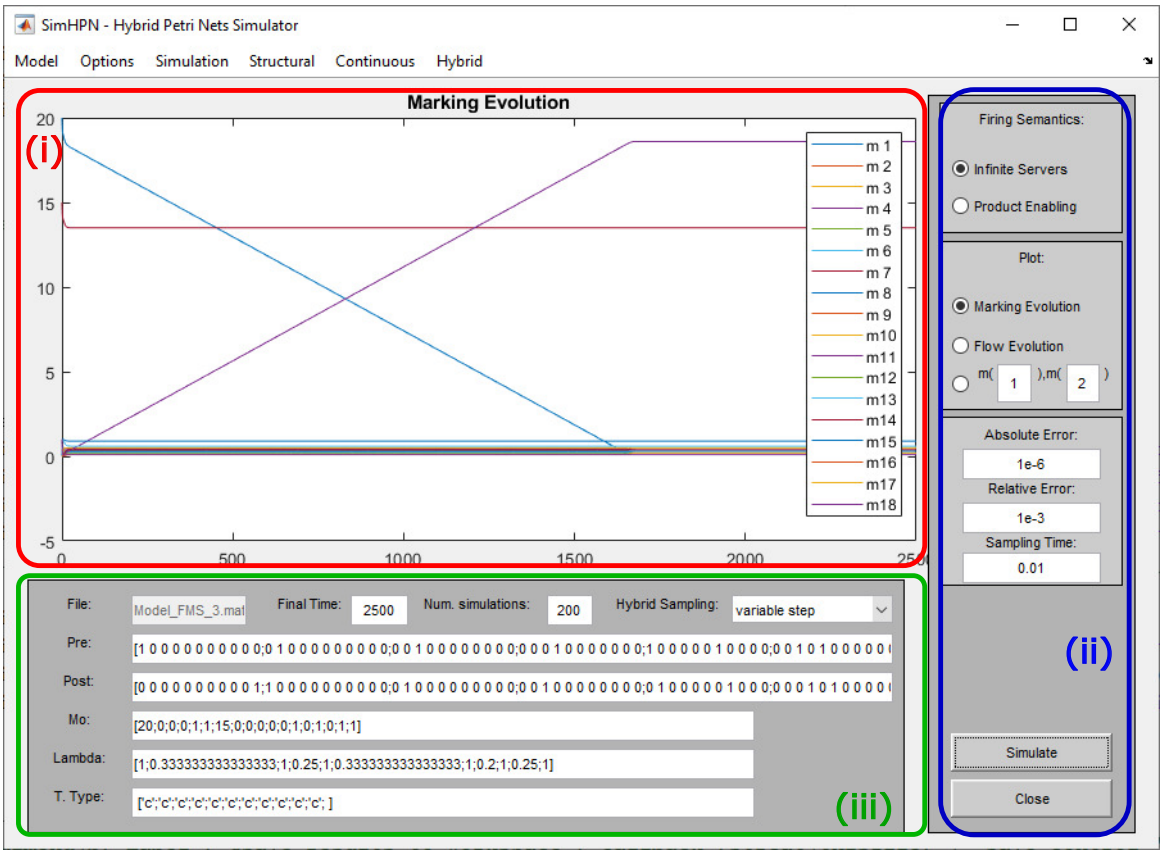

Figure 6.1. SimHPN: the toolbox used for the performance and structural controllability analysis of the system.

consult Júlvez et al. [2012].

In the previous chapters, different algorithms for the analysis of structural controllability have been developed for the case of TCPNs under infinite server semantics. The implementation of these algorithms in SimHPN provides a practical tool for researchers and practitioners to analyze complex systems modeled as TCPNs, enhancing the practical applicability and accessibility of our research. In this section, we describe the algorithms that have been adapted to SimHPN and their functionalities.

The main window of SimHPN is depicted in Fig. 6.1. The Menu bar (placed horizontally, on the top of the window) displays a set of six drop-down menus at the top of the window. In particular, the menu *Continuous menu* calls procedures for analysis and synthesis of continuous Petri nets. Our algorithms can be found on the submenu *Structural controllability analysis* (Fig. 6.2).

This submenu provides a set of various tests for determining the net rank-controllability property of a given TCPN and the computation of the sets of equilibrium markings of the system.

6.1.1. Influence of controllable transitions

This routine computes the sets of *influenced places and transitions by the controllable transitions*, P_I, and T_I. This is a necessary condition for net rank-controllability and it indicates the sets of nodes whose marking and flow can be affected by the activity on the controllable transitions, regardless of the configuration. If a controllable transition does not influence all places in the net, the net cannot be net rank-controllable. It is carried out by implementing Algorithm 1 in chapter 4.

When the user selects this routine, a window is opened and the user should introduce the set of controllable transitions. After this, the results are shown in a pop-up window containing one of two possible messages: 1) A message indicating that influence is not total and indicating the sets of influenced nodes, $P_I \subset P$ and $T_I \subset T$, 2) A message indicating that influence is total, i.e., $P_I = P$ and $T_I = T$.

6.1.2. Net rank-controllability test

This routine verifies sufficient conditions guaranteeing net rank-controllability. It is carried out by implementing Algorithm 3 (Chapter 4, section 5). It is efficiently performed by verifying some structural conditions:

• **Structural Condition 1 (SC1)**: Given $\mathcal{N}$, the influence of T_c is total.

• **Structural Condition 2 (SC2)**: Given $\mathcal{N}$, for all choice place, $p_c \in \{p \in P || p^\bullet| > 1\}$, $p_c^\bullet \subseteq T_c$.

• **Structural Condition 3 (SC3)**: Given $\mathcal{N}$, let $T_F = \{t \in T || t^\bullet| > 1\}$ be the set of fork transitions. For all $t_f \in T_F$, we assume that $|\{t_f^\bullet\}^\bullet \cap T_{nc}| \leq 1$.

When the user selects this routine, a window is opened and the user should introduce the set of controllable transitions. After this, the results are shown in a pop-up window indicating if the net fulfills the property. In case it is not fulfilled, it indicates which one of the structural conditions does not hold.

6.1.3. Equilibrium connectivity graph

This routine computes the equilibrium sets and their connectivity for a specified TCPN system. The output is a graph where each node represents a configuration of the system whose region contains equilibrium markings, and the edges indicate the connection between the equilibrium markings of the different regions. You can save the results of this analysis by selecting the "Save Equilibrium Connectivity Graph to Workspace" submenu. Additionally, if all the equilibrium sets are connected, the function will return a message indicating this.

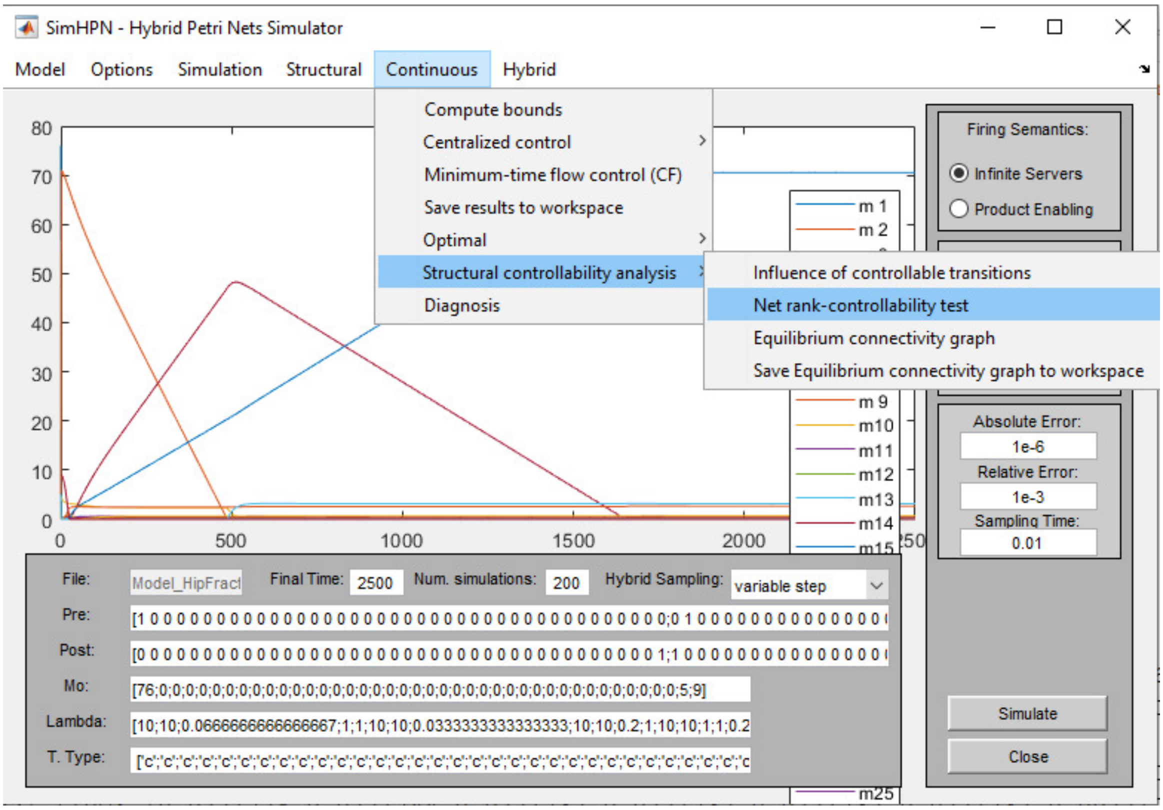

Figure 6.2. SimHPN: the toolbox used for the performance and structural controllability analysis of the system.

6.2 — A Kanban-like flexible manufacturing system

Let us consider again the Kanban-like flexible manufacturing system (FMS) consisting of two workflows that are attended by a pool of three machines (Fig. 6.3), to perform a structural controllability analysis with SimHPN. A TCPN that models the system is presented in Fig. 6.4 (this model is available in the models folder as Model_FMS_3.mat). It has 216 configurations and 11 transitions, each one representing one of the following events:

- Loading of material to the machines $(t_1, t_3, t_5, t_7, t_9)$.
- Unloading of the processed material to be stored in a buffer $(t_2, t_4, t_6, t_8, t_{10})$.
- Removing parts from the system output (t_{11}).

The timing of the net is given by $\lambda = \left[1\ \frac{1}{3}\ 1\ \frac{1}{4}\ 1\ \frac{1}{3}\ 1\ \frac{1}{5}\ 1\ \frac{1}{5}\ 1\right]^T$.

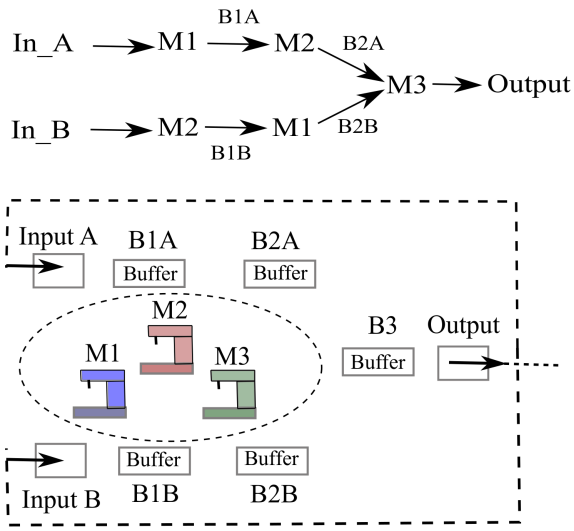

Figure 6.3. Production process of a manufacturing system.

We work based on the assumption that machines are consistently working at their nominal speed and are freed up as soon as the material is processed. As a result, we have identified $T_{nc} = \{t_2, t_4, t_6, t_8, t_{10}\}$. The remaining events are controllable because it is possible to decide when to use a specific machine to process a particular piece, and we can always empty the output buffer. This leads to T_c being $T_c = \{t_1, t_3, t_5, t_7, t_9, t_{11}\}$.

Net rank-controllability analysis: Once the model has been loaded, the test can be carried out by selecting *Continuous* → *Structural controllability analysis* → *Net rank-controllability test*. We present 3 cases:

• $T_c = \{t_1, t_5\}$: We enter this set of controllable transitions on the pop-up windows as [1 5] and we obtain the message

"*Influence is not total! Therefore, the set of controllable transitions does not guarantee net*

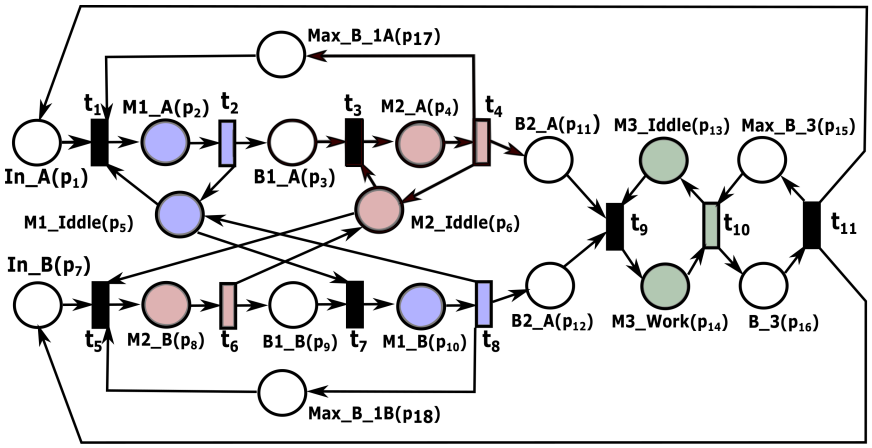

Figure 6.4. TCPN that models the flexible system in Fig. 6.3. The controllable events transitions are depicted in black.

rank-controllability. The only influenced nodes are: Places = [1 2 3 4 5 6 7 8 9 10 11 12 17 18] Transitions = [1 2 3 4 5 6 7 8]"
This means that, since the property of influence does not hold, then there are configurations in which the net is not rank-controllable.
• $T_c = \{t_1, t_5, t_9, t_{11}\}$ By entering this set of controllable transitions as [1 5 9 11] we obtain the message
"*It is not possible to decide if the timed net is net rank-controllable. The condition related to the choice places is not fulfilled.*".
In this case the test cannot conclude if the system is NRC, since one of the sufficient conditions does not hold. In particular, the one related to the choice places. This serves to give indications to the operator/researcher about where the problem may be in order to guarantee controllability.
• $T_c = \{t_1, t_3, t_5, t_7, t_9, t_{11}\}$: Here we choose the set that we will consider in our case study, which is such that it satisfies all the structural conditions for controllability and is indicated by the message: "*The timed net is net rank-controllable.*".

From the previous analysis, we conclude that the system is NRC. Moreover, this system is a live and bounded TCPN. Therefore, T_c also guarantees that the system will be controllable over its connected sets of equilibrium markings.

Equilibrium connectivity graph: This routine can be used to calculate the equilibrium connectivity graph of a system by selecting the menu *Continuous* → *Structural controllability analysis* → *Equilibrium connectivity graph* and entering the set of controllable transitions as the input. Each node of the resulting graph represents a configuration of the system whose region contains equilibrium markings, and the edges indicate the connection between the equilibrium markings of the different regions. This provides insights into the controllability of the

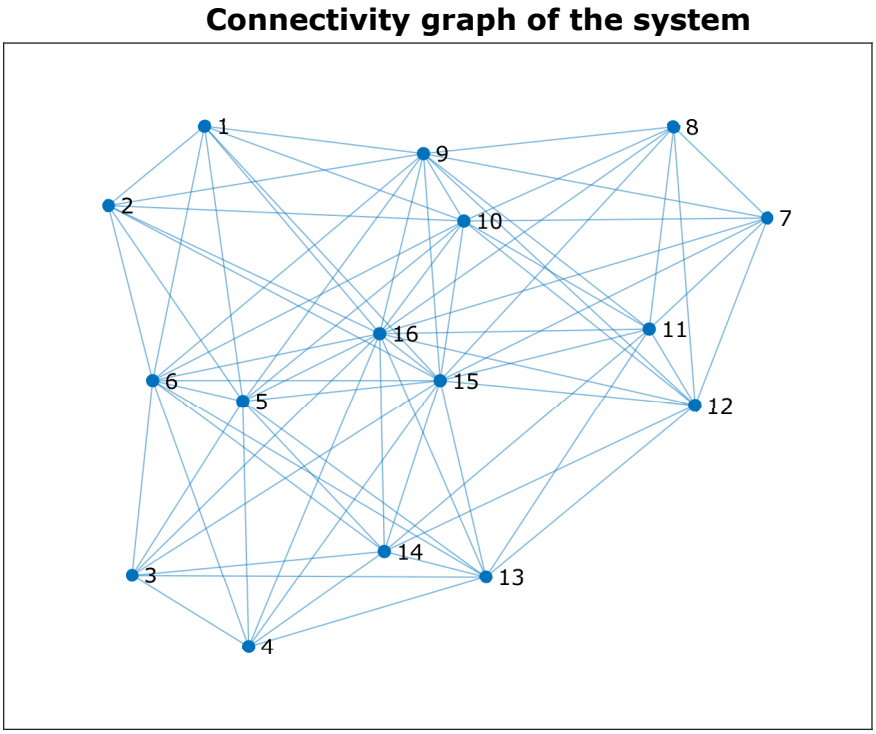

Figure 6.5. Equilibrium connectivity graph of the FMS system. Each node corresponds to a single region of the TCPN system in which it contains equilibrium markings.

system, showing the sets of equilibrium points where the controllability property holds.

Using this routine and selecting the set of controllable transitions [1 3 5 7 9 11], a matrix E_conf is obtained. Each row of this matrix represents a configuration of the system in which equilibrium markings are present in the corresponding regions. For this particular case, the results are the following:

E_conf =

1 2 3 4 7 8 9 10 13 14 16 (node 1) 1 2 3 4 7 8 9 10 13 15 16 (node 2)
1 2 3 4 18 8 9 10 12 14 16 (node 3) 1 2 3 4 18 8 9 10 12 15 16 (node 4)
1 2 3 4 18 8 9 10 13 14 16 (node 5) 1 2 3 4 18 8 9 10 13 15 16 (node 6)
17 2 3 4 7 8 9 10 11 14 16 (node 7) 17 2 3 4 7 8 9 10 11 15 16 (node 8)
17 2 3 4 7 8 9 10 13 14 16 (node 9) 17 2 3 4 7 8 9 10 13 15 16 (node 10)
17 2 3 4 18 8 9 10 11 14 16 (node 11) 17 2 3 4 18 8 9 10 11 15 16 (node 12)
17 2 3 4 18 8 9 10 12 14 16 (node 13) 17 2 3 4 18 8 9 10 12 15 16 (node 14)
17 2 3 4 18 8 9 10 13 14 16 (node 15) 17 2 3 4 18 8 9 10 13 15 16 (node 16)

For instance, the region corresponding to the configuration

$$\mathcal{C}_1 = \{(p_1, t_1), (p_2, t_2), (p_3, t_3), (p_4, t_4), (p_7, t_5), (p_8, t_6), (p_9, t_7), (p_{10}, t_8), (p_{13}, t_9), (p_{14}, t_{10}), (p_{16}, t_{11})\}$$

(node 1) contains equilibria. Furthermore, the routine generates a variable-type graph called E_graph, which has 16 nodes and 76 edges, representing the connectivity of the equilibrium sets. This graph can be plotted (as in Fig. 6.5), providing a visual representation of the equilibrium connectivity of the system. For this particular case, the equilibrium sets in all the regions are connected, meaning that the system exhibits the controllability property over all of its equilibrium markings.

6.3 — Analysis and optimization of clinical pathway

In this section, we propose a TCPN system that can be used for the analysis of a *clinical pathway* of hip fracture from the "Lozano Blesa" University Hospital in Zaragoza.

6.3.1. Motivation

This case study focuses on the analysis and optimization of healthcare systems based on *clinical pathways* [Rotter et al., 2010]. A clinical pathway is a structured approach to the treatment and management of patients with a particular diagnosis or condition. It provides a standardized set of recommendations for medical staff to follow in terms of diagnostic tests, interventions, and treatments for each step of a patient's care journey. As a case study, we consider the analysis of the clinical pathway of hip fracture from the "Lozano Blesa" University Clinical Hospital in Zaragoza, Spain.

To deal with this problem, DEDS and, in particular, Petri nets have proven to be highly appropriate for modeling the event-driven nature of healthcare systems [Augusto and Xie, 2014, Bernardi et al., 2019, Kang et al., 2019, Wang, 2023]. The advantage of this approach is that by leveraging these formalisms, healthcare professionals can gain valuable insights into the operation of these complex systems, leading to better patient outcomes and a higher quality of care. However, it is well-known that the use of analysis techniques for DEDS may become inefficient in highly populated systems since they suffer from the *state explosion problem*, requiring a substantial amount of time to complete the analysis.

In order to cope with this, we propose a model to describe the structure and dynamics of the clinical pathway using TCPNs. The proposed model is based on the one presented in Bernardi et al. [2019] where Stochastic Well-Formed (SWN) Petri nets were used to model the clinical pathway and available SWN solution techniques, such as event-driven simulation [Amparore et al., 2016], were used to obtain an estimation of different performance indices.

The advantage of our approach is that it achieves a reduction in computational complexity for analyzing the system while maintaining a good level of accuracy with respect to the behavior of the discrete model.

TCPNs have been previously used in the literature to model healthcare systems [Dotoli et al., 2009b, Fanti et al., 2012]. However, these works deal with the optimization of the system differently. For instance, Fanti et al. [2012] proposes to optimize the healthcare system by solving a linear programming problem for the determination of the optimal resources, i.e., by redesigning the system by changing its initial parameters and resource availability. In this work, we use a different approach: our goal is to manage the available resources to optimize system performance, assuming redesign is not desirable or feasible.

In order to do that, we take a control theory approach. First, we deal with the controllability analysis of the proposed model by using the results presented in the previous chapters that efficiently deal with the controllability verification. This is a crucial property of any dynamic system since if a system is not controllable, then there does not exist a controller that drives the system to the desired state. We use the implemented algorithms in SimHPN. Next, we propose a control scheme, based on the one proposed in Ross-León et al. [2014] that enables the modeled system to reach a state of maximum throughput more quickly. The scheme is based on an *On-Off* type control over the *firing speed* at the *controllable transitions* that reduces the *marking error*, i.e., the difference between the desired and actual state of the clinical pathway. In the context of the modeled system, the proposed control law can be interpreted as that it prioritizes activities that reduce the marking error, resulting in an optimized use of personnel and a more efficient system. The proposed control law can be computed easily online, despite the complexity of the system. Finally, we provide simulation results that demonstrate the effectiveness of the proposed control scheme in the model under study.

6.3.2. TCPN model of the clinical pathway

In this section, we present a TCPN model for the study of the clinical pathway of hip fracture from the "Lozano Blesa" University Clinic Hospital in Zaragoza, Spain. It is based on the model developed in Bernardi et al. [2019], as a stochastic well-formed Petri net (SWN). We validate our model by comparing the results obtained through TCPN simulation with those of the discrete system. We show how the TCPN system can be used to obtain a more efficient continuous-time analysis of the patient flow and resource utilization dynamics while maintaining a good level of accuracy, w.r.t. the original model.

The proposed TCPN model is depicted in Fig. 6.6. It contains some modifications w.r.t. the original SWN, which will be explained in the following. As in the original discrete model, it captures the clinical pathway for hip fracture treatment: it consists of all the tasks that need to be done during the pre-operative day of hospitalization (left side of the figure), the surgery (at

the bottom of figure), and the post-operative day (right side of the figure). The TCPN model includes places that represent both the patients (p_1) and the resources of the system, such as nurses (p_{41}) and doctors (p_{42}). The model shows how these entities are utilized throughout the clinical pathway.

Originally, the SWN contains *conflicts* that represent the different alternatives through the clinical pathway. For instance, p_6 models the possibility of the patient having a urinary infection or not. In the SWN (Fig. 8 in Bernardi et al. [2019]), a *choice place* is used to model this scenario and a probabilistic resolution policy is used to solve the conflict. For this particular case, statistically, only 10% of the patients suffer from urinary infection and need an urgent pre-operative study (procedure modeled from p_7 to t_9) while 90% of the cases can continue the pathway without it. For simplicity of analysis, we remove the probabilistic choices in our model by introducing equivalent structures composed by *fork transitions* (t_6, t_{10}, and t_{37}) that divide the token flow proportionally to each branch's probability. For instance, for t_6, for each token that consumes, it allocates 0.9 tokens to the first branch and 0.1 tokens to the second branch, representing the behavior of the original system.

Next, to set the parameters for performance evaluation purposes, we need to determine the timing of the transitions. For the SWN, the mean time delay of each transition is defined according to the time interval it takes to accomplish the task it represents. This information is reported in Table 1 of Bernardi et al. [2019]. The SWN model has two types of transitions: immediate and timed. The former type represents events that occur instantaneously, such as the allocation and release of resources or probabilistic choices (depicted as black transitions in Fig. 6.6). The latter represents the tasks that must be performed during the clinical path (depicted as white transitions in the figure). This information is used to define the firing rate of the transitions in the TCPN model, summarized in Table A.1. It is worth noticing that we assume that the timing of the immediate transitions is not instantaneous but only much faster than the rest of the transitions. This way, we can still consider the controllability analysis techniques from the previous chapters, which do not consider the case of immediate transitions, while still obtaining a good approximation of the original model.

Table 6.1

Firing rates of the transitions of the clinical pathway.

Transitions set	Timing (1/min)
$\{t_4, t_5, t_{12}, t_{15}, t_{16}, t_{20}\}$	1
$\{t_{11}, t_{17}, t_{29}, t_{30}, t_{34}, t_{38}\}$	1/5
$\{t_3, t_{28}\}$	1/15
$\{t_8, t_{25}, t_{31}\}$	1/30
$\{t_{23}\}$	1/120
$\{t_1, t_2, t_6, t_7, t_9, t_{10}, t_{13}, t_{14}, t_{18},$ $t_{19}, t_{21}, t_{22}, t_{24}, t_{26}, t_{27}, t_{32}, t_{33}$ $t_{35}, t_{36}, t_{37}, t_{39}, t_{40}\}$	10

Finally, the initial marking of the system is determined by the number of available entities: number of patients nP, number of nurses nN, and number of doctors nD. Initially, the marking in the rest of the places is 0, representing that no patient is receiving care. Several cases will be simulated in order to validate the model. For more information on the modeled clinical pathway, please see Bernardi et al. [2019].

6.3.3. TCPN model validation

In order to validate the proposed TCPN, we present the performance results of our model under different assumptions of patient workload and resource plan and compare them with the results obtained for the SWN in Bernardi et al. [2019]. The results are summarized in Fig. 6.7. The performance index of interest is the cycle time of t_1, CT_{t_1}, multiplied by the number of patients, nP, i.e., $CT = CT_{t_1} nP$. This measure corresponds to the mean time spent for a patient to undergo the treatment Bernardi et al. [2019]. The CT values for the discrete case were obtained by event-driven simulation using GreatSPN [1] [Amparore et al., 2016] and the SWN model.

To calculate this performance index in the TCPN system, we first obtain the cycle time of a transition by analyzing its throughput (the flow through its transitions at the steady state) [Silva et al., 2011]. This was performed by simulating the behavior of the system until it reached a steady state, using SimHPN[2]. The throughput of transition t_1 can then be obtained from the flow at the steady state, $\mathbf{f}_{ss}$, as

$$\chi_1 = \mathbf{f}_{ss}[t_1]$$

Specifically, the throughput of a transition corresponds to the inverse of its cycle time. Hence,

[1] GreatSPN2.0, available at `http://www.di.unito.it/~greatspn/index.html`

[2] The simulations are performed using the algorithms implemented on SimHPN with a computer with i5-6600 CPU @ 3.30GHz and 16GB RAM.

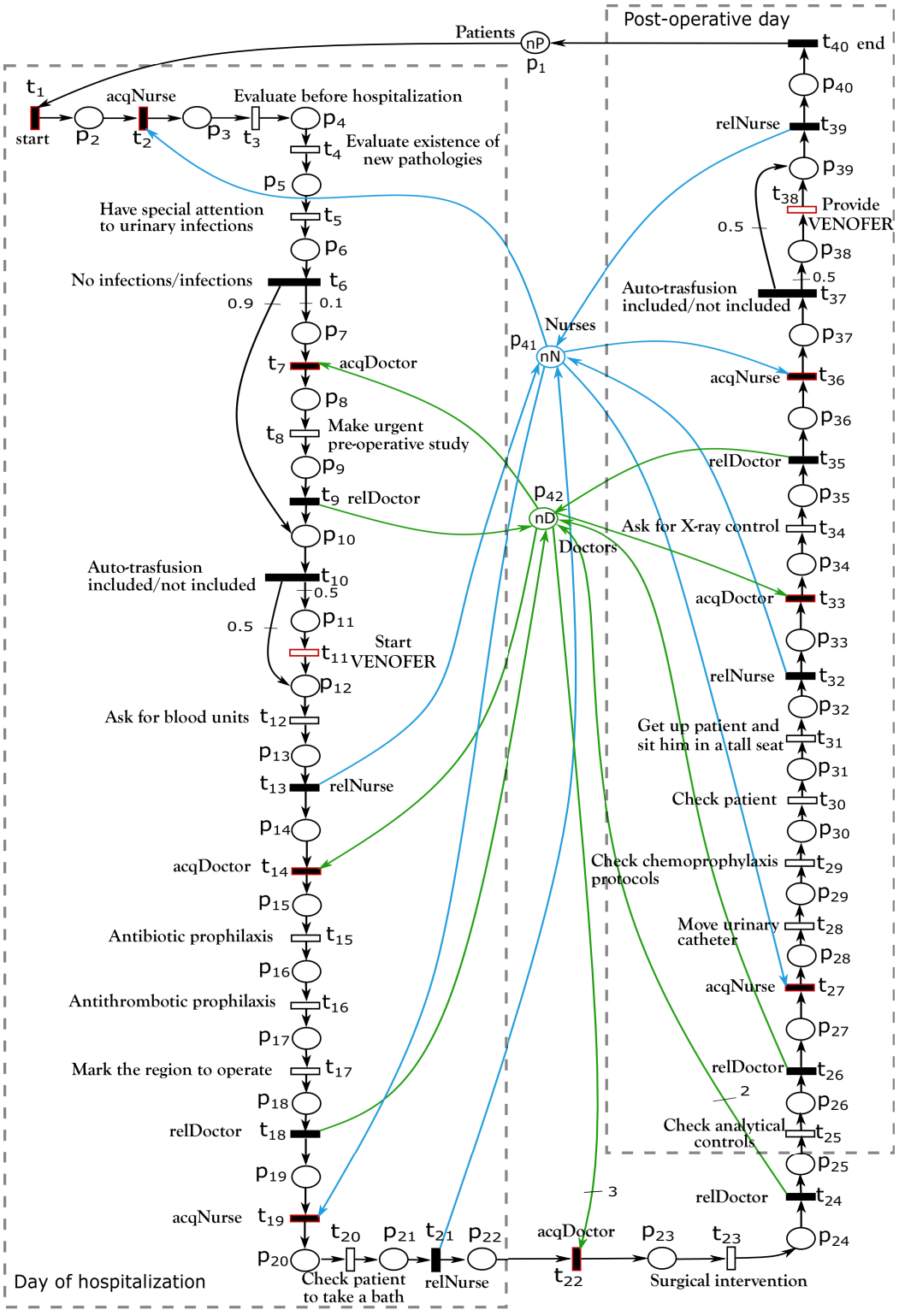

Figure 6.6. A TCPN system that models a hip fracture clinical pathway. The controllable transitions of the system are represented with a red outline. The model is contained in SimHPN's models folder as Model_HipFractureClinicalPathway_SS.mat

the overall performance index can be computed as

$$CT = \frac{1}{\chi_1} nP \frac{1}{1440}$$

where the factor $\frac{1}{1440}$ is added to convert the time units from minutes (used in the TCPN simulation) to days.

The simulation results for both models are reported in Fig. 6.7. We simulated the 26 different scenarios presented in Bernardi et al. [2019], where the authors considered several patient workloads on the interval $[1, 100]$ and different personnel resource plans. We compared the CT obtained by using our proposed fluid model (5^{th} column) against the one obtained by the event-driven simulation (8^{th} column). The table also shows the relative error between the performance values computed with both techniques (6^{th} column). The error was computed by considering the results of the event-driven simulation as reference values:

$$\text{Rel.Err} = \frac{CT^{SWN} - CT^{TCPN}}{CT^{SWN}} \times 100$$

Furthermore, the solution time for obtaining the performance values in each case is reported in columns 7 and 9.

The results in Fig. 6.7 show that the TCPN system provides a suitable approximation for the problem under consideration. Notably, the error tends to decrease as the number of tokens (resources) increases. This is likely due to the fact that fluidization typically provides a good approximation of the original system in highly marked systems Mahulea et al. [2009], which are often the most challenging cases to analyze for the SWN model. Overall, the relative error between the TCPN approximation and the SWN model is relatively low, with a maximum error of 21.05% occurring in only one scenario (case 5), in which the number of tokens is relatively low. For the rest of the scenarios, the error is below 12.25%, indicating that *the TCPN approximation provides an accurate representation of the system behavior*. Moreover, we observed that the simulation time of the SWN model worsens as the number of resources increases. In contrast, the TCPN simulation can handle larger systems with less computational time, making it a more scalable approach for complex systems.

6.3.4. Control and optimization of the fluid model

The use of the TCPN model offers the advantage of enabling the application of various analysis and design techniques developed for this formalism. In this section, we demonstrate how this feature can be leveraged to improve the performance of the system by analyzing its controllability and designing an appropriate control law. In particular, we show the implementation of a control law that enables the system to reach its state of maximum throughput more quickly.

	Resources			TCPN Sim			SWN Sim	
Case	**nP**	**nD**	**nN**	**CT**	**Rel.Err.**	**Sol. Time**	**CT**	**Sol. Time**
1	100	3	5	9.396	11.53%	303.19	10.62	11.03
2	76	3	5	7.141	11.89%	227.83	8.105	8.02
3	50	3	5	4.698	12.24%	128.77	5.353	6.01
4	26	3	5	2.443	10.97%	61.26	2.744	3.04
5	2	3	5	0.1879	21.05%	9.25	0.238	0.03
6	1	3	5	0.1712	0.71%	6.89	0.17	0.02
7	100	6	5	4.698	7.97%	134.29	5.105	59
8	76	6	5	3.5703	10.43%	99.06	3.986	40.08
9	50	6	5	2.349	9.23%	67.34	2.588	29.06
10	26	6	5	1.2214	10.91%	29.22	1.371	15.01
11	2	6	5	0.1708	0.70%	9.23	0.172	0.05
12	100	9	5	3.1318	6.99%	79.23	3.367	132.08
13	76	9	5	2.3803	8.31%	64.08	2.596	98.07
14	50	9	5	1.566	7.12%	39.78	1.686	65.08
15	26	9	5	0.8143	6.29%	21.53	0.869	36.08
16	2	9	5	0.1708	1.07%	9.45	0.169	3.07
17	100	15	5	1.879	4.62%	63.84	1.97	1123.04
18	76	15	5	1.428	5.49%	37.24	1.511	936.08
19	50	15	5	0.94	5.72%	24.37	0.997	416.01
20	26	15	5	0.488	4.87%	12.20	0.513	200.07
21	2	15	5	0.1707	1.01%	7.61	0.169	2.03
22	100	25	5	1.1503	3.58%	274.14	1.193	1293.06
23	76	25	5	0.8742	1.66%	228.07	0.889	578.08
24	50	25	5	0.575	1.71%	248.67	0.585	707.02
25	26	25	5	0.299	8.00%	202.34	0.325	106.06
26	2	25	5	0.1708	0.47%	9.79	0.17	88.02

Figure 6.7. Cycle time (CT) values estimated using TCPN (5^{th} column) and SWN simulation (8^{th} column). The relative error between both techniques is also reported (6^{th} column) and the solution time for each of the different scenarios (7^{th} and 9^{th} columns). CT values are given in days and the solution time in seconds.

We provide simulation results to demonstrate the effectiveness of our controller in practical settings.

6.3.5. Structural controllability analysis using SimHPN

In this section, we analyze the controllability of the fluid model employing the techniques developed in this thesis, which we have implemented in the toolbox SimHPN. The model and parameters of this system are included in the toolbox (to load the model select *Model* → *Import from .mat file* → *models\Model_HipFractureClinicalPathway_SS.mat*). The controllability test can be carried out by selecting *Continuous* → *Structural controllability analysis* → *Net rank-controllability test* (Fig. 6.1). This test verifies sufficient conditions for net rank-controllability efficiently. The transitions that can be controlled are depicted with a red outline in Fig. 6.6. They represent the events of the patients entering the pathway, assigning nurses and doctors to the different stages of the process and some tasks within the pathway. We present 3 control scenarios

1. $T_c = \{t_1, t_{11}, t_{38}\}$, i.e., *the events of assigning nurses and doctors cannot be controlled*: For this case, we obtain the message:
   "*Influence is not total! Therefore, the set of controllable transitions does not guarantee net rank-controllability. The only influenced nodes are: Places = [1 2 3 4 5 6 7 10 11 12 13 14 38 39 40 41] Transitions = [1 2 3 4 5 6 10 11 12 13 38 39 40]*".
   From a system point of view, total influence means that the behavior of all states in the system can be influenced by a set of controllable transitions, which is a necessary condition for NRC. In the context of a clinical pathway, if the property of influence is not fulfilled, it means that there are some modes of operation (configurations) in which the behavior of several parts of the pathway cannot be affected by means any control action.

2. $T_c = \{t_1, t_7, t_{11}, t_{14}, t_{22}, t_{38}\}$, i.e., *the events of assigning nurses cannot be controlled*: By entering this set of controllable transitions we obtain the message
   "*It is not possible to decide if the timed net is net rank-controllable. The condition related to the choice places is not fulfilled.*".
   In this case the test cannot conclude if the system is NRC, since one of the structural sufficient conditions does not hold. In particular, the one related to the choice places. This serves to give indications to the user about where the problem may be in order to guarantee controllability.

3. $T_c = \{t_1, t_2, t_7, t_{11}, t_{14}, t_{19}, t_{22}, t_{27}, t_{33}, t_{36}, t_{38}\}$, i.e., *the allocation of these resources can be decided upon*: Here we choose the set that we will consider in our case study, which is such that it satisfies all the structural conditions for controllability and is indicated by the message:
   "*The timed net is net rank-controllable.*"

6.3.6. Control law implementation

After dealing with the controllability analysis, we turn our attention to the following control design problem:
Given a TCPN system, $\langle \mathcal{N}, \boldsymbol{\lambda}, \mathbf{m}_0 \rangle$ and a required target marking, $\mathbf{m}_r$, design a control law that drives the marking of the TCPN from $\mathbf{m}_0$ to $\mathbf{m}_r$, and then keeps the marking at $\mathbf{m}_r$ indefinitely.

To solve this problem from our particular case study, we adopt a control law presented in Ross-León et al. [2014], originally designed for the case where all the transitions are controllable. This scheme is based on defining a required marking, $\mathbf{m}_r \in \mathbb{E}$ and defining the marking error as:

$$\mathbf{e}(\tau) = \mathbf{m}_r - \mathbf{m}(\tau) \tag{6.1}$$

Based on this, we can now define the *contribution degree* of a controllable transition. This is a measure of how much the firing of a particular transition contributes to reducing the overall error in the system, formally defined as:

The *contribution degree* of the k-th transition, $\Psi_k(\tau)$, is defined as:

$$\Psi_k(\tau) = \mathbf{e}^T(\tau)\mathbf{C}[\bullet, k] \tag{6.2}$$

Now, we can define the control law as follows:

Definition 6.1. *Let $\langle \mathcal{N}, \boldsymbol{\lambda}, \mathbf{m}_0 \rangle$ be a TCPN system and $\mathbf{m}_r \in \mathbb{E}$ be the required marking. For each $t_k \in T_c$, its control input at instant τ is given by:*

$$I_{ck}(\tau) = \begin{cases} 1 & \text{if } \Psi_k(\tau) > 0 \\ 0 & \text{otherwise} \end{cases} \tag{6.3}$$

The goal is to reach a state that guarantees maximum throughput, i.e., allocate the available resources to ensure the optimal performance of the system. To establish the target marking, we can use SimHPN to compute such a state using: *Continuous* → *Optimal* → *Optimal Control*. In order to compare the performance of the controlled system against the unforced system ($\mathbf{u}(\tau) = \mathbf{0}$), we choose the state of maximal throughput of the unforced system as our target. To do this, we set the value of Uncontrolled Transitions as = [1:40] (as if there are no controllable transitions), in the optimal control menu and use the default values for the "Gain Vector w.r.t. Flow: w" and "Cost Vector Due to Immobilization to Maintain the Product Flow z" options. Although other target markings could be chosen by applying additional constraints,

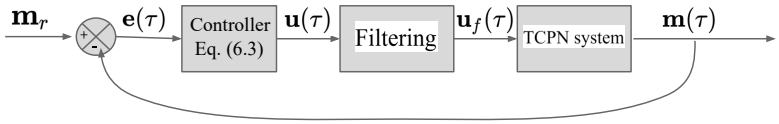

Figure 6.8. Control scheme for the TCPN system.

we select this one to enable a direct comparison. The obtained target marking is

$$\begin{aligned}\mathbf{m}_r = [&0.0022\ 0.0022\ 0.3326\ 0.0222\ 0.0222\ 0.0022\ 0.0002\ 0.0665\ 0.0002\ 0.0022\\ &0.0554\ 0.0222\ 0.0022\ 0.0022\ 0.0222\ 0.0222\ 0.1109\ 0.0022\ 0.0022\ 0.0222\\ &0.0022\ 70.5474\ 2.6607\ 0.0022\ 0.6652\ 0.0022\ 0.0022\ 0.3326\ 0.1109\ 0.1109\\ &0.6652\ 0.0022\ 0.0022\ 0.1109\ 0.0022\ 0.0022\ 0.0022\ 0.0554\ 0.0022\ 0.0022\\ &3.1659\ 0.0067]^T\end{aligned}$$

Once an optimal steady state has been computed, the objective is to reach and maintain the desired marking in the shortest amount of time possible.

Before implementing the proposed control law (Eq. 6.3), it is important to notice that due to its nature, it will generate a high-frequency control input Ross-León et al. [2014], switching between two possible states: a transition working at maximum capacity (when the value is 1) and stopping its activity (when the value is 0). Therefore, the control input may lack physical meaning for the discrete system, making its interpretation and implementation difficult. Nevertheless, we propose a solution by implementing the control scheme depicted in Fig. 6.8 that adapts the high-frequency switching input to a smoother, more physically meaningful signal, ensuring that our approach is not only feasible but also suitable for the intended application.

In particular, we filtered the On-Off control input of each transition by computing the *running mean* of the corresponding control signal and applying a first-order low-pass filter to it (using off-the-shelf functions in MATLAB). The result of this procedure is depicted in Fig. 6.9 for the control signal of t_7. The upper subplot shows the high-frequency control input computed with Eq. (6.3). The zooms on the plot show how the duty cycle of the signals changes over time. The lower subplot shows the filtered signal, which captures the control input as a smoother control signal for the controllable transitions of the system.

Figure 6.10 shows the simulation results of the implemented control: The upper subplot depicts the marking error (the difference between the desired and the current state) of the unforced case; the lower subplot depicts the marking error for the forced case. Notice that it takes more than 1700 minutes for the unforced case to reach the target. On the contrary, for the forced case it takes around 700 minutes to reach it. The filtered control signal on the different transitions is depicted in Fig. 6.11.

To interpret the physical meaning of the simulation results in the context of the clinical

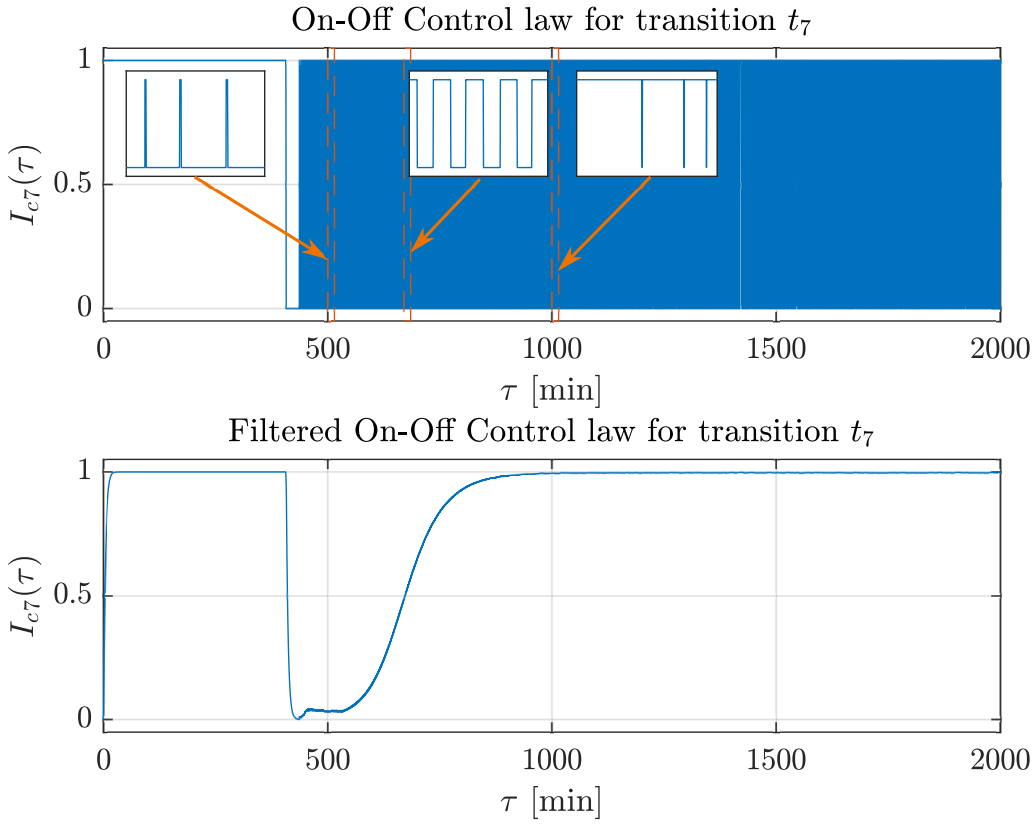

Figure 6.9. Filtering control input of transition t_7.

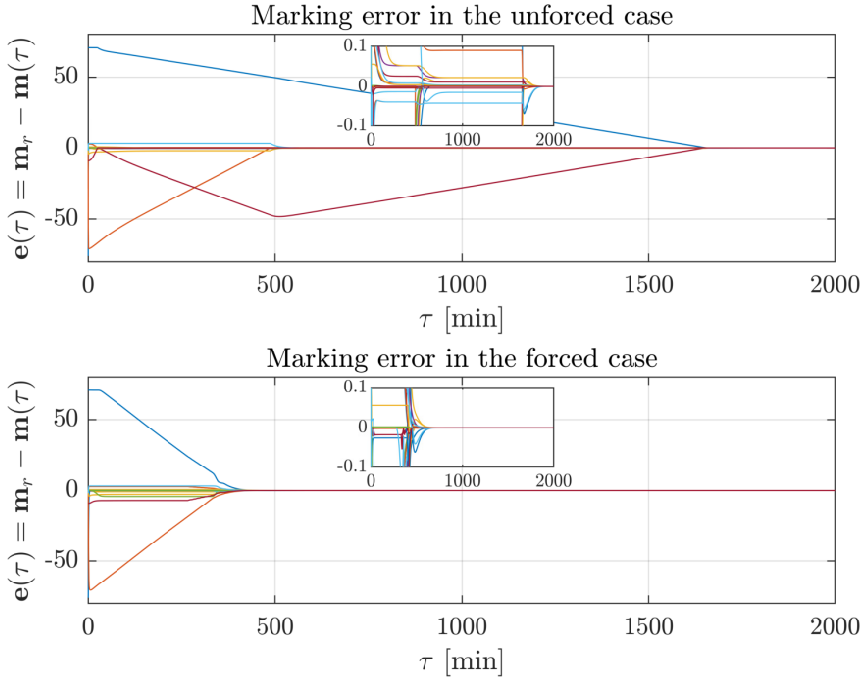

Figure 6.10. Marking error for the unforced and the forced case.

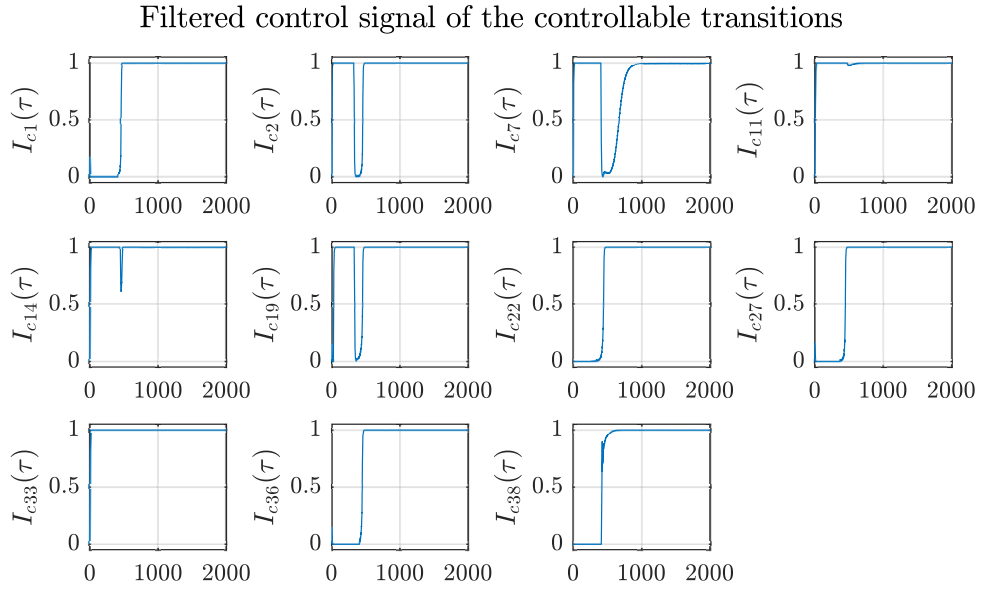

Figure 6.11. Filtered control signal of the controllable transitions.

pathway, it is important to remember that the control inputs in our model correspond to delays in the firing rate of certain transitions. In a clinical pathway model with limited resources, the delays represent the addition of extra time to certain activities to prioritize others, thus optimizing the use of the available resources to ensure that the system achieves its maximum productivity as quickly as possible. For instance, in Fig. 6.11, the delay added to transition t_1 (which represents the entrance of patients to the pathway), can be seen as the rate at which patients enter the pathway is being regulated to avoid bottlenecks in the early parts of the process and prioritize the efficient use of the available personnel. Another example is the control actions of t_7 and t_{22} which represent the use of doctors in a pre-operative phase and during the surgery, respectively: at the beginning of the process, we may prioritize the use of doctors during the preoperative stage (t_7), to ensure that patients are adequately prepared for surgery. As more patients enter the pathway and become ready for surgery, we can then shift the focus to the surgical stage (t_{22}), where doctors are needed to perform the operations. These are examples of how, by carefully controlling the flow through the controllable transitions, we can ensure that the available resources are utilized efficiently and that the system reaches its steady state as quickly as possible, optimizing the overall throughput of the system.

6.4 — Concluding remarks

In this chapter, we presented different contributions to showcase the applicability of the results presented in the previous chapters.

First, we showed the implementation of the results presented in previous chapters in the toolbox SimHPN. The implementation of these algorithms in SimHPN provides a practical tool

for researchers and practitioners to analyze complex systems modeled as TCPNs, enhancing the practical applicability and accessibility of our research.

Then, as a first case study, we showed the use of SimHPN for the analysis of a Kanban-like flexible manufacturing system, showcasing the results in the analysis of controllability and the computation of equilibrium sets.

As a second case study, we proposed a novel approach using timed continuous Petri nets to analyze and optimize healthcare systems through clinical pathways. Our approach is demonstrated through a case study of a hip fracture clinical pathway at the "Lozano Blesa" University Clinical Hospital, in Zaragoza Spain. First, it was shown that the TCPN model can be used to perform a more efficient analysis of the patient flow and resource utilization dynamics of the system while maintaining a good level of accuracy, w.r.t. the discrete techniques. Next, a control scheme that enables the modeled system to reach its state of maximum throughput more quickly, was proposed. The effectiveness of the proposed method is demonstrated using simulation results.

While a formal proof of convergence for the proposed control scheme is not provided, the chapter highlights its potential and the need for further investigation to understand its limitations. Future research can also explore the practical implementation of the proposed control scheme into the discrete system, following a similar scheme as the one proposed in Vázquez and Silva [2009].

Chapter 7

Conclusions and Future Work

This chapter summarizes the main contributions presented in this thesis and discusses some of the possible future research directions.

7.1 — Concluding remarks

This dissertation presents a structural theory for the analysis of controllability in timed continuous Petri nets under infinite server semantics:

• In Chapter 3, it was demonstrated that the analysis of *Bounded Input Controllability* (BIC) in TCPN systems, under infinite server semantics, can be studied through property of *net rank-controllability* (NRC), a *global structural property* of the TCPN. There, the relationship between both properties was established. First, the relation between NRC and BIC in a single region was stated, and then, between multiple regions in a given system. In particular, an important result was introduced: *if the system is live as untimed, then, NRC is a sufficient condition for BIC over multiple regions* (each of the Macro-regions of the system) (Thm. 3.1). Moreover, it was pointed out that *in non-live systems NRC is not sufficient nor necessary for BIC.*
Furthermore, a first necessary structural condition for NRC, was derived: the control actions must *influence* the marking at all the nodes of the net, in any given configuration. The property of influence was defined and then, intuitively explained by showing the relationship between controllability and its connection to the the structure of the net. It was shown that influence can be verified from the net structure in *polynomial* time, avoiding the analysis by configurations. However, it was established that influence is not a sufficient condition since, even if influence is fulfilled, there might exist a linear dependence between marking variations in different places (i.e., due to the existence of *uncontrollable marking invariants* corresponding to the *uncontrollable invariant subspaces* of the system [Wonham, 1985]).

• In order to deal with that, Chapter 4 introduces a series of structural conditions to guarantee NRC. This is achieved by introducing the *effective flow dynamic system*. We study the controllability of this system by defining the uncontrollable flow invariants (UFIs), which

correspond the uncontrollable invariant subspaces of the flow system. The existence of UFIs was then associated with net structural objects such as P-flows or choice places, among others, thus facilitating the characterization of the controllability of the flow system. Finally, as it was shown in Lemma 4.2 and Proposition 4.6, the controllability of the flow system can be related to the property of NRC. Taking this into consideration, in Thm. 4.2, it was demonstrated that *if total influence holds and there are no UFIs, NRC is guaranteed*. Finally, polynomial-time algorithms based only on purely structural conditions from the net for the verification of NRC (and therefore, for the verification of BIC), were provided. These algorithms are able to verify, in polynomial time, sufficient conditions for NRC (i.e., that the rank of the controllability matrices in all the configurations has its maximum possible rank), regardless of the potentially exponential number of configurations.

• In Chapter 5, different methods for analyzing the equilibrium sets of TCPN systems were presented. The study of this sets and its connectivity is closely related to the analysis of controllability, as stated extensively in Chapter 2. We defined the connectiviy graph of a system, $\langle V, E\rangle$, as a graph containing the information of the equilibrium markings in all of the different regions of the system. First, a general approach was introduced to compute this graph and analyze its connectivity. The idea is to reduce the complexity of the analysis of connectivity by means of pre-processing the TCPN information. It was tested against benchmarks of real-life systems, obtaining a significant reduction in the complexity of the analysis, compared to the brute force methods used in the literature.
Moreover, the analysis for subclasses of nets was adressed. In particular, a qualitative analysis of the equilibrium sets in Topologically Equal Conflict (TEC) systems is presented. First, for unforced, conservative, and consistent Choice-Free systems, with suitable $\mathbf{m}_0$, the relation between the number of equilibrium points of the system and the qualitative characteristics of its *maximal limiting subnet* (MLS) is presented. In particular, it was shown that when the MLS is strongly connected there exists a unique equilibrium marking in the system. Otherwise, an infinite number of them exist. Moreover, it is shown that the connectivity of the equilibrium sets is always fulfilled. Finally, those results are straightforwardly extended to unforced TEC systems. This can be used to state stronger controllability results and as a useful tool for the synthesis of controllers in TEC systems.
Regarding the analysis of controllability in TCPNs, the previous results complement the results presented in chapters 3 and 4 in the following manner:

- Given a TCPN system that is NRC, if $\langle V, E\rangle$ is strongly connected, then, the system is globally controllable, i.e., BIC over the set of all of its equilibrium markings.
- Given a TCPN system that is NRC, if $\langle V, E\rangle$ is not strongly connected, the system is BIC over the each of the Macro-Regions of the system.

Clearly, the complexity of the method is still heavily influenced by the initial number of config-

urations of the TCPN system. Nevertheless, the substantial reduction in the number of pairs to analyze when using the proposed method is a promising development.

• Finally, in Chapter 7, we presented different contributions to showcase the applicability of the results presented in the previous chapters. First, we showed the implementation of our results in the toolbox SimHPN. The implementation of these algorithms in SimHPN provides a practical tool for researchers and practitioners to analyze complex systems modeled as TCPNs, enhancing the practical applicability and accessibility of our research.
Then, as a first case study, we showed the use of SimHPN for the analysis of a Kanban-like flexible manufacturing system, showcasing the results in the analysis of controllability and the computation of equilibrium sets. As a second case study, we proposed a novel approach using timed continuous Petri nets to analyze and optimize healthcare systems through clinical pathways. Our approach is demonstrated through a case study of a hip fracture clinical pathway at the "Lozano Blesa" University Clinical Hospital, in Zaragoza Spain. First, it was shown that the TCPN model can be used to perform a more efficient analysis of the patient flow and resource utilization dynamics of the system while maintaining a good level of accuracy, w.r.t. the discrete techniques.
Next, a control scheme for TCPNs under ISS with the presence of uncontrollable transitions was proposed. The scheme is based on an On-Off type control over the firing speed at the controllable transitions that reduce the difference between the desired and actual state of the system. The proposed control law can be computed easily online, despite the complexity of a given system. In order to study the effectiveness of the proposed method, it was implemented in the case study of the clinical pathway. By using simulation results, it was shown that the control scheme enables the modeled system to reach its state of maximum throughput more quickly.
It is important to note that the proposed control scheme's applicability extends beyond the presented case study, since its general formulation allows for implementation in general TCPN systems. While a formal proof of convergence for the proposed control scheme is not provided, this chapter highlights its potential and the need for further investigation to understand its limitations.

7.2 — Future work

Considering the research done during this thesis, some of the problems which remain open or require more research, are stated below:

A first next step on this research will be to extend the study of NRC to non-live systems. By using the most recent results in the literature about the structural analysis of liveness and deadlock avoidance, a first approach would be formulating methodologies, by means of an appropriate control strategy, for enforcing liveness in a given TCPN system. After that, the

results from this thesis could be used in the resulting live system. Moreover, extending the results presented for the analysis of NRC to particular subclasses would be useful to obtain stronger results and determine supplementary information about the connection between the controllability property and the net structure.

Regarding the results related to the analysis of equilibria, as future work, it is expected to extend the results herein presented to the forced TEC systems. Since a forced system can be viewed as an unforced one with timing variations and, due to the linear behaviour of a system within each single region, it is expected that connectivity will hold for the forced case. Moreover, a possible extension of the presented work will be the study of the connectivity of equilibrium sets in more general subclasses such as Mono-T-Semiflow systems, by pursuing the structural approach herein presented.

Moreover, as in the case of the case study of the clinical pathway presented in Chapter 6, a fluid version of the model of the manufacturing process for transport platforms (Appendix A) could be developed in order to use the results presented in this thesis, allowing the analysis of different properties of the system, such as controllability, control design, and more efficient steady-state performance.

Finally, regarding the results from the presented control scheme, further investigation should be provided to guarantee its applicability in broader classes of systems. Furthermore, some future work could explore the practical implementation of the proposed control scheme into the discrete system, following a similar scheme as the one proposed in Vázquez and Silva [2009].

Este capítulo resume las principales contribuciones presentadas en esta tesis y discute algunas posibles direcciones para investigaciones futuras.

7.3 — Observaciones finales

Esta disertación presenta una teoría estructural para el análisis de la controlabilidad en redes de Petri continuas temporizadas bajo la semántica de infinitos servidores:

• En el Capítulo 3, se demostró que el análisis de la *Controlabilidad con Entrada Acotada* (BIC) en sistemas TCPN, bajo la semántica de infinitos servidores, puede estudiarse a través de la propiedad de *net rank-controllability* (NRC), una *propiedad estructural global* de la TCPN. Allí, se estableció la relación entre ambas propiedades. Primero, se indicó la relación entre NRC y BIC en una sola región, y luego, entre múltiples regiones en un sistema dado. En particular, se introdujo un resultado importante: *si el sistema es vivo, entonces, NRC es una condición suficiente para BIC sobre múltiples regiones* (las Macro-regiones del sistema) (Thm. 3.1). Además, se señaló que *en sistemas no vivos, NRC no es suficiente ni necesario para BIC.* Además, se derivó una primera condición estructural necesaria para NRC: las acciones de control deben *influir* en el marcado en todos los nodos de la red, en cualquier configuración dada. La propiedad de influencia fue definida y luego, explicada de manera intuitiva al mostrar la relación entre la controlabilidad y su conexión con la estructura de la red. Se demostró que la influencia se puede verificar desde la estructura de la red en tiempo *polinómico*, evitando el análisis por configuraciones. Sin embargo, se estableció que la influencia no es una condición suficiente, ya que, incluso si se cumple la influencia, podría existir una dependencia lineal entre las variaciones de marcado en diferentes lugares (es decir, debido a la existencia de *invariantes de marcado no controlables* correspondientes a los *subespacios invariantes no controlables* del sistema [Wonham, 1985]).

• Para abordar esto, el Capítulo 4 introduce una serie de condiciones estructurales para garantizar NRC. Esto se logra mediante la introducción del *sistema dinámico de flujo efectivo.* Estudiamos la controlabilidad de este sistema al definir los invariantes no controlables de flujo (UFIs), que corresponden a los subespacios invariantes no controlables del sistema de flujo. La existencia de UFIs luego se asoció con objetos estructurales de la red, como P-flujos o lugares de elección, entre otros, facilitando así la caracterización de la controlabilidad del sistema de flujo. Finalmente, como se mostró en el Lema 4.2 y la Proposición 4.6, la controlabilidad del sistema de flujo se puede relacionar con la propiedad de NRC. Considerando esto, en Thm. 4.2, se demostró que *si se cumple la influencia total y no hay UFIs, se garantiza NRC.* Finalmente, se proporcionaron algoritmos en tiempo polinómico basados solo en condiciones puramente estructurales de la red para la verificación de NRC (y, por lo tanto, para la verificación de BIC). Estos algoritmos pueden verificar, en tiempo polinómico, condiciones suficientes para NRC (es decir, que el rango de las matrices de controlabilidad en todas las configuraciones

tenga su rango máximo posible), independientemente del potencial número exponencial de configuraciones.

• En el Capítulo 5, se presentaron diferentes métodos para analizar los conjuntos de equilibrio de sistemas TCPN. El estudio de estos conjuntos y su conectividad está estrechamente relacionado con el análisis de la controlabilidad, como se detalla extensamente en el Capítulo 2. Definimos el grafo de conectividad de un sistema, $\langle V, E\rangle$, un grafo que contiene la información de los conjuntos de marcados de equilibrio en todas las diferentes regiones del sistema. En primer lugar, se introdujo un enfoque general para calcular este grafo y analizar su conectividad. La idea es reducir la complejidad del análisis de conectividad mediante el preprocesamiento de la información de TCPN. Se probó con benchmarks de la literatura, que modelan sistemas reales, obteniendo una reducción significativa en la complejidad del análisis, en comparación con los métodos de fuerza bruta utilizados en la literatura. Además, se abordó el análisis de subclases de redes. En particular, se presenta un análisis cualitativo de los conjuntos de equilibrio en sistemas Conflictos Topológicamente Igualados (TEC). Primero, para sistemas no forzados, conservativos y consistentes sin elecciones (CF), con un $\mathbf{m}_0$ adecuado, se presenta la relación entre el número de puntos de equilibrio del sistema y las características cualitativas de su *Maximal Limiting Subnet* (MLS). En particular, se mostró que cuando la MLS está fuertemente conectada, existe un marcado de equilibrio único en el sistema. De lo contrario, existen infinitos. Además, se muestra que la conectividad de los conjuntos de equilibrio siempre se cumple. Finalmente, esos resultados se extienden directamente a sistemas TEC no forzados. En cuanto al análisis de la controlabilidad en TCPNs, los resultados anteriores complementan los resultados presentados en los capítulos 3 y 4 de la siguiente manera:

- Dado un sistema TCPN que es NRC, si $\langle V, E\rangle$ es fuertemente conexo, entonces, el sistema es globalmente controlable, es decir, BIC sobre el conjunto de todos sus marcados de equilibrio.
- Dado un sistema TCPN que es NRC, si $\langle V, E\rangle$ no es fuertemente conexo, el sistema es BIC sobre cada una de las Macro-Regiones del sistema.

Claramente, la complejidad del método sigue estando fuertemente influenciada por el número inicial de configuraciones del sistema TCPN. No obstante, la reducción sustancial en la cantidad de pares a analizar al utilizar el método propuesto es un desarrollo prometedor.

• Finalmente, en el Capítulo 7, presentamos diferentes contribuciones para demostrar la aplicabilidad de los resultados presentados en los capítulos anteriores. En primer lugar, mostramos la implementación de nuestros resultados en el toolbox de MATLAB, SimHPN. La implementación de estos algoritmos en SimHPN proporciona una herramienta práctica para que investigadores y profesionales analicen sistemas complejos modelados como TCPNs, mejorando la aplicabilidad práctica y accesibilidad de nuestra investigación. Luego, como primer caso de estudio, mostramos el uso de SimHPN para el análisis de un sistema de fabricación flexible tipo

Kanban, exhibiendo los resultados en el análisis de la controlabilidad y el cálculo de conjuntos de equilibrio. Como segundo estudio de caso, propusimos un enfoque nuevo utilizando redes de Petri continuas temporizadas para analizar y optimizar sistemas de atención médica a través de trayectorias clínicas. Nuestro enfoque se demostró a través de un caso de estudio de una vía clínica de fractura de cadera en el Hospital Clínico Universitario "Lozano Blesa" de Zaragoza, España. Primero, se mostró que el modelo TCPN puede utilizarse para realizar un análisis más eficiente de la dinámica de flujo de pacientes y la utilización de recursos del sistema, manteniendo un buen nivel de precisión en comparación con las técnicas discretas.
A continuación, se propuso un esquema de control para TCPNs bajo ISS con la presencia de transiciones no controlables. El esquema se basa en un control tipo On-Off sobre la velocidad de disparo en las transiciones controlables que reduce la diferencia entre el estado deseado y real del sistema. La ley de control propuesta puede calcularse fácilmente en línea, a pesar de la complejidad de un sistema dado. Para estudiar la efectividad del método propuesto, se implementó en el caso de estudio de la vía clínica. Mediante resultados de simulación, se mostró que el esquema de control permite que el sistema modelado alcance su estado de máxima capacidad más rápidamente.
Es importante señalar que la aplicabilidad del esquema de control propuesto se extiende más allá del caso de estudio presentado, ya que su formulación general permite su implementación en sistemas TCPN generales. Aunque no se proporciona una prueba formal de convergencia para el esquema de control propuesto, este capítulo destaca su potencial y la necesidad de una investigación adicional para comprender sus limitaciones.

7.4 — Trabajo futuro

Considerando la investigación realizada durante esta tesis, se presentan a continuación algunos de los problemas que aún están abiertos o requieren más investigación:

Un primer paso siguiente en esta investigación será extender el estudio de NRC a sistemas no vivos. Utilizando los resultados más recientes en la literatura sobre el análisis estructural de vivacidad y evitación de bloqueos, un primer enfoque sería formular metodologías, mediante una estrategia de control adecuada, para hacer cumplir la vivacidad en un sistema TCPN dado. Después de eso, los resultados de esta tesis podrían utilizarse en el sistema en vivo resultante. Además, extender los resultados presentados para el análisis de NRC a subclases particulares sería útil para obtener resultados más sólidos y determinar información adicional sobre la conexión entre la propiedad de controlabilidad y la estructura de la red.

En relación con los resultados relacionados con el análisis de equilibrios, como trabajo futuro, se espera extender los resultados presentados aquí a sistemas TEC forzados. Dado que un sistema forzado puede considerarse como uno no forzado con variaciones temporales y, debido al comportamiento lineal de un sistema dentro de cada región única, se espera que

la conectividad se mantenga para el caso forzado. Además, una posible extensión del trabajo presentado será el estudio de la conectividad de los conjuntos de equilibrios en subclases más generales, como los sistemas Mono-T-Semiflow, siguiendo el enfoque estructural presentado aquí.

Además, como en el caso de estudio de la vía clínica presentada en el Capítulo 6, se podría desarrollar una versión fluida del modelo del proceso de fabricación para plataformas de transporte (Apéndice A) para utilizar los resultados presentados en esta tesis, permitiendo el análisis de diferentes propiedades del sistema, como la controlabilidad, el diseño del control y un rendimiento más eficiente en estado estacionario.

Finalmente, en cuanto a los resultados del esquema de control presentado, se debe realizar una investigación adicional para garantizar su aplicabilidad en clases más amplias de sistemas. Además, algún trabajo futuro podría explorar la implementación práctica del esquema de control propuesto en el sistema discreto, siguiendo un esquema similar al propuesto en Vázquez and Silva [2009].

References

Abdul-Hussin, M. (2015). Design of a Petri net based deadlock prevention policy supervisor for S3PR. In *2015 6th International Conference on Intelligent Systems, Modelling and Simulation*, pages 46–52.

Aguayo-Lara, E., Ramírez-Treviño, A., and Ruiz-León, J. (2011). Invariant subspaces and sensor placement for observability in continuous timed Petri nets. In *2011 IEEE International Conference on Automation Science and Engineering*, pages 607–612. IEEE.

Aguayo-Lara, E., Ramírez-Treviño, A., and Ruiz-León, J. (2014). Sensor placement for distinguishability and single structure observer design in continuous timed Petri nets. *Nonlinear Analysis: Hybrid Systems*, 12:20–32.

Amparore, E. G., Balbo, G., Beccuti, M., Donatelli, S., and Franceschinis, G. (2016). 30 years of GreatSPN. In *Principles of Performance and Reliability Modeling and Evaluation*, pages 227–254. Springer.

Augusto, V. and Xie, X. (2014). A modeling and simulation framework for health care systems. *IEEE Transactions on Systems, Man, and Cybernetics: Systems*, 44(1):30–46.

Baeten, J. C. and Weijland, W. P. (1991). *Process algebra*. Cambridge University Press.

Balbo, G. (2007). Introduction to generalized stochastic Petri nets. *Formal Methods for Performance Evaluation: 7th International School on Formal Methods for the Design of Computer, Communication, and Software Systems, Advanced Lectures 7*, pages 83–131.

Beccuti, M., Fornari, C., Franceschinis, G., Halawani, S., Barukab, O., Ahmad, A., and Balbo, G. (2013). From symmetric nets to differential equations exploiting model symmetries. *The Computer Journal*, 58(1):23–39.

Bemporad, A., Ferrari-Trecate, G., and Morari, M. (2000). Observability and controllability of piecewise affine and hybrid systems. *IEEE Transactions on Automatic Control*, 45(10):1864–1876.

Bernardi, S., Mahulea, C., and Albareda, J. (2019). Toward a decision support system for the clinical pathways assessment. *Discrete Event Dynamic Systems*, 29:91–125.

Bernardo, M., Budd, C., Champneys, A. R., and Kowalczyk, P. (2008). *Piecewise-smooth Dynamical Systems: Theory and Applications*. Springer.

Blondel, V. D. and Tsitsiklis, J. N. (1999). Complexity of stability and controllability of elementary hybrid systems. *Automatica*, 35(3):479–489.

Campos, J., Seatzu, C., and Xie, X. (2018). *Formal methods in manufacturing*. CRC press.

Casas Carrillo, R., Begovich Mendoza, O., Ramírez-Treviño, A., and Ruiz-León, J. (2021). Sufficient structural conditions for diagnosability and heuristic diagnoser design in timed continuous Petri nets. *International Journal of Control, Automation and Systems*, 19(11):3588–3597.

Cassandras, C. G. and Lafortune, S. (2008). *Introduction to discrete event systems*. Springer.

Chen, C. T. (1998). *Linear System Theory and Design*. Oxford University Press, Inc., New York, USA.

Coogan, S., Arcak, M., and Belta, C. (2017). Formal methods for control of traffic flow: Automated control synthesis from finite-state transition models. *IEEE Control Systems Magazine*, 37(2):109–128.

David, R. and Alla, H. (2010). *Discrete, Continuous, and Hybrid Petri Nets*. Springer-Verlag Berlin Heidelberg.

Dotoli, M., Fanti, M., Mangini, A., and Ukovich, W. (2009a). A continuous Petri net model for the management and design of emergency cardiology departments. *IFAC Proceedings Volumes*, 42(17):50 – 55.

Dotoli, M., Fanti, M. P., Mangini, A. M., and Ukovich, W. (2009b). A continuous Petri net model for the management and design of emergency cardiology departments. *IFAC Proceedings Volumes*, 42(17):50–55. 3rd IFAC Conference on Analysis and Design of Hybrid Systems.

Fanti, M. P., Mangini, A. M., Dotoli, M., and Ukovich, W. (2012). A three-level strategy for the design and performance evaluation of hospital departments. *IEEE Transactions on Systems, Man, and Cybernetics: Systems*, 43(4):742–756.

Habets, L., Collins, P., and van Schuppen, J. (2006). Reachability and control synthesis for piecewise-affine hybrid systems on simplices. *IEEE Transactions on Automatic Control*, 51(6):938–948.

Jacobson, S. H., Hall, S. N., and Swisher, J. R. (2013). Discrete-event simulation of health care systems. *Patient flow: Reducing delay in healthcare delivery*, pages 273–309.

Jiménez, E., Júlvez, J., Recalde, L., and Silva, M. (2005). On controllability of timed continuous Petri net systems: the join free case. In *IEEE CONFERENCE ON DECISION AND CONTROL*, volume 44, page 7645. IEEE; 1998.

Júlvez, J. and Boel, R. (2010). A continuous Petri net approach for model predictive control of traffic systems. *IEEE Transactions on Systems, Man, and Cybernetics - Part A: Systems and Humans*, 40(4):686–697.

Júlvez, J., Mahulea, C., and Vázquez, C.-R. (2012). Simhpn: A matlab toolbox for simulation, analysis and design with hybrid Petri nets. *Nonlinear Analysis: Hybrid Systems*, 6(2):806 – 817.

Júlvez, J., Recalde, L., and Silva, M. (2003). On reachability in autonomous continuous Petri net systems. In *International Conference on Application and Theory of Petri Nets*, pages 221–240. Springer.

Kang, C. W., Imran, M., Omair, M., Ahmed, W., Ullah, M., and Sarkar, B. (2019). Stochastic-Petri net modeling and optimization for outdoor patients in building sustainable healthcare system considering staff absenteeism. *Mathematics*, 7(6).

Kara, R., Ahmane, M., Loiseau, J., and Djennoune, S. (2009). Constrained regulation of continuous Petri nets. *Nonlinear Analysis: Hybrid Systems*, 3(4):738–748.

Kloetzer, M., Mahulea, C., Belta, C., and Silva, M. (2010). An automated framework for formal verification of timed continuous Petri nets. *IEEE Transactions on Industrial Informatics*, 6(3):460–471.

Lee, K., Jeong, H., Park, C., and Park, J. (2002). Development of a decision-support system for the formulation of manufacturing strategy. *International journal of production research*, 40(15):3913–3930.

Li, R. and Reveliotis, S. (2015). Performance optimization for a class of generalized stochastic Petri nets. *Discrete Event Dynamic Systems*, 25:387–417.

Liu, G. and Barkaoui, K. (2016). A survey of siphons in Petri nets. *Information Sciences*, 363:198–220.

Mahulea, C., Giua, A., Recalde, L., Seatzu, C., and Silva, M. (2008a). Optimal model predictive control of timed continuous Petri nets. *IEEE Transactions on Automatic Control*, 53(7):1731–1735.

Mahulea, C., Ramirez-Trevino, A., Recalde, L., and Silva, M. (2008b). Steady-state control reference and token conservation laws in continuous Petri net systems. *IEEE Transactions on Automation Science and Engineering*, 5(2):307–320.

Mahulea, C., Recalde, L., and Silva, M. (2009). Basic server semantics and performance monotonicity of continuous Petri nets. *Discrete Event Dynamic Systems*, 19(2):189–212.

Mahulea, C., Recalde, L., and Silva, M. (2010). Observability of continuous Petri nets with infinite server semantics. *Nonlinear Analysis: Hybrid Systems*, 4(2):219–232. IFAC World Congress 2008.

Mahulea, C., Seatzu, C., Cabasino, M. P., and Silva, M. (2012). Fault diagnosis of discrete-event systems using continuous Petri nets. *IEEE Transactions on Systems, Man, and Cybernetics-Part A: Systems and Humans*, 42(4):970–984.

Melani, A. H. d. A., Michalski, M. A. d. C., Murad, C. A., Caminada Netto, A., and de Souza, G. F. M. (2022). Generalized stochastic Petri nets for planning and optimizing maintenance logistics of small hydroelectric power plants. *Energies*, 15(8):2742.

Meyer, A. (2012). Discontinuity induced bifurcations in timed continuous Petri nets. *IFAC Proceedings Volumes*, 45(29):28 – 33. 11th IFAC Workshop on Discrete Event Systems.

Molloy, M. K. (1982). Performance analysis using stochastic Petri nets. *IEEE Trans. Comput.*, 31(09):913–917.

Murata, T. (1989). Petri nets: Properties, analysis and applications. *Proceedings of the IEEE*, 77(4):541–580.

Navarro-Gutiérrez, M., Fraustro-Valdez, J. A., Ramírez-Treviño, A., and Silva, M. (2020). Problematic configurations and choice-join pairs on mono-t-semiflow nets: Towards the characterization of behavior-structural properties. *Discrete Event Dynamic Systems*, 30:175–209.

Navarro-Gutiérrez, M., Ramírez-Treviño, A., and Silva, M. (2022a). Dual perspectives of equilibrium throughput properties of continuous mono-t-semiflow Petri nets: Firing rate and initial marking variations. *Automatica*, 136:110074.

Navarro-Gutiérrez, M., Ramírez-Treviño, A., and Silva, M. (2022b). Fluid net models: From behavioral properties to structural objects. *Applied Sciences*, 12(12):6123.

Ramadge, P. J. and Wonham, W. M. (1989). The control of discrete event systems. *Proceedings of the IEEE*, 77(1):81–98.

Ratzer, A. V., Wells, L., Lassen, H. M., Laursen, M., Qvortrup, J. F., Stissing, M. S., Westergaard, M., Christensen, S., and Jensen, K. (2003). CPN tools for editing, simulating, and analysing coloured Petri nets. In *Proceedings of Applications and Theory of Petri Nets 2003: 24th International Conference (ICATPN)*, pages 450–462. Springer.

Recalde, L., Mahulea, C., and Silva, M. (2006). Improving analysis and simulation of continuous Petri nets. In *2006 IEEE International Conference on Automation Science and Engineering*, pages 9–14.

Recalde, L. and Silva, M. (2001). Petri nets fluidification revisited: Semantics and steady state. *European Journal of Automation APII-JESA*, 35:435–449.

Recalde, L., Teruel, E., and Silva, M. (1998). Modeling and analysis of sequential processes that cooperate through buffers. *IEEE Transactions on Robotics and Automation*, 14(2):267–277.

Rodríguez, R. J., Bernardi, S., and Zimmermann, A. (2018). An evaluation framework for comparative analysis of generalized stochastic Petri net simulation techniques. *IEEE Transactions on Systems, Man, and Cybernetics: Systems*, 50(8):2834–2844.

Rodríguez, R. J., Bernardi, S., and Zimmermann, A. (2020). An evaluation framework for comparative analysis of generalized stochastic Petri net simulation techniques. *IEEE Transactions on Systems, Man, and Cybernetics: Systems*, 50(8):2834–2844.

Ross-León, R., Ramírez-Treviño, A., Ruiz-León, J., and Aguayo-Lara, E. (2014). Local control law for live and bounded timed continuous Petri nets. *IFAC Proceedings Volumes*, 47(2):129–134.

Ross-León, R., Ramírez-Treviño, A., Morales, J., and Ruiz-León, J. (2010). Control of metabolic systems modeled with timed continuous Petri nets. In *ACSD/Petri Nets Workshops, volume 827 of CEUR Workshop Proceedings*, pages 87–102.

Rotter, T., Kinsman, L., James, E. L., Machotta, A., Gothe, H., Willis, J., Snow, P., and Kugler, J. (2010). Clinical pathways: effects on professional practice, patient outcomes, length of stay and hospital costs. *Cochrane database of systematic reviews*, (3).

Seatzu, C. (2019). Modeling, analysis, and control of automated manufacturing systems using Petri nets. In *2019 24th IEEE International Conference on Emerging Technologies and Factory Automation*, pages 27–30.

Shao, G., Jain, S., Laroque, C., Lee, L. H., Lendermann, P., and Rose, O. (2019). Digital twin for smart manufacturing: the simulation aspect. In *2019 Winter Simulation Conference (WSC)*, pages 2085–2098. IEEE.

Silva, M. (1985). *Las Redes de Petri: en la Automática y la Informática*. Madrid: Editorial AC, DL.

Silva, M., Fraca, E., and Wang, L. (2014). Performance evaluation and control of manufacturing systems: A continuous Petri nets view. In *Formal Methods in Manufacturing*, pages 409–452. CRC Press.

Silva, M., Júlvez, J., Mahulea, C., and Vázquez, C. R. (2011). On fluidization of discrete event models: observation and control of continuous Petri nets. *Discrete Event Dynamic Systems*, 21(4):427–497.

Silva, M., Terue, E., and Colom, J. M. (1998). Linear algebraic and linear programming techniques for the analysis of place/transition net systems. *Lectures on Petri Nets I: Basic Models: Advances in Petri Nets 3*, pages 309–373.

Souissi, Y. and Beldiceanu, N. (1988). Deterministic systems of sequential processes: Theory and tools. In *CONCURRENCY 88: International Conference on Concurrency*, pages 380–400. Springer Berlin Heidelberg.

Taleb, M., Leclercq, E., and Lefebvre, D. (2014). Control design of timed Petri nets via model predictive control with continuous Petri nets. *IFAC Proceedings Volumes*, 47(2):149–154.

Teruel, E., Colom, J. M., and Silva, M. (1997). Choice-free Petri nets: A model for deterministic concurrent systems with bulk services and arrivals. *IEEE Transactions on Systems, Man, and Cybernetics-Part A: Systems and Humans*, 27(1):73–83.

Vázquez, C. R. and Ramírez-Treviño, A. (2012). Structural and generic conditions for controllability of timed continuous Petri nets. *IFAC Proceedings Volumes*, 45(29):41–46.

Vázquez, C. R., Ramírez-Treviño, A., and Silva, M. (2014). Controllability of timed continuous Petri nets with uncontrollable transitions. *International Journal of control*, 87(3):537–552.

Vázquez, C. R. and Silva, M. (2009). Performance control of markovian Petri nets via fluid models: A stock-level control example. In *2009 IEEE International Conference on Automation Science and Engineering*, pages 30–36. IEEE.

Wang, J. (2023). Patient flow modeling and optimal staffing for emergency departments: A Petri net approach. *IEEE Transactions on Computational Social Systems*, 10(4):2022–2032.

Wonham, W. (1985). *Linear Multivariable Control: A Geometric Approach.* Springer-Verlag New York.

Xu, J. and Xie, L. (2005). Null controllability of discrete-time planar bimodal piecewise linear systems. *International Journal of Control*, 78(18):1486–1496.

Xu, J. and Xie, L. (2014). *Control and estimation of piecewise affine systems.* Elsevier.

Zimmermann, A. and Knoke, M. (2001). Timenet 4.0.

Publications

The following publications have been generated while developing this thesis, and to an extent have guided the thesis into what it has become:

International peer-reviewed conferences

César Arzola, Carlos Renato Vázquez, Manuel Silva, & Antonio Ramírez-Treviño (2020). *Structural Characterization of Controllability in Timed Continuous Petri Nets using Invariant Subspaces.* 21st IFAC World Congress Berlin, Germany, 11–17 July 2020, IFAC-PapersOnLine, 53(2), 2087-2094, https://doi.org/10.1016/j.ifacol.2020.12.2527

César Arzola, Antonio Ramírez-Treviño, & Manuel Silva. *On the Equilibrium Sets of Topologically Equal Conflict Timed Continuous Petri Nets.* 15th IFAC Workshop on Discrete Event Systems — Rio de Janeiro, Brazil, 11-13 November 2020,IFAC-PapersOnLine 53.4 (2020): 363-370. https://doi.org/10.1016/j.ifacol.2021.04.072

César Arzola, Cristian Mahulea, & Jorge Júlvez. "Analysis and optimization of clinical pathways using timed continuous Petri nets.," 2023 IEEE 28th International Conference on Emerging Technologies and Factory Automation (ETFA), Sinaia, Romania, 2023, pp. 1-8, https://10.1109/ETFA54631.2023.10275390.

César Arzola, Daniel Latorre, Germán Sacramento, Cristian Mahulea, & Jorge Júlvez. *Modeling and performance analysis of an industrial transport platform manufacturing process*, 2023 IEEE 28th International Conference on Emerging Technologies and Factory Automation (ETFA), Sinaia, Romania, 2023, pp. 1-4, https://10.1109/ETFA54631.2023.10275422

Journal Articles

César Arzola, Carlos Renato Vázquez, Antonio Ramírez-Treviño, & Manuel Silva (2023). *Structural controllability in timed continuous Petri nets.* Automatica, 153, 111005, https://doi.org/10.1016/j.automatica.2023.111005

Appendix A

Analysis of an industrial manufacturing process

In order to showcase the capabilities of Petri net formalisms, this appendix focuses on the modeling and performance analysis of the manufacturing process for *transport platforms* at the Alimak Group facility in La Muela, Spain. The objective is to leverage formal tools to gain insights into this complex manufacturing process and explore potential applications such as control and optimization. This section presents a preliminary study, where a *Generalized Stochastic Petri net* model of the manufacturing process is proposed to be used for simulation, performance analysis, and optimization of the system.

A.1 — Introduction

In the modern era of complex systems, industries face the challenge of effectively managing intricate processes while striving for efficiency and optimal performance. This is particularly evident in the manufacturing sector, where companies aim to deliver high-quality products within tight timelines, all while maintaining cost-effectiveness. To tackle these challenges, it has become imperative to employ formal tools that can provide valuable insights into the underlying processes and aid in the design of efficient operational techniques [Campos et al., 2018, Seatzu, 2019, Shao et al., 2019].

Alimak Group, a renowned player in the manufacturing industry, specializes in the production of vertical access solutions, including elevators and work platforms. The manufacturing process of such systems involves numerous interconnected stages, encompassing production, assembly, quality control, and logistics. To optimize this intricate process, Alimak Group acknowledges the importance of adopting formal tools that can aid in analysis and decision-making, ultimately leading to improved operational efficiency and product quality.

To showcase this, in this secwion, we propose a *Petri net-based formal model* to represent the manufacturing process of transport platforms, depicted in Fig. A.1, at the Alimak Group

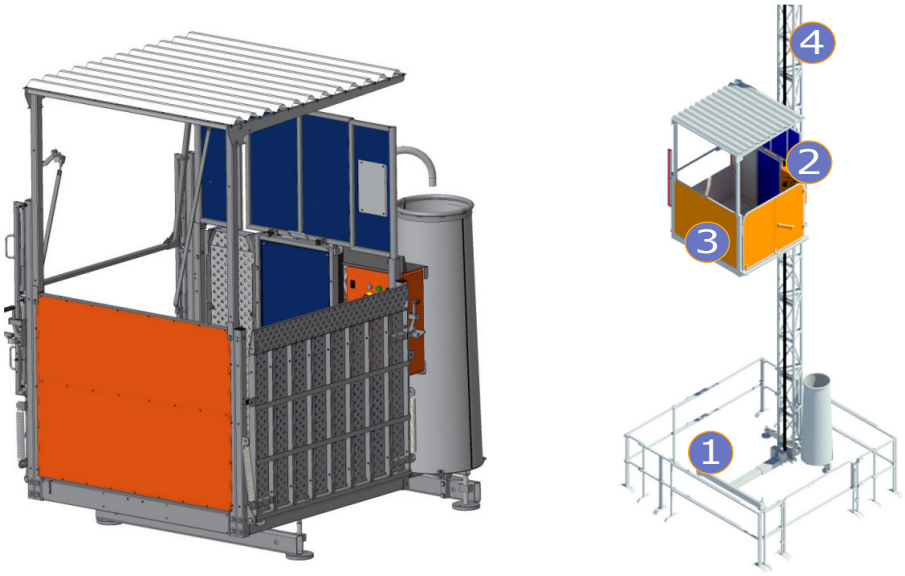

Figure A.1. The standard configuration of the transport platform and its main components: 1) the erection platform, 2) the drive unit, 3) the frame, 4) the mast unit.

facility in La Muela, Spain. In particular, we use *Generalized Stochastic Petri nets* (GSPNs) [Balbo, 2007] to model the system under consideration. One key motivation for employing GSPN models is their ability to estimate essential performance measures that provide insights into system behavior [Lee et al., 2002, Li and Reveliotis, 2015, Melani et al., 2022]. Parameters such as *throughput*, *resource utilization*, and *system efficiency* can be accurately evaluated using *state-based techniques* and/or *event-driven simulation*, leveraging the capabilities of GSPN models [Amparore et al., 2016, Ratzer et al., 2003, Rodríguez et al., 2018, Zimmermann and Knoke, 2001]. These quantitative measures provide valuable information for decision-making and process optimization, such as identifying bottlenecks, optimizing resource allocation, the assessment of different scenarios, and evaluation of alternative strategies without disrupting the actual production process.

A.2 — Production process of transport platforms

In this section, we describe the production process of the standard configuration of the transport platforms (TPL), which are produced at the Alimak Group facility in La Muela, Spain. The layout of the manufacturing process is depicted in Fig. A.2: it consists of a storage area for the parts, four production spots for TPLs, an adjacent spot for assembling 4 drive units in parallel, and an output buffer. Additionally, the production process is supported by a test bench (consisting of a mobile mast unit and masses for the load tests) and a forklift, to be used during the different stages of the process. The production of a TPL is composed of the sequential assembly of its main components:

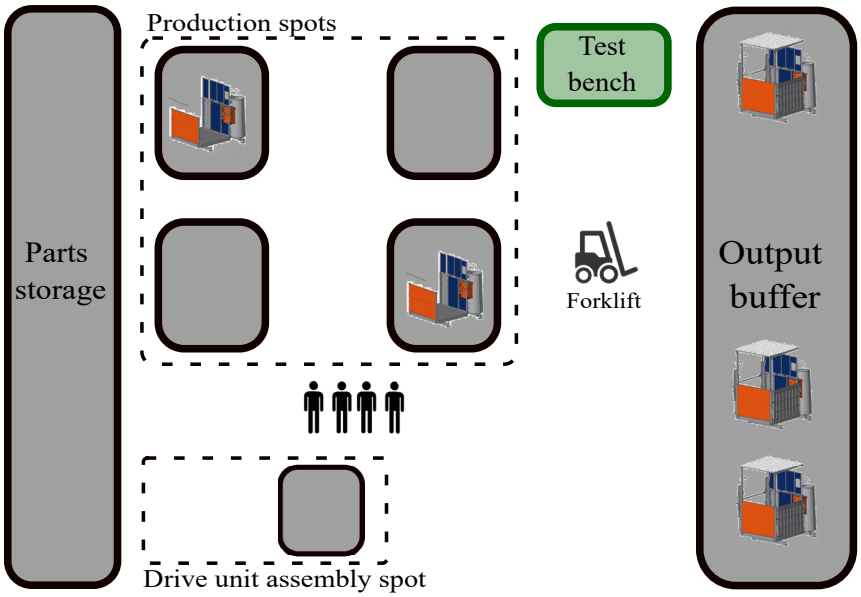

Figure A.2. General layout of the production process.

1. *Erection platform*: The erection platform is the base of the system. It serves as a facilitator for efficient mast fastening during erection and secure attachment of mast ties to the wall.

2. *Drive unit*: The drive unit is responsible for driving the TPL along the mast sections via a series of guide rollers. The gear motor, overload system, and safety device system are all installed in this unit.

3. *Frame of the unit*: It consists of the base platform (floor's self-supporting structure) to which the front panel, back panel (removable panel in front of machinery and safety device), and the falling object protection structure (roof) are attached.

4. *Electric control panel*: This panel acts as a centralized unit that integrates all the necessary commands for platform operation and the control of safety systems.

A.2.1. Assembly of the transport platforms

The production process can be divided into two main activities that are carried out in parallel:

On one hand, the drive units are built on the adjacent production spot, installing, the gear motor, overload system, and safety device system on the drive frame (Procedure 1, in Fig A.3). Four drive units can be produced in parallel.

On the other hand, the TPLs are assembled on the 4 production spots (4 TPLs can be assembled in parallel). Firstly, the erection platform is installed on an available production spot, installing the cable basket and a mast section on it. Subsequently, one of the finished drive units and the control panel are installed (Procedure 2, in Fig A.3). Finally, the four

elements composing the frame are integrated to complete the assembly (Procedure 3, in Fig A.3).

The parts that are required for the TPL assembly are stored in the general storage area. As the TPL production process progresses, operators carry the necessary parts from the storage area. Depending on the complexity of the different tasks (often requiring carrying heavy parts from the storage), they can be performed by either one, two operators or two operators utilizing a forklift, depending on its difficulty.

After assembly, the unit undergoes testing on a movable test bench. This test bench is transported to the production spot using a forklift, with the two operators ensuring its safe transfer. The test bench enables critical safety checks, including maximum velocity testing and assessment of safety device functionality through drop tests. Upon successful completion of the tests, the unit is transferred to the output buffer area (Procedure 4 in Fig. A.3).

It is worth highlighting that, given the overall process throughput is relatively slow, the need to model the arrival of new parts to the storage area is deemed unnecessary as the slow utilization rate ensures consistent availability of parts at all times in the unit storage.

A.3 — Petri net model of the manufacturing process

To model the manufacturing process, we propose a Generalized Stochastic Petri Net (GSPN) model. For a deeper insight on the formalism, the interested reader can consult Balbo [2007]. The GSPN model serves as a powerful tool for accurately representing and analyzing the complex dynamics of the manufacturing system under investigation. Due to the complexity of the proposed model, we do not include it in this section but it is available online at `https://github.com/arzola91/PNModels.git`. In order to give some general insight into the model, Fig. A.3 depicts the main PN structures that model the different procedures described in the previous section:

P1 models the assembly of the drive units, which is carried out in parallel with the rest of the production process. As mentioned early, 4 drive units can be assembled in parallel, resulting in a PN structure with four branches, each resembling the assembly process represented by P1.

Similarly, the sequential procedures for completing a TPL are represented by the procedures depicted in P2, P3, and P4. The composition of these 3 structures represents the activities performed at a specific production spot. Since the system contains 4 production spots, the proposed model also exhibits four parallel branches, with each branch representing the sequential activities (P2 $\Longrightarrow$ P3 $\Longrightarrow$ P4) performed at different production spots within the system.

The model contains other places, representing the shared resources to be used during the

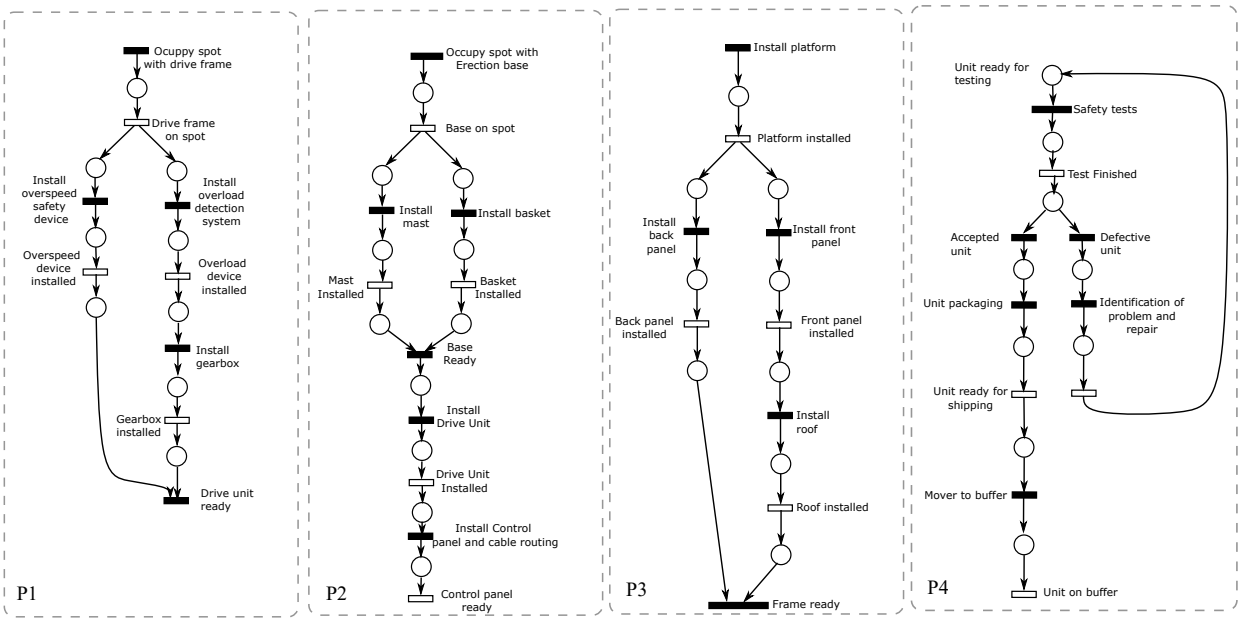

Figure A.3. Main procedures involved in the assembly of a TPL, represented by Petri net structures. P1 is carried out in parallel to the rest, which are carried out in a sequential manner P2 $\Longrightarrow$ P3 $\Longrightarrow$ P4.

process: available operators, available forklifts, available test bench availability of a production spot, output buffer, etcetera. Those places are pre-conditions for the different transitions of the system. Those places, however, are not depicted here for the sake of readability. Clearly, for each transition, these pre-conditions will depend on the complexity of each task. This is depicted clearly and without ambiguity on the complete model.

A.3.1. Model parameters

In order to assess the system performance, time delays must be associated with transitions. The mean time delay of each transition is defined according to the time interval it takes to accomplish the task it represents. This information is obtained in collaboration with the expert engineers of Alimak and is summarized in Table A.1. The model has two types of transitions: immediate and timed. The former type represents events that occur instantaneously, such as the allocation of resources and the decisions that can be taken during the process (depicted as black transitions in Fig. A.3). The latter represents the completion of the different stages of the process. (depicted as white transitions in Fig. A.3).

The initial marking distribution of the system is determined by the number of available resources: number of operators, number of production spots (4), output buffer size (8 units)[1],

[1]In the following, the number of production spots and output buffer size is considered constant since redesign of the layout and production plant is neither desirable nor feasible.

Table A.1

Delay times of each of the events included in the manufacturing process.

Event	**Time delay**
Base on spot	40 min
Basket installed	60 min
Mast installed	60 min
Drive frame on spot	40 min
Overspeed device installed	60 min
Overload device installed	60 min
Gearbox installed	80 min
Drive unit installed	80 min
Control panel + cable routing ready	90 min
Platform installed	80 min
Back panel installed	60 min
Front panel installed	60 min
Roof installed	60 min
Test finished	80 min
Unit ready for shipping	40 min
Unit on buffer	30 min

number of forklifts and, number of test benches. Initially, the marking in the rest of the places is 0, representing that no unit is being processed.

A.4 — Performance analysis of the system

In this section, we present a performance analysis of the system. In particular, Alimak aims to optimize the process to reduce production time while maintaining or improving quality. Currently, they can produce, on average, four TPLs in 40 hours using 4 operators, 1 forklift, and 1 test bench. Therefore, the selected goal of this contribution is to study how different distributions of resources (operators and forklifts) may affect the production time of the TPLs. We simulated 6 scenarios, considering different personnel/resource cases.

In order to carry out the performance analysis, we use event-driven simulation techniques (GreatSPN). The considered performance index was the *throughput* of the output transition of the system, χ_{out}, i.e., a measure of how many units of TPLs can be processed in a given amount of time. This was obtained by simulating[2] the behavior of the system until it reached a steady state, using the *steady state simulation* module of GreatSPN (solver: *GreatSPN Legacy*; confidence: 95%).

Once this performance index is obtained, we can compare its performance with the real production plant. To compare it with the current layout, the performance index chosen for

[2]The simulations were performed using a computer with an 11th Gen Intel(R) Core(TM) i7-1165G7 @ 2.80GHz processor and 16GB RAM.

	Resources				
Case	#Op	#FkL	PT (Hrs.)	Avg. #Idle_Op	Avg. #Idle_FkL
1	4	1	37.68	1.078	0.083
2	6	1	35.19	2.868	0.016
3	8	1	34.63	4.823	0.003
4	4	2	29.11	0.223	0.810
5	6	2	20.78	0.721	0.339
6	8	2	18.50	2.043	0.128

Figure A.4. Production time (PT) values estimated using GreatSPN for different resource situations. PT values are given in hours. The second (#Op) and third (#FkL) columns indicate the number of operators and the number of forklifts considered in each case, respectively. Moreover, the fifth and sixth columns indicate the average number of idle operators and idle forklifts, respectively

our analysis was the time required to produce four TPLs. This production time, PT, can be computed as $PT = \frac{1}{\chi_{out}} \times 4$ (the amount it takes to produce one TPL multiplied by four, i.e., the amount it takes to produce 4 TPLs).

To ensure the reliability of our model, we validated it by considering Case 1 as the baseline scenario (which represents the production implementation currently employed at the manufacturing plant). By comparing the model's predictions with the actual performance data obtained from Case 1, we were able to assess the accuracy and validity of our model. After this, we simulated different cases to study how different distributions of resources may affect the production time of the TPLs, compared to the baseline scenario. These results are summarized in Fig. A.4.

Other performance indices considered were the number of average idle operators and average idle forklifts, i.e., the number of operators or forklifts that, on average, were not actively engaged in productive tasks. This information is useful to understand if a resource might be underutilized or if there are potential bottlenecks in the system. For instance, if the average idle operators value is consistently high, it suggests that there may be an imbalance between the available workforce and the workload, indicating a potential excess of operators. On the other hand, a low average idle forklifts value signifies efficient utilization of forklifts, indicating that they are effectively supporting the production process.

A.4.1. Discussion

The results obtained from the event-driven simulation provide insights into the impact of resource allocation on the system performance. For instance, in this particular case, the obtained results reveal that the availability of forklifts plays a crucial role in determining the production time. Scenarios with limited forklift capacity (cases 1-3), even with an increased number of operators, experienced prolonged production times due to a lack of ability to perform parallel task execution (since most of the parallelizable tasks during the production process require the use of the forklift). This can be seen also in the number of average idle operators of case 3 (8 operators and 1 forklift), indicating that the lack of resources to carry out the operations does not allow to parallelize tasks in the system, even with a high amount of personnel. Therefore, minimal improvements in efficiency were obtained in these cases.

On the other hand, an increase in the number of forklifts shows a significant improvement in production times, even in the case of only 4 operators. This is due to the fact that this improvement allows the operators to perform several tasks in parallel, reducing production times. Clearly, it is imperative to establish a balanced allocation of both operators and forklifts. This ensures improved coordination among resources, enables parallel task execution, and enhances overall efficiency.

A.5 — Concluding remarks

In order to showcase the capabilities of Petri net formalisms, this appendix proposes a *Generalized Stochastic Petri net* (GSPN) model to analyze and optimize the manufacturing process for *transport platforms* at the Alimak Group facility in La Muela, Spain. It was shown that the GSPN model can be used to perform the analysis of the production time and resource utilization dynamics of the system under consideration. In addition, a preliminary study was conducted to examine how different resource plans can affect the productivity of the system. Through this study, it was observed that the GSPN model effectively enables the identification of the specific resources that have a greater impact on the overall productivity of the system.

Future research can focus on

- Collaborating closely with Alimak and gathering comprehensive data to enhance the accuracy and reliability of the GSPN model. Rigorous validation against real production data will verify the model's fidelity.
- Exploring and adapting existing optimization algorithms and resource allocation tools developed for GSPNs, identifying efficient resource allocation strategies to maximize productivity.

- Implementation of the optimization results in the actual manufacturing process, achieving tangible improvements.

Moreover, as in the case of the case study of the clinical pathway presented in section 6, a fluid version of this model could be developed in order to use the results presented in this thesis, allowing the analysis of different properties of the system, such as controllability, control design, and more efficient steady-state performance.